

Multistage Linear Multiuser Receivers: Large-System Design and Analysis

Mohsen Ghotbi

A Thesis
in
The Department
of
Electrical and Computer Engineering

Presented in Partial Fulfillment of the Requirements
for the Degree of Doctor of Philosophy at
Concordia University
Montréal, Québec, Canada

March 2005

© Mohsen Ghotbi, 2005



Library and
Archives Canada

Bibliothèque et
Archives Canada

Published Heritage
Branch

Direction du
Patrimoine de l'édition

395 Wellington Street
Ottawa ON K1A 0N4
Canada

395, rue Wellington
Ottawa ON K1A 0N4
Canada

Your file *Votre référence*
ISBN: 0-494-09972-0
Our file *Notre référence*
ISBN: 0-494-09972-0

NOTICE:

The author has granted a non-exclusive license allowing Library and Archives Canada to reproduce, publish, archive, preserve, conserve, communicate to the public by telecommunication or on the Internet, loan, distribute and sell theses worldwide, for commercial or non-commercial purposes, in microform, paper, electronic and/or any other formats.

The author retains copyright ownership and moral rights in this thesis. Neither the thesis nor substantial extracts from it may be printed or otherwise reproduced without the author's permission.

AVIS:

L'auteur a accordé une licence non exclusive permettant à la Bibliothèque et Archives Canada de reproduire, publier, archiver, sauvegarder, conserver, transmettre au public par télécommunication ou par l'Internet, prêter, distribuer et vendre des thèses partout dans le monde, à des fins commerciales ou autres, sur support microforme, papier, électronique et/ou autres formats.

L'auteur conserve la propriété du droit d'auteur et des droits moraux qui protègent cette thèse. Ni la thèse ni des extraits substantiels de celle-ci ne doivent être imprimés ou autrement reproduits sans son autorisation.

In compliance with the Canadian Privacy Act some supporting forms may have been removed from this thesis.

Conformément à la loi canadienne sur la protection de la vie privée, quelques formulaires secondaires ont été enlevés de cette thèse.

While these forms may be included in the document page count, their removal does not represent any loss of content from the thesis.

Bien que ces formulaires aient inclus dans la pagination, il n'y aura aucun contenu manquant.


Canada

ABSTRACT

Multistage Linear Multiuser Receivers: Large-System Design and Analysis

Mohsen Ghotbi, Ph. D.

Concordia University, 2005

This thesis introduces an analytical method for large-system design and analysis of multistage linear multiuser (MLMU) receivers for direct-sequence (DS-) code division multiple access (CDMA) systems. The figure of merit to evaluate performance is the signal to interference plus noise ratio (SINR) that is calculated for a case where the number of active users and the processing gain tend towards infinity, while their ratio remains finite. The large-system performance will be a function of the number of the interference cancellation stages, the moments of the eigenvalues of the covariance matrix, the system load and the SNR. Compared to other recently-proposed methods, our proposed method offers a more efficient approach to finding the large-system performance by introducing a new expression for the covariance matrix of the interference term. A simplified multistage scheme to estimate the multipath channel gains is also introduced. It will be shown that by applying this new method method for data detection and channel estimation, the performance of the MLMU receiver will converge to that of the minimum mean-squared error (MMSE) receiver.

To My Family

ACKNOWLEDGEMENTS

I would like to show my sincerest gratitude to my advisor Dr. M. Reza Soleymani for his devoted guidance and constant encouragement. Working with professor Soleymani has been my invaluable and delightful experience and his keen advice has helped me both professionally and personally. His immense patience and incredible meticulousness has left an indelible effect on me. Special appreciation to the committee members, Dr. Lim, Dr. Harutyunyan, Dr. Plotkin and Dr. Shayan for their ideas and invaluable comments.

I wish to express my deepest appreciation to my dearest parents, sisters, and brothers for their support and encouragement. I am also grateful for Mrs. Juliet O'Neill Dunphy for the proofreading of this thesis.

This thesis was partially supported by Natural Sciences and Engineering Research Council of Canada (NSERC) IPS II and NSERC discovery grant OGPIN01.

TABLE OF CONTENTS

LIST OF TABLES	ix
LIST OF FIGURES	x
LIST OF ACRONYMS	xvi
LIST OF SYMBOLS	xvi
1 Introduction	1
1.1 Multiple Access Schemes	1
1.2 Multiuser Detection	4
1.3 Large CDMA System	4
1.4 Objective	5
1.5 Contributions	5
1.6 Organization	6
2 Multistage Linear Multiuser Receivers: An Overview	8
2.1 Computing PCFs for Multistage PPIC Receiver	9
2.1.1 System Model	9
2.1.2 Derivation of PCFs	10
2.2 Computing SINR for Multistage PPIC Receivers	13
2.2.1 System Model	13
2.2.2 MMSE-Based Multistage Linear PPIC Receiver with a constant PCF	14
2.2.3 Decorrelator-Based Multistage Linear PPIC Receiver with a Variable PCF	15
2.3 Multiuser Detection and Channel Estimation over Multipath Fading Channels	17
2.3.1 System Model	17
2.3.2 Data Estimation	18

2.3.3	Channel Estimation	18
2.4	Asynchronous CDMA Systems	20
2.4.1	System Model	21
2.5	Large CDMA System	23
3	A Simple Method for Computing PCFs for Multistage PPIC Receiver	26
3.1	Derivation of PCF	27
3.2	Numerical Results	29
3.2.1	Equal-Power Case	29
3.2.2	Unequal-Power Case	35
3.3	Summary	38
4	Large-System Design and Analysis of Multistage PPIC Receiver with a Constant PCF	39
4.1	System Model	40
4.2	Performance of Multistage PPIC Receiver	41
4.3	Numerical Results and Discussions	43
4.4	Summary	51
5	Large-System Design and Analysis of Multistage Linear PPIC Receiver with a Variable PCF	52
5.1	MMSE-Based Multistage Multiuser Receiver with a variable PCF	53
5.2	Numerical Results and Discussion	56
5.2.1	Equal-Power Case	56
5.2.2	Unequal-Power Case	70
5.3	Summary	76
6	Multistage Multiuser Detection and Channel Estimation over Multipath Fading Channels	77

6.1	Data Estimation	78
6.2	Channel Estimation	83
6.3	Summary	89
7	Multistage PPIC Receiver for Asynchronous CDMA Systems	94
7.1	Multistage Linear PPIC Receiver	95
7.2	Performance Evaluation	95
7.2.1	Performance Versus Number of Stages	96
7.2.2	Performance Versus System Load	99
7.2.3	Performance Versus SNR	100
7.3	Summary	103
8	Conclusions and Suggestions for Future Work	104
8.1	Conclusions	104
8.2	Directions for Further Research	106
A	Proof of Theorem 6.1.1	107
B	Proof of Theorem 6.2.1	110
	Bibliography	113

LIST OF TABLES

- 2.1 Coefficients of Equations (2.68) and (2.69) for $i = 1, 2, 3, 4,$ and 5 . . . 25

LIST OF FIGURES

1.1	FDMA and TDMA techniques.	2
1.2	A DS-CDMA technique, a) pure CDMA, b) CTDMA (CDMA & TDMA).	3
2.1	An m -stage PPIC receiver.	11
2.2	Asynchronous CDMA timing diagram.	21
2.3	The effect of interferer k on user 1 in an asynchronous CDMA.	22
3.1	The p.d.f of the eigenvalues of the covariance matrix for the two cases of analytical i.i.d and simulation i.i.d. entries with $K = 16$, $N = 32$ and $\beta = K/N = 0.5$	30
3.2	Comparison of performance improvement of the PPIC receiver by applying two methods of PCF optimization for $K = 15$, $N = 31$ and $SNR = 10dB$	31
3.3	Convergence of the performance of the PPIC receiver to that of the MMSE receiver using two methods of PCF optimization for $K = 15$, $N = 31$ and $SNR = 7dB$	32
3.4	Comparison of the performance of the multistage linear PPIC receiver with optimum PCF using proposed method for $m = 14$ with that of the MMSE and SUMF receivers versus the number of active users, $N = 32$ and $SNR = 8.0dB$	33
3.5	Comparison of the performance of the multistage linear PPIC receiver with optimum PCF using proposed method for $m = 14$ with that of the MMSE and SUMF receivers versus SNR, $\beta = 0.5$	34

3.6	Large-system performance of the PPIC receiver for CDMA system over a Rayleigh-fading channel versus number of interference cancellation stages ($\beta = 0.5$ and $SNR = 12dB$).	36
3.7	Comparison of the large-system performance of the PPIC receiver with MMSE and SUMF receivers for a CDMA system over a frequency-flat Rayleigh fading channel versus SNR ($\beta = 0.5$ and $m = 10$).	37
4.1	Large-system performance of the PPIC receiver for CDMA system over a Rayleigh-fading channel versus PCF ($\beta = 0.5$, $m = 8$, and $SNR = 12dB$).	44
4.2	Comparison of the Large-system SINR of synchronous CDMA with SUMF, MMSE, and PPIC ($m = 1, 3, 5, 8$) receivers over a Rayleigh-fading channel for $SNR = 12dB$	45
4.3	Large-system SINR of synchronous CDMA with SUMF, MMSE, and PPIC ($m = 1, 3, 5, 8$) receivers over AWGN channel for $SNR = 12dB$	46
4.4	SINR improvement of the multistage PPIC receiver for a CDMA system over a Rayleigh-fading channel versus the number of interference cancellation stages, $SNR = 12$	48
4.5	BER improvement of the multistage PPIC receiver for a CDMA system over a Rayleigh-fading channel for different stages, $SNR = 12$	49
4.6	Comparison of the large-system analytical and simulation results for a CDMA system over a Rayleigh-fading channel with PPIC receiver, $N = 16, 32$, and 64 , $SNR = 12$ dB, $m = 1$, and $\mu = 0.165$	50
5.1	SINR of the MMSE-based multistage linear PPIC receiver with constant PCF for a large CDMA system over an AWGN channel versus system load, SNR= 12.0 dB.	57

5.2	SINR of the MMSE-based multistage linear PPIC receiver with constant PCF for a large CDMA system over an AWGN channel versus SNR, $\beta = 0.75$	58
5.3	BER of the MMSE-based multistage linear PPIC receiver with constant PCF for a large CDMA system over an AWGN channel versus system load, SNR= 12.0 dB.	59
5.4	BER of the MMSE-based multistage linear PPIC receiver with constant PCF for a large CDMA system over an AWGN channel versus SNR, $\beta = 0.75$	60
5.5	SINR of the decorrelator-based multistage linear PPIC receiver with different PCF for a large CDMA system over an AWGN channel versus system load, SNR= 12.0 dB.	62
5.6	SINR of the decorrelator-based multistage linear PPIC receiver with variable PCF for a large CDMA system over an AWGN channel versus SNR, $\beta = 0.75$	63
5.7	BER of the Decorrelator-based multistage linear PPIC receiver with variable PCF for a large CDMA system over an AWGN channel versus system load, SNR= 12.0 dB.	64
5.8	BER of the decorrelator-based multistage linear PPIC receiver with variable PCF for a large CDMA system over an AWGN channel versus SNR, $\beta = 0.75$	65
5.9	SINR of the MMSE-based multistage linear PPIC receiver with variable PCF for a large CDMA system over an AWGN channel versus system load, SNR= 12.0 dB.	66
5.10	SINR of the multistage linear PPIC receiver with variable PCF for a large CDMA system over an AWGN channel versus SNR, $\beta = 0.75$	67

5.11	BER of the MMSE-based multistage linear PPIC receiver with variable PCF for a large CDMA system over an AWGN channel versus system load, SNR= 12.0 dB.	68
5.12	BER of the MMSE-based multistage linear PPIC receiver with variable PCF for a large CDMA system over an AWGN channel versus SNR, $\beta = 0.75$	69
5.13	SINR of the MMSE-based multistage linear PPIC receiver with constant PCF for a large CDMA system over a Rayleigh frequency-flat fading channel versus system load, SNR= 12.0 dB.	71
5.14	SINR of the MMSE-based multistage linear PPIC receiver with variable PCF for a large CDMA system over a Rayleigh frequency-flat fading channel versus system load, SNR= 12.0 dB.	72
5.15	SINR of the MMSE-based multistage linear PPIC receiver with variable PCF for a large CDMA system over a Rayleigh frequency-flat fading channel versus SNR, $\beta = 0.75$	73
5.16	BER of the MMSE-based multistage linear PPIC receiver with variable PCF for a large CDMA system over a Rayleigh frequency-flat fading channel versus system load, SNR= 12.0 dB.	74
5.17	BER of the MMSE-based multistage linear PPIC receiver with variable PCF for a large CDMA system over a Rayleigh frequency-flat fading channel versus SNR, $\beta = 0.75$	75
6.1	Large-system SINR of the MMSE-based MLMU receiver in a multipath fading channel versus system load for $L = 2$ and $SNR = 12.0$ dB.	81
6.2	Large-system SINR of the MMSE-based MLMU receiver in a multipath fading channel versus SNR for $L = 3$ and $\beta = 0.5$	82

6.3	Large-system SINR of the MMSE-based MLMU receiver in a multi-path fading channel versus the number of resolvable paths for $SNR = 12.0$ dB and $\beta = 0.5$	84
6.4	Large-system BER of the MMSE-based MLMU receiver in a multi-path fading channel versus system load for $L = 2$ and $SNR = 12.0$ dB.	85
6.5	Large-system BER of the MMSE-based MLMU receiver in a multi-path fading channel versus SNR for $L = 3$ and $\beta = 0.5$	86
6.6	Large-system BER of the MMSE-based MLMU receiver in a multi-path fading channel versus L for $SNR = 12.0$ dB and $\beta = 0.5$	87
6.7	Large-system multistage MSE versus system load. $\tau = 10$, $L = 2$, and $SNR = 12.0$ dB.	90
6.8	Large-system multistage MSE versus number of training symbols. $\beta = 0.5$, $L = 2$, and $SNR = 12.0$ dB.	91
6.9	Large-system multistage MSE versus number of resolvable paths. $\tau = 10$, $\beta = 0.5$, and $SNR = 12.0$ dB.	92
6.10	Large-system multistage MSE versus SNR. $\tau = 10$, $\beta = 0.5$, and $L = 2$	93
7.1	SINR improvement of the multistage linear PPIC receiver for an asynchronous CDMA system over an AWGN channel versus PCF (μ) and the number of the interference cancellation stages (m), $SNR = 12.0$ dB, $K = 16$, $N = 32$ (system load $\beta = K/N = 0.5$).	97
7.2	SINR improvement of the multistage linear PPIC receiver for an asynchronous CDMA system over an AWGN channel versus m , $SNR = 12.0$ dB, $K = 16$, $N = 32$ ($\beta = 0.5$), and $\mu = 0.4$	98
7.3	SINR of the multistage linear PPIC receiver for an asynchronous CDMA system over an AWGN channel versus μ and β , $SNR = 12.0$ dB, $N = 32$, $m = 15$	99

7.4	SINR of the multistage linear PPIC receiver for an asynchronous CDMA system over an AWGN channel versus β , $SNR = 12.0dB$, $N = 32$, $m = 15$, and $\mu = 0.3$	100
7.5	SINR of the multistage linear PPIC receiver for an asynchronous CDMA system over an AWGN channel versus μ and SNR, $N = 32$, $K = 16$, $m = 15$	101
7.6	SINR of the multistage linear PPIC receiver for an asynchronous CDMA system over an AWGN channel versus μ and SNR, $N = 32$, $K = 16$, $m = 15$, $\mu = 0.5$	102

LIST OF ACRONYMS

AWGN	Additive White Gaussian Noise
BER	Bit Error Rate
CDMA	Code Division Multiple Access
DS-CDMA	Direct-Sequence Code Division Multiple Access
FDMA	Frequency Division Multiple Access
MAI	Multiple Access Interference
ML	Maximum Likelihood
MLMU	Multistage Linear Multiuser
MMSE	Minimum Mean-Squared Error
MSE	Mean Square Error
MUD	Multiuser Detection
PCF	Partial Cancellation Factor
PIC	Parallel Interference Cancellation
PPIC	Partial Parallel Interference Cancellation
SINR	Signal to Interference plus Noise Ratio
SNR	Signal to Noise Ratio
SULB	Single User Lower Bound
SUMF	Single User Matched Filter
TDMA	Time Division Multiple Access

LIST OF SYMBOLS

K	Number of active users
N	Processing gain
β	System load
\mathbf{r}	Received signal vector
\mathbf{A}	Amplitude matrix
\mathbf{s}	Signature sequence of user k
\mathbf{b}	Information data vector
\mathbf{n}	Additive white Gaussian noise vector
H	Hermitian transposition
m	Number of interference cancellation stages
\mathbf{c}	Multistage linear multuser receiver
\mathbf{I}	Identity matrix
μ_i	Partial cancellation factor at stage i
$\boldsymbol{\theta}$	Combination of vector of partial cancellation factors
\mathbf{R}	Covariance matrix
λ	eigenvalue of covariance matrix
\mathbf{S}_1	Signature sequence matrix of interfering users
P	Transmitted power of each user
P/σ^2	Signal to noise ratio (SNR)
$\boldsymbol{\Lambda}$	Vector of the moments
L	Number of resolvable paths in fading channel

Chapter 1

Introduction

1.1 Multiple Access Schemes

The main goal of using multiple access schemes is to share a limited network resource among different users as efficiently as possible. There are three major multiple access techniques, each of which will be explained as follows.

The first type of multiple access technique is Frequency Division Multiple Access (*FDMA*). In this method, the available frequency band is divided among the users and they are supposed to transmit their data simultaneously. Hence, the whole bandwidth consists of non-overlapping slots of frequency and each slot is assigned to one user (Figure 1.1).

The second type of multiple access technique is Time Division Multiple Access (*TDMA*). In this approach, users are aligned in time slots rather than frequency slots. These time slots are non-overlapping to each other to provide no interference from one user to another. Figure 1.1 shows a simple picture of this scheme as well.

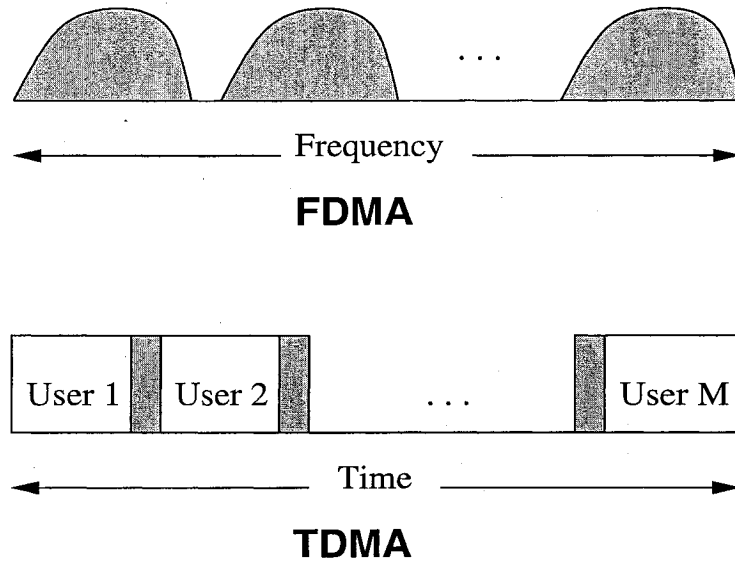


Figure 1.1: FDMA and TDMA techniques.

The main drawback of both FDMA and TDMA is that they are hard-capacity limited. This means that after filling up the available frequency bands or time slots, adding new users is not possible since all the available frequency bands or time slots have already been allocated to the existing users. In order to overcome this issue, Code Division Multiple Access (*CDMA*) as a candidate for providing soft capacity limit has emerged (see [1] and references therein). This technique has become popular in the telecommunications industry due to its exceptional properties such as multipath diversity, narrowband interference rejection and low probability of interception. These properties make CDMA a promising air interface for satellite and wireless communications since all users share the available bandwidth simultaneously. In CDMA, a unique signature sequence or waveform is assigned to each user. Such signature sequences have a bandwidth well beyond that of information data. Coding the data with these signature sequences results in spread spectrum communication. The number of signature sequence pulses (chips) in one bit duration is called the *processing gain*.

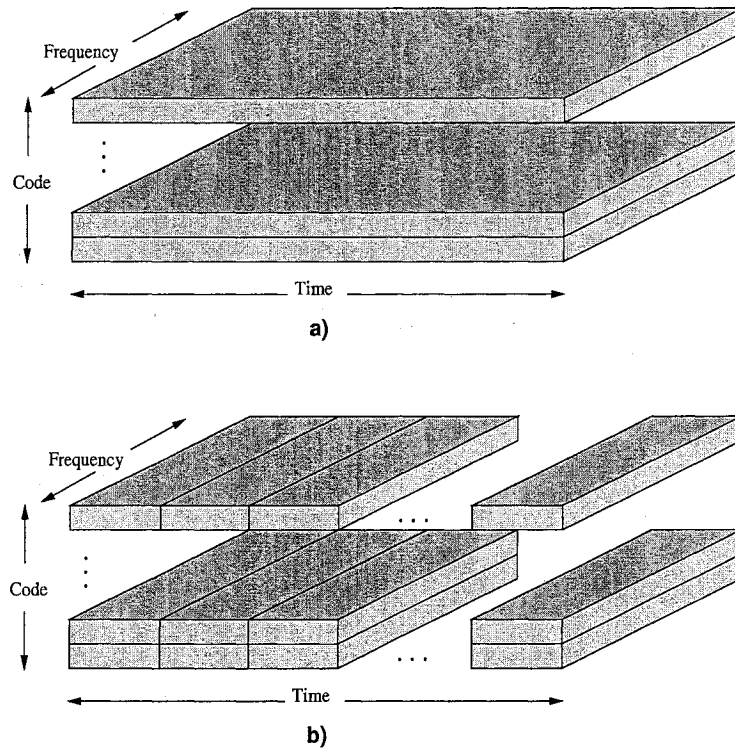


Figure 1.2: A DS-CDMA technique, a) pure CDMA, b) CTDMA (CDMA & TDMA).

Among spread-spectrum techniques, the most popular one is the Direct-Sequence (*DS*-) CDMA, where each active user's data is modulated (multiplied) by a unique signature sequence. Figure 1.2 shows such a scheme where a hybrid technique as a combination of CDMA and TDMA is also introduced as an evolutionary technique since present-day satellite communications are mostly based on the TDMA technique. When the signature sequences in CDMA are not orthogonal, each user will suffer from Multiple Access Interference (*MAI*) originating from other users.

1.2 Multiuser Detection

In order to cancel or mitigate the effect of the MAI, Multiuser Detection (*MUD*) is proposed where the information of other users is employed in order to recover a more accurate version of users' data to be detected or fed to a soft error-control decoder. Several multiuser receivers have been proposed in the literature. In [2], Verdu devised an optimal Maximum Likelihood (*ML*) receiver. The complexity of the ML multiuser receiver grows exponentially with the number of users. This type of receiver becomes too complicated to be implemented, even when the number of active users is low. Therefore, the goal of suppressing or mitigating the MAI has been compromised in order to find schemes that sacrifice optimality for the sake of implementation feasibility. As a result of such endeavors, some suboptimal multiuser receivers have been introduced.

Among suboptimal multiuser receivers, linear multiuser receivers are of special interest since they offer a simple circuitry by applying a linear transformation on the received signal in order to estimate the transmitted data. The most popular linear receivers are decorrelator and Minimum Mean-Squared Error (*MMSE*) receivers. In these receivers, the calculation of the inverse of the covariance matrix of the signature sequences is needed. This calculation becomes more complicated when a large number of users attempts to share the available channel. Therefore, an approximation of the inverse of the covariance matrix by admitting a small degradation in performance merits special attention.

1.3 Large CDMA System

Recently, the analytical studies about linear multiuser receivers such as single-user matched-filter (SUMF), minimum mean-squared error (MMSE) and partial parallel interference cancellation (PPIC) receivers have attracted a lot of attention. These

studies are usually done for a case where the number of active users and the processing gain tend towards infinity while their ratio remains finite. The reason for the attention paid to the large-system scenario is that in this case, the performance has a closed-form expression. Therefore, large-system assumption makes the performance easier to track analytically. The figure of merit to evaluate the performance is the Signal-to-Interference-plus-Noise Ratio (**SINR**). For more details on large CDMA system one can refer to [3]-[27].

1.4 Objective

The objective of this thesis is large-system design and analysis of an efficient multi-stage linear multiuser receiver (MLMU) for different channel conditions.

1.5 Contributions

The contributions to this thesis are as follows:

- We present an explicit formula for the PCF that is a function of the moments of the eigenvalues of the covariance matrix of the signature sequences. By employing the presented method, there is no need to know the number of interference cancellation stages *a priori*. Moreover, the calculated PCFs are applied as they are without any need for ordering. Finally, since the PCFs are explicit functions of moments of the eigenvalues of the covariance matrix, the circuitry will be even simpler.
- We find an explicit expression for the SINR of a CDMA system with a PPIC receiver when the users arrive at the receiver with different power levels by applying a constant PCF.

- We introduce a multistage linear PPIC receiver whose performance will converge to that of the MMSE receiver by applying a variable PCF. We analyze the large-system performance of our proposed scheme and compare it with that of the existing schemes. It will be shown that the large-system performance is a function of the moments of the eigenvalues of the covariance matrix.
- We introduce a new tool for large-system design and analysis of the MLMU receiver for a multipath fading channel by taking a simpler and more efficient approach.
- We evaluate the performance of the multistage PPIC receiver for an asynchronous user CDMA system through numerical simulations of the random covariance matrix of the signature sequences. The investigating receiver is suitable for a satellite system with CDMA or a combination of CDMA and TDMA, which is referred to as slotted CDMA in [28].

1.6 Organization

This thesis continues as follows:

Chapter 2 gives an overview of multistage linear multiuser (MLMU) receivers.

Chapter 3 introduces an easy-to-compute expression for finding the optimum partial cancellation factors (PCF) for the multistage linear partial parallel interference cancellation (PPIC) receiver. These factors are found in a DS-CDMA system over additive white Gaussian noise (AWGN) and frequency-flat fading channels for a large-system case. It will be shown that the expression for the PCF is a function of the moments of the eigenvalues of the covariance matrix, the number of interference cancellation stages, the system load (users per chip) and the signal to noise ratio (SNR).

Chapter 4 introduces an analytical tool for finding the large-system performance of a multistage linear PPIC receiver using the moments of the eigenvalues

of the covariance matrix of the spreading sequences for a CDMA system over a frequency-flat fading channel by applying a constant PCF. The figure of merit to evaluate the performance is the signal-to-interference-plus-noise ratio (SINR) that is calculated under a large-system condition. It is shown that the large-system performance is a function of the system load, the partial cancellation factor (PCF), the number of interference cancellation stages, the SNR and the received powers of the interfering users. Furthermore, for practical applications, the physical meaning of the large system will be described by numerical simulations.

Chapter 5 introduces a multistage linear PPIC receiver with a variable PCF whose performance converges to that of the minimum mean-squared error (MMSE) receiver. It is shown that the large-system performance is a function of the number of the interference cancellation stages, the moments of the eigenvalues of the covariance matrix and the SNR.

Chapter 6 introduces a simple method for large-system design and analysis of a multistage linear multiuser (MLMU) receiver for a DS-CDMA system over a multipath fading channel. Compared to recently-proposed methods, our method offers a more efficient approach to analyzing the large-system performance by introducing a new expression for the covariance matrix of the interference. In addition, a simple multistage scheme to estimate the multipath channel gains is introduced.

Chapter 7 introduces a low-complexity multistage linear PPIC receiver for an asynchronous DS-CDMA system. This receiver is suitable for satellite systems using either CDMA or a combination of time division multiple access (TDMA) and CDMA. The optimum performance of the investigating receiver will be established by adjusting different system parameters such as the partial cancellation factor (PCF), the number of interference cancellation stages, the system load and the SNR.

Finally, Chapter 8 concludes this thesis and gives some directions for further research.

Chapter 2

Multistage Linear Multiuser Receivers: An Overview

In order to avoid the covariance matrix inversion, one of the alternatives is the multistage linear Parallel Interference Cancellation (*PIC*) receiver. This type of receiver is a suitable scheme for mitigating the MAI, taking into consideration the performance, the complexity and the processing delay [29]. In this scheme the MAI affecting each user is removed by taking a parallel approach. However, in most cases, this receiver suffers from a drawback in that a complete cancellation of the MAI, results in a poor performance [30]. This is due to the fact that the information at the early stages is not reliable enough to be used to calculate the MAI. In order to address this problem, an improved version of the PIC receiver, called the Partial Parallel Interference Cancellation (*PPIC*) receiver, is proposed. In this scheme, a fraction of the MAI is cancelled in each stage by introducing a Partial Cancellation Factor (*PCF*). It has been shown ([31]-[36]) that the PPIC receiver performs considerably better than the PIC receiver.

2.1 Computing PCFs for Multistage PPIC Receiver

The value of the PCF has a crucial impact on the performance of the PPIC receiver such that a wrong selection of this factor results in a performance inferior even to that of the Single-User Matched Filter (**SUMF**). Nevertheless, by choosing an appropriate value for PCF, the multistage PPIC receiver can be directed to provide a performance converging to that of the decorrelator ([37]-[39]) or the minimum mean-squared error (MMSE) receiver [40].

In [41], [42] and [43], interesting methods for finding the optimum PCFs were proposed. It was shown that the empirical and theoretical results are almost the same. However, there is a problem in that two stages of interference cancellation are not sufficient, especially for the cases where the **system load** (users per chip) is high. In [44] an expression for the PCF when the number of interference cancellation stages is known *a priori* was derived. The criterion to find the expression for the optimum PCF was to minimize the Mean Square Error (**MSE**) between the m th stage output and the transmitted data. Therefore, in this case, the PCFs for all stages would be ready simultaneously. This approach has some problems. First of all, the number of cancellation stages should be known *a priori*. Secondly, there will be a performance fluctuation in the middle stages and, in order to have a monotonic improvement in performance, the PCFs should be ordered. This is another issue which will make the circuitry more complex. Finally, PCFs are found by using some matrix inversion. This results in even more complexity.

2.1.1 System Model

A K -user synchronous CDMA system with a binary antipodal modulation is considered. All vectors and matrices are shown in boldface throughout this thesis. The processing gain is denoted by N . The baseband received signal sampled at chip rate

is shown as

$$\mathbf{r} = \mathbf{A}\mathbf{b} + \mathbf{n} \quad (2.1)$$

where \mathbf{r} is an $N \times 1$ received vector defined as $\mathbf{r} = [r_1, r_2, \dots, r_N]^H$, $\mathbf{A} = [a_1\mathbf{s}_1, a_2\mathbf{s}_2, \dots, a_K\mathbf{s}_K]$ is an $N \times K$ matrix including the amplitude a_k and the signature sequence \mathbf{s}_k for any user k with $\mathbf{s}_k = 1/\sqrt{N}[s_{k1}, s_{k2}, \dots, s_{kN}]^H$ and $\mathbf{b} = [b_1, b_2, \dots, b_K]^H$ is the $K \times 1$ transmitted data vector. The $N \times 1$ noise vector is additive white Gaussian noise (AWGN) defined as $\mathbf{n} = [n_1, n_2, \dots, n_N]^H$ with zero mean and variance of σ^2 ; and $[\cdot]^H$ denotes the Hermitian transposition. The multistage linear PPIC receiver (Figure 2.1) applies a linear transformation on the received signal such that the output at the m th stage is $\mathbf{b}^{(m)} = \mathbf{C}_m^H \mathbf{r}$ where \mathbf{C}_m^H is a $K \times N$ filter defined as [40]

$$\mathbf{C}_m^H = \left[\mathbf{I} - \prod_{i=1}^m (\mathbf{I} - \mu_i (\mathbf{R} + \sigma^2 \mathbf{I})) \right] (\mathbf{R} + \sigma^2 \mathbf{I})^{-1} \mathbf{A}^H \quad (2.2)$$

where \mathbf{I} is a $K \times K$ identity matrix and μ_i is the PCF at stage i . The $K \times K$ matrix $\mathbf{R} = \mathbf{A}^H \mathbf{A}$ is called the covariance matrix. It can be shown that

$$\mathbf{R} = \mathbf{U}\mathbf{\Lambda}\mathbf{U}^H \quad (2.3)$$

with $\mathbf{U}\mathbf{U}^H = \mathbf{I}$ and $\mathbf{\Lambda} = \text{diag}[\lambda_1, \lambda_2, \dots, \lambda_K]$ where λ_k are the eigenvalues of the covariance matrix for $k = 1, 2, \dots, K$. If \mathbf{R} is full rank, which corresponds to the case where the signature sequences from all K users are linearly independent, then \mathbf{R} has only positive eigenvalues.

2.1.2 Derivation of PCFs

It is found in [44] that the *Mean Square Error* (MSE) is

$$J^{(m)}(\mu_i, \alpha) = J_{MMSE} + J_{ex}^{(m)}(\mu_i, \alpha) \quad (2.4)$$

where

$$J_{MMSE} = \sum_{k=1}^K \frac{\sigma^2}{\lambda_k + \sigma^2} \quad (2.5)$$

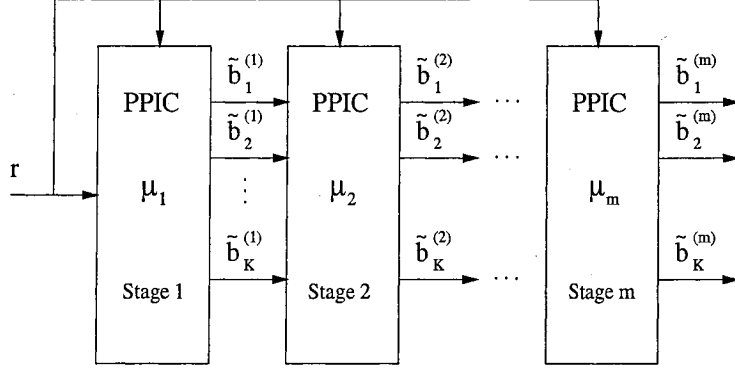


Figure 2.1: An m -stage PPIC receiver.

and

$$J_{ex}^{(m)}(\mu_i, \alpha) = \sum_{k=1}^K \frac{\lambda_k \varphi_k}{\gamma_k^2} \left| \frac{\sigma^2 - \alpha}{\varphi_k} - \prod_{i=1}^m (1 - \mu_i \gamma_k) \right|^2 \quad (2.6)$$

with $\varphi_k = \lambda_k + \sigma^2$ and $\gamma_k = \lambda_k + \alpha$. The optimization criterion is to minimize the MSE. If we assume that $\alpha = \sigma^2$ (MMSE receiver), then

$$J_{ex}^{(m)}(\mu_i, \sigma^2) = \sum_{k=1}^K \frac{\lambda_k}{\varphi_k} \left| \prod_{i=1}^m (1 - \mu_i \varphi_k) \right|^2 \quad (2.7)$$

if the coefficients are identical

$$J_{ex}^{(m)}(\mu_i, \sigma^2) = \sum_{k=1}^K \frac{\lambda_k}{\varphi_k} (1 - \mu \varphi_k)^{2m} \quad (2.8)$$

differentiating with respect to μ yields

$$\frac{\partial J_{ex}^{(m)}(\mu, \alpha)}{\partial \mu} = -2m \sum_{k=1}^K \lambda_k (1 - \mu \varphi_k)^{2m-1} \quad (2.9)$$

the second derivative is

$$\frac{\partial^2 J_{ex}^{(m)}(\mu, \alpha)}{\partial \mu^2} = \sum_{k=1}^K (2m)(2m-1) \lambda_k \varphi_k (1 - \mu \varphi_k)^{2m-2} > 0 \quad (2.10)$$

where it shows that the found μ always gives the minimum. Equating (2.9) to zero, we can find that

$$(1 - \mu \varphi_k) = 0 \quad (2.11)$$

which gives

$$\mu = \frac{1}{\lambda_k + \sigma^2} \quad (2.12)$$

For the case with a variable PCF, assume that for m stage we have $\mu = (\mu_1, \mu_2, \dots, \mu_m)$. Denote

$$x_i = (-1)^i \sum_{i=1}^m \prod_i \quad (2.13)$$

where $\sum_{i=1}^m \prod_i$ means the sum of the i -ary product of μ_i for $i = 1, 2, \dots, m$. This means that

$$\begin{aligned} x_1 &= (-1) (\mu_1 + \mu_2 + \dots + \mu_m) \\ x_2 &= (-1)^2 (\mu_1 \mu_2 + \mu_1 \mu_3 + \dots + \mu_{m-1} \mu_m) \\ &\vdots \\ x_m &= (-1)^m (\mu_1 \mu_2 \dots \mu_{m-1} \mu_m) \end{aligned} \quad (2.14)$$

It can be shown that

$$\prod_{j=1}^m (1 - \mu_j \varphi_k) = 1 + \sum_{i=1}^{(m)} x_i \varphi_k^i \quad (2.15)$$

Define

$$t_k^{(i)} = \prod_{j=1}^{i-1} (1 - \mu_j \gamma_k) = 1 + \sum_{j=1}^{(i-1)} x_j \gamma_k^j = 1 + \sum_{j=1}^{(i-1)} x_j \phi_k^j \quad (2.16)$$

Differentiating 2.6 with respect to μ_i yields

$$\frac{\partial J_{ex}^{(m)}(\mu_i, \alpha)}{\partial \mu} = \sum_{k=1}^K \frac{\lambda_k \phi_k}{\gamma_k} \left[\frac{\sigma^2 - \alpha}{\phi_k} t_k^{(i)} - (1 - \mu_i \gamma_k) \left| t_k^{(i)} \right|^2 \right] \quad (2.17)$$

equating this equation to zero gives the optimum μ_i as

$$\mu_i = \frac{\sum_{k=1}^K \frac{\lambda_k}{\gamma_k} \left[\phi_k \cdot \left| t_k^{(i)} \right|^2 - (\sigma^2 - \alpha) \cdot \left| t_k^{(i)} \right|^2 \right]}{\sum_{k=1}^K \lambda_k \phi_k \cdot \left| t_k^{(i)} \right|^2} \quad (2.18)$$

Therefore, in order to calculate the weights for an m -stage PPIC receiver, the $2m$ moments of the eigenvalues of covariance matrix are needed.

2.2 Computing SINR for Multistage PPIC Receivers

In the previous section, it is not possible to have a closed-form expression for the SINR. In order to do so, the received signal can be decomposed to the desired user, the MAI and the background noise. In [45], a multistage linear PPIC receiver with a constant PCF was introduced, whose performance converges to that of the MMSE receiver when synchronous users arrive at the receiver with the same power level. However, as is seen in [46], it is not clear how to calculate the optimum PCF analytically when the users undergo fading. In addition, given that the optimum PCF is available, a large number of interference cancellation stages is needed in order to force the performance to converge to that of the MMSE receiver. In [4] and [5], a polynomial multiuser receiver using the Gram-Schmidt orthogonalization algorithm was proposed.

2.2.1 System Model

The baseband-sampled received signal is given by

$$\mathbf{r} = Ab_1\mathbf{s}_1 + \sum_{k=2}^K Ab_k\mathbf{s}_k + \mathbf{n} \quad (2.19)$$

where the first, the second, and the third terms in (2.19) are the useful signal, the multiple access interference (MAI), and the background noise, respectively. Furthermore, $E[Ab_k] = 0$ and $E[Ab_k^2] = P$ where P is the transmitted power of each user. A linear multiuser receiver for user 1 (as the one of interest) applies a linear transformation on the received signal, *i.e.*, $\tilde{b}_1 = \mathbf{c}_1^H \cdot \mathbf{r}$ where \tilde{b}_1 is the soft decision on first user's data and $\mathbf{c}_1 \in \mathbb{R}^N$. The signal-to-interference-plus-noise ratio (SINR) in general is defined as the ratio of the useful signal to the MAI plus noise at the

receiver end. Therefore, SINR for user 1 becomes

$$\begin{aligned} SINR_1 &= \frac{E[(Ab_1\mathbf{c}_1^H.\mathbf{s}_1)^2]}{E[(\sum_{k=2}^K Ab_k\mathbf{c}_1^H.\mathbf{s}_k)^2] + E[(\mathbf{c}_1^H.\mathbf{n})^2]} \\ &= \frac{P.(\mathbf{c}_1^H.\mathbf{s}_1)^2}{\sum_{k=2}^K P.[(\mathbf{c}_1^H.\mathbf{s}_k)^2 + \sigma^2(\mathbf{c}_1^H.\mathbf{c}_1)]} \end{aligned} \quad (2.20)$$

or in matrix format

$$SIR_1 = \frac{P.(\mathbf{c}_1^H.\mathbf{s}_1)^2}{\mathbf{c}_1^H(P\mathbf{S}_1\mathbf{S}_1^H + \sigma^2\mathbf{I})\mathbf{c}_1} \quad (2.21)$$

where \mathbf{S}_1 is an $N \times (K - 1)$ matrix of the spreading sequences of the $(K - 1)$ synchronous interferers, *i.e.*,

$$\mathbf{S}_1 = [\mathbf{s}_2, \mathbf{s}_3, \dots, \mathbf{s}_K] \quad (2.22)$$

and \mathbf{I} is an $N \times N$ identity matrix. For SUMF and MMSE receivers, performance analysis has been established in [47], [48] and [49] for different channel situations.

2.2.2 MMSE-Based Multistage Linear PPIC Receiver with a constant PCF

In this case, the performance of the multistage linear PPIC receiver tends to converge to that of the MMSE receiver by applying a constant PCF to all interference cancellation stages. The m -stage receiver is defined as [45]

$$\mathbf{c}_{1,m}^{PPIC} = \mu \left(\sum_{i=0}^m \left[\mathbf{I} - \mu \left(\mathbf{S}_1\mathbf{S}_1^H + \frac{\sigma^2}{P}\mathbf{I} \right) \right]^i \right) \mathbf{s}_1 \quad (2.23)$$

where the subscripts in $\mathbf{c}_{1,m}^{PPIC}$ denote the user of interest and the number of interference cancellation stages, respectively. The constant μ is called the partial cancellation factor (PCF). The $N \times N$ matrix $\mathbf{R} = \mathbf{S}_1\mathbf{S}_1^H$ is the covariance matrix. Finally, P/σ^2 is defined to be the signal to noise ratio (SNR). The SINR for this receiver using [45] becomes

$$SINR_{1,m}^{PPIC} = \frac{(\eta_m)^2}{\nu_m} \quad (2.24)$$

where

$$\eta_m = \sum_{i=0}^m (-\mu)^i \sum_{j=0}^i \left(\frac{\sigma^2}{P} - \frac{1}{\mu} \right)^{i-j} \binom{i}{j} M_j, \quad (2.25)$$

$$\nu_m = \sum_{i=0}^m \sum_{j=0}^m (-\mu)^{i+j} \sum_{l=0}^{i+j} \left(\frac{\sigma^2}{P} - \frac{1}{\mu} \right)^{i+j-l} \binom{i+j}{l} \left(M_{l+1} + \frac{\sigma^2}{P} M_l \right) \quad (2.26)$$

with

$$M_i = \mathbf{s}_1^H (\mathbf{S}_1 \mathbf{S}_1^H)^i \mathbf{s}_1. \quad (2.27)$$

As will be seen in Section 5.2, this receiver suffers from the following drawbacks. First of all, the calculation of the optimum PCF for different channel situations is not an easy task [46]. Secondly, given that the optimum PCF is available, a large number of interference cancellation stages is needed in order to force the performance of this receiver to converge to that of the MMSE receiver.

2.2.3 Decorrelator-Based Multistage Linear PPIC Receiver with a Variable PCF

In [50], a simple polynomial multiuser receiver was proposed whose performance converges to that of the decorrelator receiver. The advantage of this receiver is that the performance of the decorrelator receiver is achieved with fewer stages of interference cancellation. However, this receiver suffers from a drawback in the sense that since it eventually provides the performance of a decorrelator receiver, its performance degrades very fast when a large number of active users attempts to share the available channel simultaneously. The performance of this receiver will converge to that of the decorrelator receiver by applying a variable PCF to different interference cancellation stages. The optimum PCF and the SINR of this receiver were found in [50] as

$$\boldsymbol{\theta}_{opt} = \frac{\mathbf{R}^{-1} \mathbf{M}}{a_1^2 \mathbf{M}^H \mathbf{R}^{-1} \mathbf{M} + 1} \quad (2.28)$$

and

$$\text{SINR} = a_1^2 \mathbf{M}^H \mathbf{R}^{-1} \mathbf{M} \quad (2.29)$$

where

$$\boldsymbol{\theta} = [\theta_0, \theta_1, \dots, \theta_m] \quad (2.30)$$

with

$$\begin{aligned} \theta_0 &= (-1) (\mu_0 + \mu_1 + \dots + \mu_m) \\ \theta_1 &= (-1)^2 (\mu_0 \mu_1 + \mu_0 \mu_2 + \dots + \mu_{m-1} \mu_m) \\ &\vdots \\ \theta_m &= (-1)^{m+1} (\mu_0 \mu_1 \dots \mu_{m-1} \mu_m). \end{aligned} \quad (2.31)$$

The $(m+1) \times 1$ matrix \mathbf{M} is defined as

$$\mathbf{M} = \begin{bmatrix} M_0 \\ M_1 \\ \vdots \\ M_m \end{bmatrix} \quad (2.32)$$

where M_i is defined according to (2.27) and the matrix \mathbf{R} is an $(m+1) \times (m+1)$ Hankel matrix with the first column as

$$[M_1 + \frac{\sigma^2}{P} M_0, M_2 + \frac{\sigma^2}{P} M_1, \dots, M_{m+1} + \frac{\sigma^2}{P} M_m]^H \quad (2.33)$$

and the last row as

$$[M_{m+1} + \frac{\sigma^2}{P} M_m, M_{m+2} + \frac{\sigma^2}{P} M_{m+1}, \dots, M_{2m+1} + \frac{\sigma^2}{P} M_{2m}] \quad (2.34)$$

As will be seen in Section 5.2, the performance of this receiver degrades very fast when the system is highly loaded.

2.3 Multiuser Detection and Channel Estimation over Multipath Fading Channels

As was mentioned earlier, due to its multipath diversity, the CDMA technique is a promising air interface for wireless communications since real wireless channels deliver a multitude of replicas of the transmitted signal to the receiver end. In [50] and [51], the Multistage Linear Multi-User (*MLMU*) receiver was proposed for a multipath fading channel.

2.3.1 System Model

The system model is formulated for K synchronous users where each user undergoes L distinct paths and the processing gain is N . The discrete-time baseband received vector at time p can be written as

$$\mathbf{r}(p) = \sum_{k=1}^K b_k(p) \sum_{l=1}^L \sqrt{P} a_{kl}(p) \mathbf{s}_{kl}(p) + \mathbf{n}(p) \quad (2.35)$$

where $\mathbf{r}(p)$ is an $N \times 1$ received vector, $b_k(p)$ is the information data of user k at time p , P is the transmitted power that is assumed to be the same for all users and all paths, a_{kl} is the channel gain of user k for path l , \mathbf{s}_{kl} is the signature sequence of user k for path l ; and finally, $\mathbf{n}(p)$ is an $N \times 1$ additive white Gaussian noise (AWGN) vector. It is assumed that $E[b_k(p)] = 0$, $E[b_k(p)b_k^*(p)] = 1$, $E[\mathbf{n}(p)] = \mathbf{0}$, $E[\mathbf{n}(p)\mathbf{n}^H(p)] = \sigma^2\mathbf{I}$ where $\mathbf{0}$ is an $N \times 1$ zero vector and \mathbf{I} is an $N \times N$ identity matrix. The signature sequence $\mathbf{s}_{kl}(p)$ is an N -dimensional vector of independent and identically distributed (i.i.d.) random variables with zero mean and variance of $1/N$. We may drop the index p by considering a one-bit observation window. Therefore, the received signal would be

$$\mathbf{r} = \sum_{k=1}^K b_k \sum_{l=1}^L \sqrt{P} a_{kl} \mathbf{s}_{kl} + \mathbf{n} \quad (2.36)$$

or in matrix format,

$$\mathbf{r} = \sqrt{P}\mathbf{S}\mathbf{A}^{1/2}\mathbf{b} + \mathbf{n} \quad (2.37)$$

where $\mathbf{r} = [r^{(1)}, r^{(2)}, \dots, r^{(N)}]^H$; $\mathbf{S} = [\mathbf{s}_1, \mathbf{s}_2, \dots, \mathbf{s}_K]$; $\mathbf{s}_k = [s_{k1}, s_{k2}, \dots, s_{kL}]$; $\mathbf{s}_{kl} = [s_{kl}^{(1)}, s_{kl}^{(2)}, \dots, s_{kl}^{(N)}]^H$; $\mathbf{A}^{1/2} = \text{diag}[\mathbf{a}_1, \mathbf{a}_2, \dots, \mathbf{a}_K]$ with $\mathbf{a}_k = [a_{k1}, a_{k2}, \dots, a_{kL}]^H$ for $k = 1, 2, \dots, K$ and $l = 1, 2, \dots, L$. Finally, $\mathbf{b} = [b_1, b_2, \dots, b_K]^H$ and $\mathbf{n} = [n^{(1)}, n^{(2)}, \dots, n^{(N)}]^H$ where $(\cdot)^H$ denotes the Hermitian transposition.

2.3.2 Data Estimation

The MMSE demodulator for the first user that is assumed to be the one of interest with a small modification is [48]

$$\mathbf{c}_1 = \left(\mathbf{S}_1 \mathbf{A}_1 \mathbf{S}_1^H + \frac{\sigma^2}{P} \mathbf{I} \right)^{-1} \mathbf{s}_1 \mathbf{a}_1. \quad (2.38)$$

where $\mathbf{S}_1 = [\mathbf{s}_2, \dots, \mathbf{s}_K]$; $\mathbf{A}_1 = \text{diag}(E[\mathbf{a}_2 \mathbf{a}_2^H], \dots, E[\mathbf{a}_K \mathbf{a}_K^H])$; and the signal to noise ratio is defined as $SNR = P/\sigma^2$ per user per path. By separating the contribution of the first user, the received signal can be written as

$$\mathbf{r} = b_1 \mathbf{s}_1 \mathbf{a}_1 + \mathbf{S}_1 \mathbf{A}_1^{1/2} \mathbf{b}_1 + \mathbf{n} \quad (2.39)$$

where b_1 is the information bit of user 1, $\mathbf{A}_1^{1/2} = \text{diag}[\mathbf{a}_2, \dots, \mathbf{a}_K]$, and $\mathbf{b}_1 = [b_2, \dots, b_K]$. The decision statistic for user 1 is

$$\tilde{b}_1 = \mathbf{c}_1^H \cdot \mathbf{r} = \mathbf{a}_1^H \mathbf{s}_1^H \left(\mathbf{S}_1 \mathbf{A}_1 \mathbf{S}_1^H + \frac{\sigma^2}{P} \mathbf{I} \right)^{-1} \cdot \mathbf{r}. \quad (2.40)$$

2.3.3 Channel Estimation

Similar to [48] and [51], we only consider estimation of the channel gains and the intersymbol interference is neglected. When estimating channel parameters, the training symbols and the distribution of the channel gains are assumed to be known to the estimator. An estimation window of τ symbols is considered. The received

signal can be shown as ([48] and [51])

$$\bar{\mathbf{r}} = \tau^{1/2} \bar{\mathbf{S}} \mathbf{a} + \bar{\mathbf{n}} \quad (2.41)$$

where

$$\bar{\mathbf{r}} = [\mathbf{r}^H(1), \mathbf{r}^H(2), \dots, \mathbf{r}^H(\tau)]^H \quad (2.42)$$

$$\bar{\mathbf{S}} = \tau^{-1/2} [\mathbf{S}^H(1), \mathbf{S}^H(2), \dots, \mathbf{S}^H(\tau)]^H \quad (2.43)$$

$$\mathbf{a} = [a_{11}, a_{12}, \dots, a_{1L}, \dots, a_{K1}, a_{K2}, \dots, a_{KL}]^H \quad (2.44)$$

$$\bar{\mathbf{n}} = [\mathbf{n}^H(1), \mathbf{n}^H(2), \dots, \mathbf{n}^H(\tau)]^H \quad (2.45)$$

$$\underline{\mathbf{r}}(p) = [r^{(1)}(p), r^{(2)}(p), \dots, r^{(N)}(p)]^H \quad (2.46)$$

$$\mathbf{S}(p) = [b_1(p)\mathbf{s}_{11}(p), \dots, b_1(p)\mathbf{s}_{1L}(p), \dots, b_K(p)\mathbf{s}_{K1}(p), \dots, b_K(p)\mathbf{s}_{KL}(p)] \quad (2.47)$$

$$\underline{\mathbf{n}}(p) = [n^{(1)}(p), n^{(2)}(p), \dots, n^{(N)}(p)]^H \quad (2.48)$$

with $p = 1, 2, \dots, \tau$. The estimated channel gain is

$$\tilde{\mathbf{a}} = \mathbf{c}^H \bar{\mathbf{r}} \quad (2.49)$$

where \mathbf{c} is the estimator vector. The covariance matrix of the MSE between the estimated and the original channel gains is

$$\mathbf{MSE} = E[(\mathbf{c}^H \bar{\mathbf{r}} - \mathbf{a})(\mathbf{c}^H \bar{\mathbf{r}} - \mathbf{a})^H] \quad (2.50)$$

Minimizing the MSE with respect to \mathbf{c} with a small modification yields [48]

$$\mathbf{c} = \tau^{-1/2} \left(\bar{\mathbf{S}} \mathbf{A} \bar{\mathbf{S}}^H + \frac{1}{\tau} \frac{\sigma^2}{P} \mathbf{I} \right)^{-1} \bar{\mathbf{S}} \mathbf{A} \quad (2.51)$$

where $\mathbf{A} = E[\mathbf{a}\mathbf{a}^H]$ is the channel covariance matrix. The expression of the normalized MSE for a_{11} (which is the (1,1) element of the MSE) is [48]

$$MSE_{11} = \frac{1}{1 + \Gamma} \quad (2.52)$$

where

$$\Gamma = \bar{\mathbf{s}}_{11}^H \left(\bar{\mathbf{S}}_{11} \mathbf{A}_{11} \bar{\mathbf{S}}_{11}^H + \frac{1}{\tau} \frac{\sigma^2}{P} \mathbf{I} \right)^{-1} \bar{\mathbf{s}}_{11} \quad (2.53)$$

and

$$\bar{\mathbf{S}}_{11} = [\bar{s}_{12}, \dots, \bar{s}_{1L}, \dots, \bar{s}_{K1}, \dots, \bar{s}_{KL}] \quad (2.54)$$

$$\mathbf{A}_{11} = E[\mathbf{a}_{11}\mathbf{a}_{11}^H] \quad (2.55)$$

$$\mathbf{a}_{11} = [a_{12}, \dots, a_{1L}, a_{21}, \dots, a_{2L}, a_{K1}, \dots, a_{KL}]^H \quad (2.56)$$

with

$$\bar{s}_{kl} = \tau^{-1/2}[b_k(1)\mathbf{s}_{kl}^H(1), \dots, b_k(\tau)\mathbf{s}_{kl}^H(\tau)]^H. \quad (2.57)$$

2.4 Asynchronous CDMA Systems

Concerning the asynchronous CDMA system, in [45], an expression for the SINR of a multistage linear PPIC receiver with a user-synchronous CDMA system over an Additive White Gaussian Noise (**AWGN**) channel was derived. In that paper, the linear multistage receiver is based on the first-order stationary linear iterative method that has only one PCF. Generalization of the proposed receiver in [45] to an asynchronous case is possible along the lines of [49], [52] and [53]. In [49], the performance of the MMSE receiver for a symbol-asynchronous but chip-synchronous CDMA system over an AWGN channel was found. A symbol-asynchronous but chip-synchronous CDMA system is a system where the relative delays are assumed to be multiples of chip duration. The main idea in [49] is that the $(K - 1)$ asynchronous users interfering with any given user are transformed into $2(K - 1)$ synchronous interferers in order to make the asynchronous system more easy-to-track. This was done by extending the random covariance matrix of signature sequences in the SINR expression for the MMSE receiver.

2.4.1 System Model

A K -user asynchronous CDMA system under perfect power control is assumed. A binary antipodal modulation is applied and the processing gain is N . The continuous-time received signal for a $(2M + 1)$ bit sequence can be shown as

$$r(t) = \sum_{k=1}^K \sum_{i=-M}^M \sqrt{P} b_k[i] s_k(t - iT - \tau_k) + n(t) \quad (2.58)$$

where $b_k[i]$ is the transmitted symbol of user k at time $iT < t < (i + 1)T$ and P is the transmitted power that is assumed to be the same for all users. The s_k is the unit-energy spreading sequence of user k defined as

$$s_k = \frac{1}{\sqrt{N}} [s_{k1}, s_{k2}, \dots, s_{kN}]^H \quad (2.59)$$

where the independent and identically distributed (i.i.d) random variables s_{ki} take values ± 1 for $k = 1, 2, \dots, K$ and $i = 1, 2, \dots, N$, and τ_k is the relative delay of user k . Figure 2.2 shows the timing diagram where in this figure it is assumed that $\tau_1 < \tau_2 < \dots < \tau_K < T$. In the special case of synchronous, we have $\tau_1 = \tau_2 = \dots = \tau_K = 0$. The noise $n(t)$ is an additive white Gaussian noise (AWGN) with zero mean and variance of σ^2 .

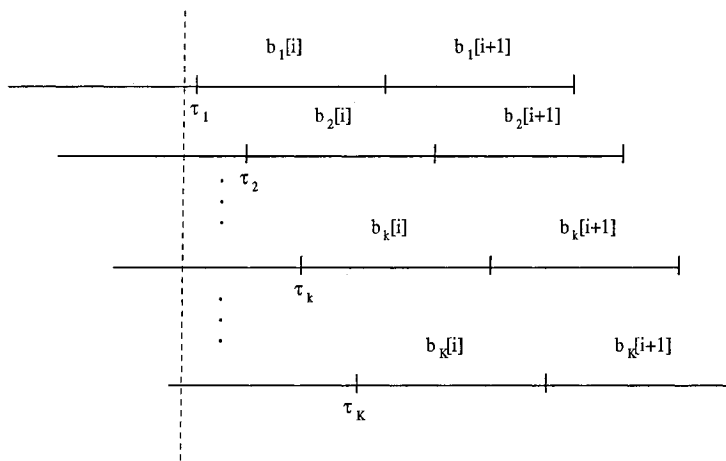


Figure 2.2: Asynchronous CDMA timing diagram.

The discrete-time model used for the asynchronously received signal is based on what was proposed in [49]. Figure 2.3 shows the effect of any general interferer k on user 1. Assume that the first user is the one of interest and the observation window is one-symbol duration (N chips). The sampled received signal is given by

$$\mathbf{r} = \sqrt{P}b_1\mathbf{s}_1 + \sum_{k=2}^K \sqrt{P}x_k\mathbf{u}_k + \sum_{k=2}^K \sqrt{P}y_k\mathbf{v}_k + \mathbf{n} \quad (2.60)$$

where x_k and y_k are two consecutive symbols of user k that overlap with user 1 in the observation window and $\mathbf{u}_k, \mathbf{v}_k$ are the spreading sequences of x_k and y_k , respectively. Denote by d_k the random variable representing the relative delay, in chips for the k th user with respect to user 1. The first d_k elements of \mathbf{u}_k are the last d_k elements of \mathbf{s}_k and the rest are zero. Likewise, the first d_k elements of \mathbf{v}_k are zero and the last $N - d_k$ elements are the first $N - d_k$ elements of \mathbf{s}_k . Such a system is called symbol-asynchronous, chip-synchronous system.

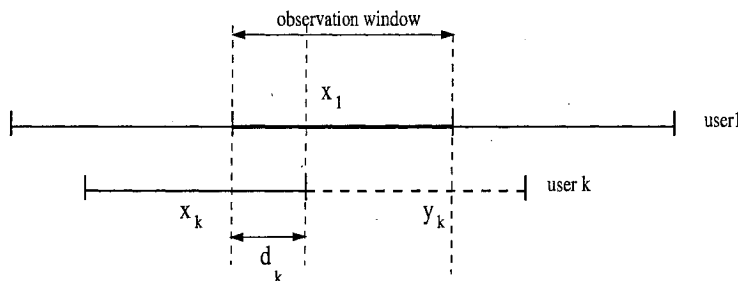


Figure 2.3: The effect of interferer k on user 1 in an asynchronous CDMA.

As a result, by separating each interfering user's signature \mathbf{s}_k into two signatures \mathbf{u}_k and \mathbf{v}_k , the problem is translated into the case with $2(K - 1)$ synchronous interferers. A linear multiuser receiver for user 1 (as the one of interest) applies a linear transformation on the received signal, i.e., $\tilde{b}_1 = \mathbf{c}_1^H \cdot \mathbf{r}$ where \tilde{b}_1 is the soft decision on first user's data and $\mathbf{c}_1 \in \mathbb{R}^N$.

The SINR for the first user is

$$\begin{aligned} SINR_1 &= \frac{E[(\sqrt{P}b_1\mathbf{c}_1^H\mathbf{s}_1)^2]}{E[(\sum_{k=2}^K\sqrt{P}x_k\mathbf{c}_1^H\mathbf{u}_k)^2] + E[(\sum_{k=2}^K\sqrt{P}y_k\mathbf{c}_1^H\mathbf{v}_k)^2] + E[(\mathbf{c}_1^H\mathbf{n})^2]} \\ &= \frac{P.(\mathbf{c}_1^H.\mathbf{s}_1)^2}{\sum_{k=2}^K P.[(\mathbf{c}_1^H.\mathbf{u}_k)^2 + (\mathbf{c}_1^H.\mathbf{v}_k)^2] + \sigma^2(\mathbf{c}_1^H.\mathbf{c}_1)} \end{aligned} \quad (2.61)$$

or in matrix format

$$SINR_1 = \frac{P.(\mathbf{c}_1^H\mathbf{s}_1)^2}{\mathbf{c}_1^H(PS_1\mathbf{S}_1^H + \sigma^2\mathbf{I})\mathbf{c}_1} \quad (2.62)$$

where \mathbf{S}_1 is an $N \times 2(K-1)$ matrix of the spreading sequences of the $(K-1)$ asynchronous interferers or $2(K-1)$ equivalent synchronous interferers, i.e.,

$$\mathbf{S}_1 = [\mathbf{u}_2, \mathbf{u}_3, \dots, \mathbf{u}_K, \mathbf{v}_2, \mathbf{v}_3, \dots, \mathbf{v}_K] \quad (2.63)$$

and \mathbf{I} is an $N \times N$ identity matrix. For the synchronous case we have

$$SINR_1 = \frac{P.(\mathbf{c}_1^H\mathbf{s}_1)^2}{P.\sum_{k=2}^K(\mathbf{c}_1^H\mathbf{s}_k)^2 + \sigma^2.(\mathbf{c}_1^H\mathbf{c}_1)} \quad (2.64)$$

2.5 Large CDMA System

For a large-system scenario, as K and N tend towards infinity but their ratio (system load) remains finite (i.e., $K, N \rightarrow \infty$, $\beta = K/N < \infty$), the moments of the eigenvalues of the covariance matrix will have closed-form expression. The asymptotic *Probability Density Function* (p.d.f) for eigenvalues of the covariance matrix (AWGN channel) becomes [20]

$$f(\lambda) = \frac{1}{2\pi\beta\lambda} \sqrt{(\lambda - \lambda_{min})(\lambda_{max} - \lambda)} \quad \lambda_{min} < \lambda < \lambda_{max} \quad (2.65)$$

where $\lambda_{min} = (1 - \sqrt{\beta})^2$ and $\lambda_{max} = (1 + \sqrt{\beta})^2$. The r th moment is shown to be a polynomial in N and K that can be expressed as

$$M_r = \sum_{j=0}^{r-1} \frac{1}{j+1} \binom{r}{j} \binom{r-1}{j} (\beta)^j \quad (2.66)$$

Having changed the situation from an equal-power to a fading case, the definition of the covariance matrix will change. In this case, unlike the case introduced in [45], the covariance matrix is a function of the received powers of the interferers as well. For a fading case, the moments of the eigenvalues of the covariance matrix were found in [54] that will be explained in more details in this section. In order to do so, it can be shown that [45]

$$M_i \simeq \text{trace}(\mathbf{A}^H \mathbf{A})^i = E[\lambda^i]. \quad (2.67)$$

where $E[\lambda^i]$ is the i th moment of the eigenvalues of the covariance matrix defined as

$$E[\lambda^i] = \sum_{j=1}^i \beta^j \sum_{m_1+\dots+m_j=m} c(m_1, \dots, m_j) E[\Delta^{m_1}] \dots E[\Delta^{m_j}] \quad (2.68)$$

where Δ is a nonnegative random variable whose distribution is the limit distribution of \mathbf{A} , and

$$c(m_1, m_2, \dots, m_j) = \frac{m!}{(m-j+1)! f(m_1, m_2, \dots, m_j)} \quad (2.69)$$

where $f(m_1, m_2, \dots, m_j)$ is defined below:

Take a vector of j integers (m_1, m_2, \dots, m_j) . Partition the indices $1, 2, \dots, j$ into l sets of S_1, S_2, \dots, S_l where each set consists of those indices having a given value v_q . Denote the cardinality of set S_i by f_i for $i = 1, 2, \dots, l$. Then the function $f(m_1, m_2, \dots, m_j)$ is defined as:

$$f(m_1, m_2, \dots, m_j) = f_1! f_2! \dots f_l! \quad (2.70)$$

As an example, for a vector of 5 integers $(5, 2, 3, 2, 7)$ the related sets and functions are defined, respectively as $S_1 = \{1\}$, $f_1 = 1$, $S_2 = \{2, 4\}$, $f_2 = 2$, $S_3 = \{3\}$, $f_3 = 1$, $S_4 = \{5\}$, $f_4 = 1$.

Table 2.1 shows the required coefficients to calculate the moments for $i = 1, 2, 3, 4$, and 5.

Table 2.1: Coefficients of Equations (2.68) and (2.69) for $i = 1, 2, 3, 4$, and 5.

i	j	m_1	m_2	m_3	m_4	m_5	$f(m_1, m_2, \dots, m_j)$
1	1	1	0	0	0	0	1!
2	1	2	0	0	0	0	1!
2	2	1	1	0	0	0	2!
3	1	3	0	0	0	0	1!
3	2	1	2	0	0	0	1!1!
3	3	1	1	1	0	0	3!
4	1	4	0	0	0	0	1!
4	2	1	3	0	0	0	1!1!
4	2	2	2	0	0	0	2!
4	3	1	1	2	0	0	2!1!
4	4	1	1	1	1	0	4!
5	1	5	0	0	0	0	1!
5	2	1	4	0	0	0	1!1!
5	2	2	3	0	0	0	1!1!
5	3	1	1	3	0	0	2!1!
5	3	1	2	2	0	0	1!2!
5	4	1	1	1	2	0	3!1!
5	5	1	1	1	1	1	5!

Chapter 3

A Simple Method for Computing PCFs for Multistage PPIC Receiver

This chapter introduces a simple expression for finding the optimum partial cancellation factors (PCF) for the multistage linear partial parallel interference cancellation (PPIC) receiver. These factors are found in a direct-sequence code division multiple access (DS-CDMA) system over additive white Gaussian noise (AWGN) and frequency-flat fading channels for a large-system case according to [55] and [21]. In this case, the number of active users and the processing gain tend towards infinity while their ratio is finite. In this chapter, the performance is bit error rate (BER) that is measured by numerical simulations. It will be shown that the expression for the PCF is a function of the moments of the eigenvalues of the covariance matrix, the number of interference cancellation stages, the system load (users per chip) and the signal to noise ratio (SNR). In addition, by choosing these PCFs, the performance of the PPIC receiver will converge to that of the minimum mean-squared error (MMSE) receiver. Compared to recently-proposed methods, our method has the following advantages: a) It is less complex because the calculated PCFs are explicit functions of the moments of the eigenvalues of the covariance matrix; b)

there is no need to order the PCFs; and c) it is not necessary to know the number of interference cancellation stages *a priori*.

This chapter continues as follows. The closed-form expression of the optimal PCF is calculated in Section 3.1. Some numerical results are shown in Section 3.2; and Section 3.3 concludes this chapter.

3.1 Derivation of PCF

Suppose that the PCF for an m -stage PPIC receiver is $\mu_1, \mu_2, \dots, \mu_m$. By assuming that the multistage linear PPIC receiver will converge to the MMSE receiver, the optimum PCF expression introduced in [44] and (2.18) is simplified to

$$\mu_i = \frac{E \left[\sum_{k=1}^K \lambda_k \cdot |t_k^{(i)}|^2 \right]}{E \left[\sum_{k=1}^K \lambda_k \varphi_k \cdot |t_k^{(i)}|^2 \right]} = \frac{E \left[\frac{1}{K} \sum_{k=1}^K \lambda_k \cdot |t_k^{(i)}|^2 \right]}{E \left[\frac{1}{K} \sum_{k=1}^K \lambda_k \varphi_k \cdot |t_k^{(i)}|^2 \right]}. \quad (3.1)$$

where $t_k^{(i)}$ is defined as [44]

$$t_k^{(i)} \stackrel{\text{def}}{=} 1 + \sum_{j=1}^{i-1} x_j \varphi_k^j, \quad (3.2)$$

with

$$x_i \stackrel{\text{def}}{=} (-1)^i \sum_{j=1}^m \prod_i \mu_j \quad (3.3)$$

where $\sum_{j=1}^m \prod_i \mu_j$ denotes the sum of the i -ary product of μ_j for $j = 1, 2, \dots, m$ and

$$\varphi_k \stackrel{\text{def}}{=} \lambda_k + \sigma^2. \quad (3.4)$$

From (3.2), we get

$$\left| t_k^{(i)} \right|^2 = \left(1 + \sum_{j=1}^{i-1} x_j \varphi_k^j \right)^2 = 1 + 2 \sum_{j=1}^{i-1} x_j \varphi_k^j + \sum_{j=2}^{2i-2} x'_j \varphi_k^j \quad (3.5)$$

with

$$x'_j = \sum_{l=1}^{j-1} x_{j-l} x_l. \quad (3.6)$$

The numerator of (3.1) becomes

$$\begin{aligned}
& E \left[\frac{1}{K} \sum_{k=1}^K \lambda_k \cdot |t_k^{(i)}|^2 \right] \\
&= E \left\{ \frac{1}{K} \sum_{k=1}^K \lambda_k \cdot \left[1 + 2 \sum_{j=1}^{i-1} x_j \varphi_k^j + \sum_{j=2}^{2i-2} x'_j \varphi_k^j \right] \right\} \\
&= E \left\{ \frac{1}{K} \sum_{k=1}^K \lambda_k \left[1 + 2 \sum_{j=1}^{i-1} x_j (\lambda_k + \sigma^2)^j + \sum_{j=2}^{2i-2} x'_j (\lambda_k + \sigma^2)^j \right] \right\} \\
&= E \left[\frac{1}{K} \sum_{k=1}^K \lambda_k \right] + 2 \sum_{j=1}^{i-1} x_j \sum_{l=0}^j \binom{j}{l} \sigma^{2(j-l)} E \left[\frac{1}{K} \sum_{k=1}^K \lambda_k^{l+1} \right] \\
&\quad + \sum_{j=2}^{2i-2} x'_j \sum_{l=0}^j \binom{j}{l} \sigma^{2(j-l)} E \left[\frac{1}{K} \sum_{k=1}^K \lambda_k^{l+1} \right]. \tag{3.7}
\end{aligned}$$

By defining the r th moment of the eigenvalues of the covariance matrix as

$$M_r = E \left\{ \frac{1}{K} \sum_{k=1}^K \lambda_k^r \right\} \tag{3.8}$$

and

$$M'_j = \sum_{l=0}^j \binom{j}{l} \sigma^{2(j-l)} M_{l+1}, \tag{3.9}$$

the numerator of (3.1) eventually becomes

$$E \left[\sum_{k=1}^K \lambda_k \cdot |t_k^{(i)}|^2 \right] = M_1 + 2 \sum_{j=1}^{i-1} x_j M'_j + \sum_{j=2}^{2i-2} x'_j M'_j \tag{3.10}$$

by doing the same manipulation in the denominator of (3.1) the equation for the PCF at i th stage is found as

$$\mu_i = \frac{\eta_i}{\nu_i} \tag{3.11}$$

where

$$\eta_i = M_1 + 2 \sum_{j=1}^{i-1} x_j M'_j + \sum_{j=2}^{2i-2} x'_j M'_j \tag{3.12}$$

and

$$\nu_i = M_2 + \sigma^2 M_1 + 2 \sum_{j=1}^{i-1} x_j (M_j'' + \sigma^2 M_j') + \sum_{j=2}^{2i-2} x_j' (M_j'' + \sigma^2 M_j') \quad (3.13)$$

with

$$M_j'' = \sum_{l=0}^j \binom{j}{l} \sigma^{2(j-l)} M_{l+2} \quad (3.14)$$

In summary, once the system load, the SNR and the moments of the eigenvalues of the covariance matrix are known, one can easily calculate the optimum PCF. The PCF of each stage depends on the PCF of the previous stages as well.

3.2 Numerical Results

3.2.1 Equal-Power Case

In all simulations, purely random signature sequences are assumed. Simulations are run for 1000000 bit sequences. In order to find out the physical meaning of a large system, in Figure 3.1, the analytical p.d.f. of the eigenvalues of the covariance matrix is compared with the simulation results for $K = 16$, $N = 32$ (i.e., $\beta = K/N = 0.5$). From this figure it is seen that the difference between analytical and simulation results is negligible. Therefore, for the case of $N \geq 32$, the system can be considered as a large system. This point was discussed in [3] by introducing a different approach.

Figure 3.2 compares the performance improvement of the method proposed in [40] without ordering (hereafter, being called the first method) with the method that was calculated in this chapter (hereafter, being called the second method). The SNR is defined as P/σ^2 where for the sake of simplicity, it is assumed that $P = 1$. As is seen from this figure, there is no fluctuation in performance for the second method. Moreover, by defining a proper stopping criterion, e.g., the difference between two consecutive PCFs, we can proceed to any stage of interference cancellation. In

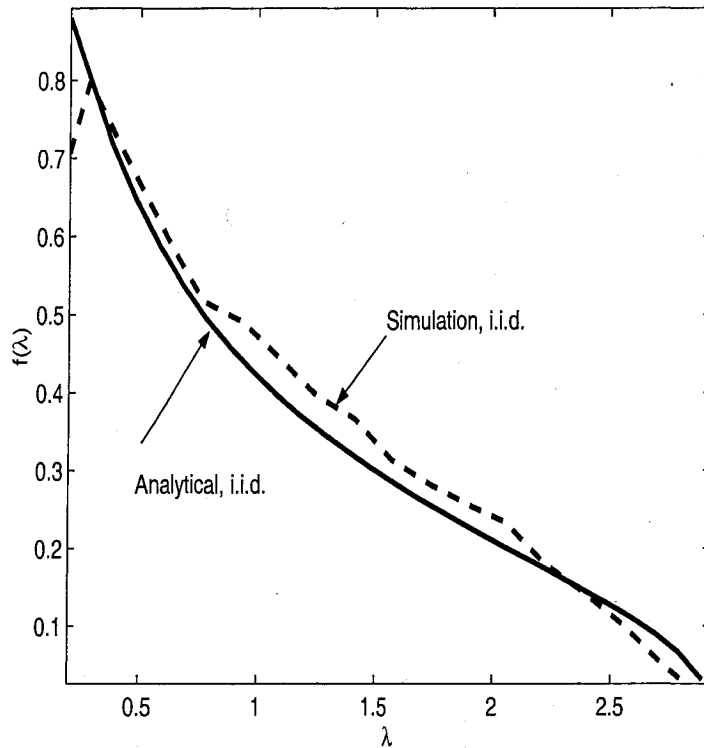


Figure 3.1: The p.d.f of the eigenvalues of the covariance matrix for the two cases of analytical i.i.d and simulation i.i.d. entries with $K = 16$, $N = 32$ and $\beta = K/N = 0.5$.

the first method, a matrix inversion is applied for the calculation of the PCFs. In addition, the PCFs need to be ordered for obtaining a monotonically improving performance in the middle stages of interference cancellation. Since the second method needs none of the above mentioned tasks, it turns out to have much less complexity.

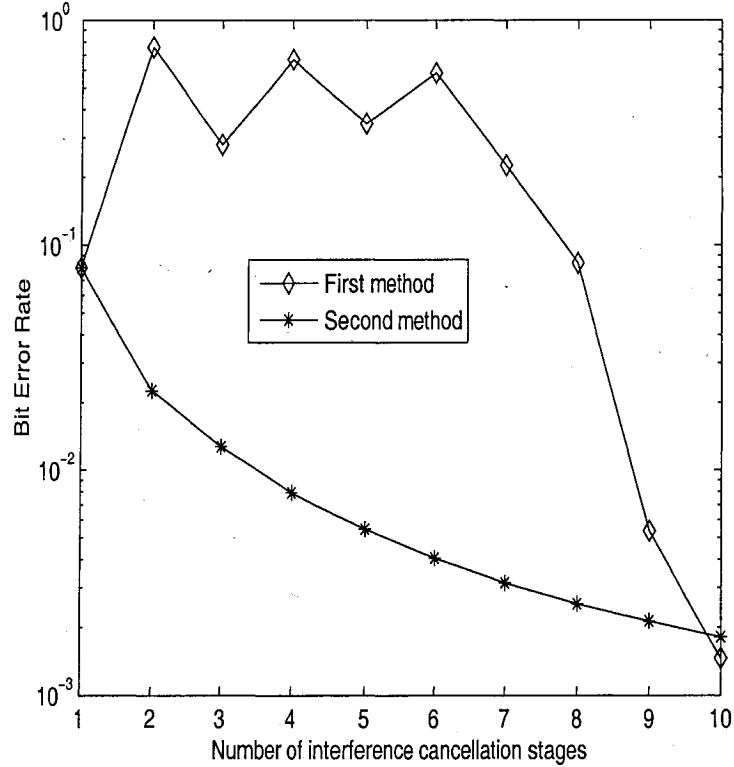


Figure 3.2: Comparison of performance improvement of the PPIC receiver by applying two methods of PCF optimization for $K = 15$, $N = 31$ and $SNR = 10dB$.

Figure 3.3 shows the convergence of performance of the PPIC receiver to that of the MMSE receiver using two methods. In the first method, in order to produce the same smooth convergence as that of the second method, the ordering has a complexity of $O(m^3)$ where m is the number of interference cancellation stages. It should be noted that the difference between the performances of the two methods at the final stage of interference cancellation is due to the simulation result that was obtained for $N = 31$, which results in a negligible error to model a large system since we have used large-system expression for the moments, as Figure 3.1 proves. Therefore, using larger processing gains (*e.g.*, $N \geq 64$) will overcome the

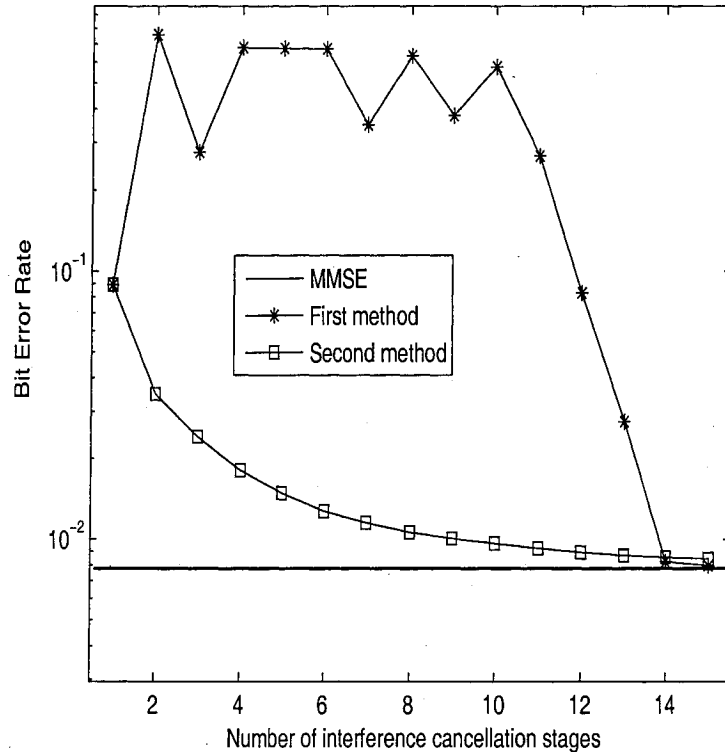


Figure 3.3: Convergence of the performance of the PPIC receiver to that of the MMSE receiver using two methods of PCF optimization for $K = 15$, $N = 31$ and $SNR = 7dB$.

issue. However, considering the simulation time length, the choice of $N = 32$ is an acceptable solution.

Figure 3.4 compares the performance of the multistage linear PPIC receiver with optimum PCF using the method proposed in this chapter with that of MMSE and SUMF receivers. As is seen, the performance of the multistage linear PPIC receiver becomes almost the same as that of the MMSE receiver for a different number of active users. Moreover, this performance is improved monotonically as the number of interference cancellation stages increases. It is noted that more interference cancellation stages are needed if the multistage PPIC receiver is to provide the same

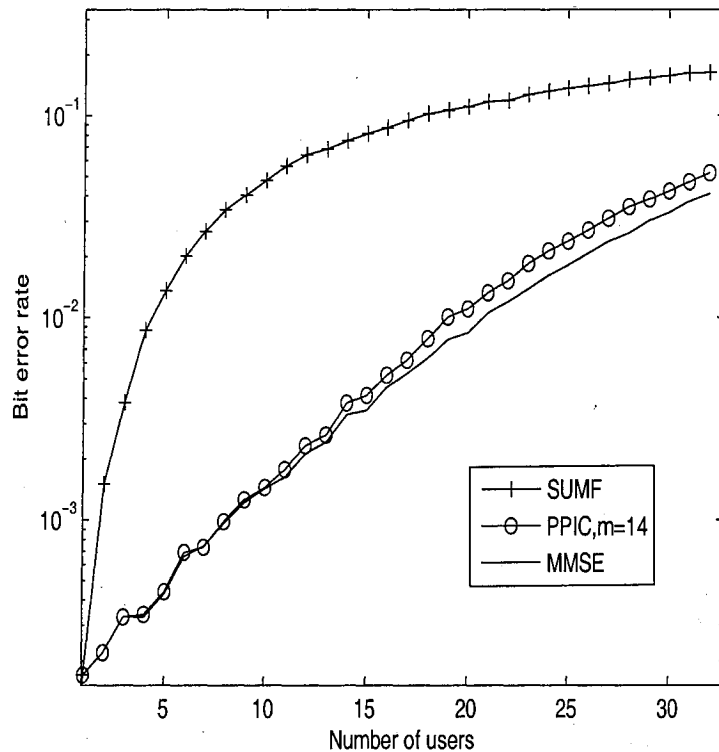


Figure 3.4: Comparison of the performance of the multistage linear PPIC receiver with optimum PCF using proposed method for $m = 14$ with that of the MMSE and SUMF receivers versus the number of active users, $N = 32$ and $SNR = 8.0\text{dB}$.

performance as that of the MMSE receiver for higher number of active users.

Figure 3.5 compares the performance of the multistage linear PPIC receiver with optimum PCF using the method proposed in this chapter with that of MMSE and SUMF receivers for different SNR levels. This figure once more shows that MMSE and multistage linear PPIC receivers provide almost the same performance. As mentioned before, for higher SNR levels, more interference cancellation stages are needed to direct the multistage PPIC receiver to converge to the MMSE receiver.

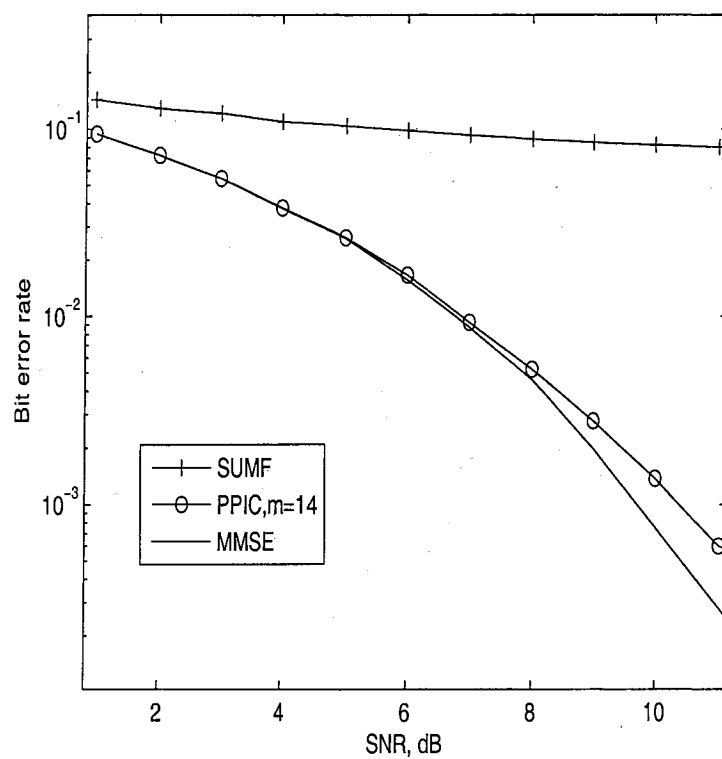


Figure 3.5: Comparison of the performance of the multistage linear PPIC receiver with optimum PCF using proposed method for $m = 14$ with that of the MMSE and SUMF receivers versus SNR, $\beta = 0.5$.

3.2.2 Unequal-Power Case

For this case, it is assumed that the channel is a frequency-flat Rayleigh fading with $E[a_k^2] = 1$ where a_k is the fading coefficient for user k . Signature sequences are i.i.d. random variables. The simulations are run for 100000 bit sequences. Figure 3.6 shows the performance improvement of the PPIC receiver with optimum PCF for the CDMA system over a frequency-flat Rayleigh fading channel versus the number of interference cancellation stages. In this figure, $\beta = 0.5$ and $SNR = 12dB$. It is seen that the performance of the PPIC receiver converges to that of the MMSE receiver. However, by choosing arbitrary PCFs, the performance could be worse than that of the SUMF.

Figure 3.7 compares the bit error rate (BER) versus SNR of a ten-stage PPIC receiver with that of the MMSE and SUMF multiuser receivers for a CDMA system over a frequency-flat Rayleigh fading channel. It is seen that at low SNR levels, there is a slight difference between the performances of the MMSE and PPIC receivers. However, this difference become noticeable for higher SNR levels. The reason is two-fold. Firstly, the MMSE receiver always attempts to find the optimum signal-to-interference-plus-noise ratio (SINR) according to [47]. Secondly, when we deal with a fading channel, the received data are less reliable. Therefore, a smaller PCF is applied in order to cancel the MAI. This makes the performance of the PPIC receiver converge to that of the MMSE receiver with a slower rate compared to the equal-power case. Regarding the complexity issue, the PPIC receiver still offers an acceptable performance.

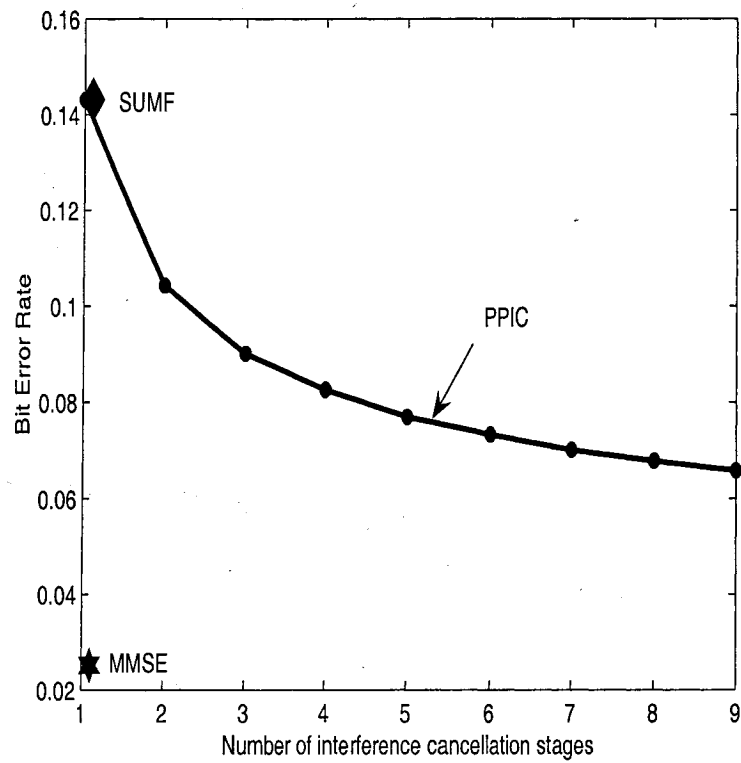


Figure 3.6: Large-system performance of the PPIC receiver for CDMA system over a Rayleigh-fading channel versus number of interference cancellation stages ($\beta = 0.5$ and $SNR = 12dB$).

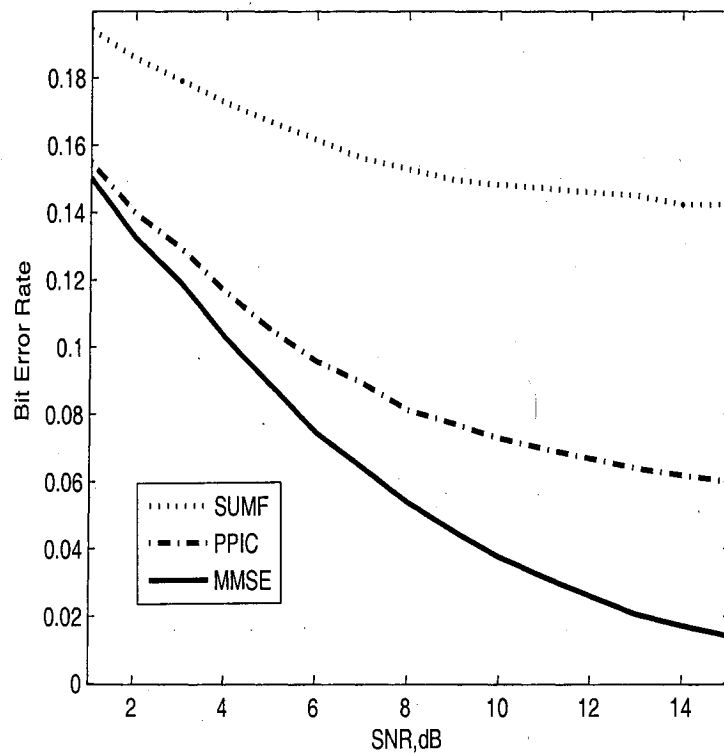


Figure 3.7: Comparison of the large-system performance of the PPIC receiver with MMSE and SUMF receivers for a CDMA system over a frequency-flat Rayleigh fading channel versus SNR ($\beta = 0.5$ and $m = 10$).

3.3 Summary

A simple approach for calculating the optimum partial cancellation factors (PCF) for the partial parallel interference cancellation (PPIC) receiver in a synchronous CDMA system over AWGN and frequency-flat fading channels was introduced in this chapter. These factors were found for a case where the number of active users and the processing gain tend towards infinity while their ratio is finite. The found PCF is a function of the number of interference cancellation stages, the moments of the eigenvalues of the covariance matrix, the system load and the signal-to-noise ratio (SNR). Simulation results showed that by using the proposed method, the performance of the PPIC receiver converges to that of the minimum mean-squared error (MMSE) receiver. When comparing the proposed method with the previously proposed methods, one can point out some advantages. Firstly, it is less complex due to the fact that the calculated PCFs are explicit functions of the moments of the eigenvalues of the covariance matrix. Secondly, there is no need to know the number of interference cancellation stages *a priori*. Finally, there is no need for the PCFs to be ordered. This last advantage results in even more simplicity in circuitry. As was seen in this chapter, it is not clear how to find the performance of the PPIC receiver analytically. In the next chapter, we will find an analytical tool to calculate the SINR of the multistage PPIC receiver with a constant PCF over a fading channel.

Chapter 4

Large-System Design and Analysis of Multistage PPIC Receiver with a Constant PCF

This chapter introduces an analytical tool for finding the large-system performance of a multistage linear partial parallel interference cancellation (PPIC) receiver using the moments of the eigenvalues of the covariance matrix for a code division multiple access (CDMA) system over a frequency-flat fading channel. The figure of merit to evaluate the performance is the signal-to-interference-plus-noise ratio (SINR) that is calculated under a large-system condition. In this case, the number of active users and the processing gain tend towards infinity while their ratio is a fixed value. Our contribution is to consider a frequency-flat fading channel instead of an additive white Gaussian noise (AWGN) channel introduced in [45]. In this condition, the expression found in [45] for performance analysis, cannot be applied anymore. This is due to the fact that the received powers of users play a key role in analyzing the performance for fading conditions. The performance is a function of the moments of the eigenvalues of the covariance matrix. The expression for these moments changes by introducing the fading condition. This expression cannot be taken from [45] and,

therefore, another tool should be sought. This issue is addressed by using the method introduced in [54] to find the final closed-form expression for the performance. It is shown that the large-system performance is a function of the system load, the partial cancellation factor (PCF), the number of interference cancellation stages, the signal-to-noise ratio (SNR), and the received powers of the interfering users. Furthermore, for practical applications, the physical meaning of the large system will be described by numerical simulations.

This chapter continues by presenting the system model for a frequency-flat fading case in Section 4.1. The performance of the PPIC receiver in fading condition is found in Section 4.2. Some numerical results are presented in Section 4.3; and finally, Section 4.4 concludes this chapter.

4.1 System Model

The system model for a synchronous CDMA system over a frequency-flat fading channel is formulated for K active users and the processing gain of N . The continuous-time synchronous received signal over a frequency-flat fading channel for a $(2M + 1)$ bit sequence is written as

$$r(t) = \sum_{k=1}^K \sum_{i=-M}^M A_k[i] b_k[i] \mathbf{s}_k(t - iT) + n(t) \quad (4.1)$$

where $A_k[i]$ and $b_k[i]$ are the amplitude and transmitted symbol of user k at time $iT < t < (i + 1)T$, respectively. The spreading sequence of user k is denoted by the unit-energy vector \mathbf{s}_k ,

$$\mathbf{s}_k = [s_{1k}, s_{2k}, \dots, s_{Nk}]^H \quad (4.2)$$

where $[\cdot]^H$ denotes the Hermitian transposition and the i.i.d random variables s_{pk} take values $\pm 1/\sqrt{N}$ with an equal probability for $p = 1, 2, \dots, N$ and $k = 1, 2, \dots, K$. The noise $n(t)$ is AWGN with zero mean and a power spectral density of σ^2 . The

sampled received signal, considering the first user as the one of interest, is given by,

$$\mathbf{r} = \sqrt{P_1}b_1\mathbf{s}_1 + \sum_{k=2}^K \sqrt{P_k}b_k\mathbf{s}_k + \mathbf{n} \quad (4.3)$$

where $P_k = A_k^2$ is the transmitted power of user k for $k = 1, 2, \dots, K$. The first, the second, and the third terms of (4.3) are the useful signal, the MAI, and the noise, respectively. For an equal-power case we have $A_1 = A_2 = \dots = A_K = A$. A linear multiuser receiver for user 1 applies a linear transformation to the received signal, such that $\tilde{b}_1 = \mathbf{c}_1^H \cdot \mathbf{r}$ where $\mathbf{c}_1 \in \mathbb{R}^N$. The SINR is defined as the ratio of the useful signal to the MAI plus the thermal noise. Therefore,

$$\begin{aligned} SINR_1 &= \frac{E[(A_1b_1\mathbf{c}_1^H \cdot \mathbf{s}_1)^2]}{E[(\sum_{k=2}^K A_k b_k \mathbf{c}_1^H \cdot \mathbf{s}_k)^2] + E[(\mathbf{c}_1^H \cdot \mathbf{n})^2]} \\ &= \frac{P_1(\mathbf{c}_1^H \cdot \mathbf{s}_1)^2}{\sum_{k=2}^K P_k(\mathbf{c}_1^H \cdot \mathbf{s}_k)^2 + \sigma^2 \cdot (\mathbf{c}_1^H \cdot \mathbf{c}_1)} \end{aligned} \quad (4.4)$$

or in matrix format

$$SINR_1 = \frac{P_1(\mathbf{c}_1^H \cdot \mathbf{s}_1)^2}{\mathbf{c}_1^H (\mathbf{S}_1 \mathbf{P}_1 \mathbf{S}_1^H + \sigma^2 \mathbf{I}) \mathbf{c}_1} \quad (4.5)$$

where \mathbf{S}_1 is an $N \times (K - 1)$ matrix of the spreading sequences of the $(K - 1)$ interferers defined as

$$\mathbf{S}_1 = [\mathbf{s}_2, \mathbf{s}_3, \dots, \mathbf{s}_K] \quad (4.6)$$

and \mathbf{P}_1 is the diagonal matrix of the received powers of interferers defined as

$$\mathbf{P}_1 = \text{diag}[P_2, P_3, \dots, P_K] \quad (4.7)$$

and finally, \mathbf{I} is an $N \times N$ identity matrix.

4.2 Performance of Multistage PPIC Receiver

The multiuser receiver that is presented in this chapter is the multistage first-order linear PPIC receiver. Such a multiuser receiver has m stages but only one partial cancellation factor (PCF) for all stages denoted by μ . This receiver is applied to a

CDMA system over a frequency-flat fading channel. For an m -stage PPIC receiver, the demodulator \mathbf{c}_1 is defined as

$$\mathbf{c}_{1,m}^{PPIC} = \mu \left(\sum_{i=0}^m \left[\mathbf{I} - \frac{\mu}{P} (\mathbf{S}_1 \mathbf{P}_1 \mathbf{S}_1^H + \sigma^2 \mathbf{I}) \right]^i \right) \mathbf{s}_1 \quad (4.8)$$

where the subscripts of \mathbf{c} denote the user of interest and the number of interference cancellation stages and; \mathbf{S}_1 , \mathbf{P}_1 , and \mathbf{s}_1 are defined in (4.6), (4.7), and (4.2), respectively. The demodulator $\mathbf{c}_{1,m}^{PPIC}$ defined by (4.8) is the generalization of the receiver proposed in [45] to a situation where the users arrive at the receiver with different power levels. This receiver depends on the received powers of the interferers. For the equal-power case, \mathbf{P}_1 is defined as

$$\mathbf{P}_1 = \text{diag}[P, P, \dots, P] = P \mathbf{I}_{K-1} \quad (4.9)$$

where \mathbf{I}_{K-1} denotes a $(K-1) \times (K-1)$ identity matrix. Substituting the $\mathbf{c}_{1,m}^{PPIC}$ from (4.8) into (4.4) and doing some manipulations, the SINR of the PPIC receiver for the first user becomes

$$SINR_{1,m}^{PPIC} = E \left[\frac{a_1^2 (\eta_m)^2}{\nu_m} \right] \quad (4.10)$$

where

$$\eta_m = \sum_{i=0}^m (-\mu)^i \sum_{j=0}^i \left(\frac{\sigma^2}{P} - \frac{1}{\mu} \right)^{i-j} \binom{i}{j} M_j \quad (4.11)$$

and

$$\begin{aligned} \nu_m &= \sum_{i=0}^m \sum_{j=0}^m (-\mu)^{i+j} \sum_{l=0}^{i+j} \left(\frac{\sigma^2}{P} - \frac{1}{\mu} \right)^{i+j-l} \binom{i+j}{l} \\ &\quad \times \left(M_{l+1} + \frac{\sigma^2}{P} M_l \right) \end{aligned} \quad (4.12)$$

with $M_i = \mathbf{s}_1^H (\mathbf{S}_1 \mathbf{A}_1 \mathbf{S}_1^H)^i \mathbf{s}_1$ and $\mathbf{A}_1 = \mathbf{P}_1 / P = \text{diag}[a_2^2, \dots, a_K^2]$ is the diagonal matrix of fading coefficients of the interfering users. The ratio $\beta = K/N$ is called the system load and $SNR = P/\sigma^2$ where P is the transmitted power that is assumed to be the same for all users. The matrix $\mathbf{R} = \mathbf{S}_1 \mathbf{A}_1 \mathbf{S}_1^H$ denotes the covariance matrix of signature sequences and amplitudes of the interfering users for a fading case. When

we deal with small K and N , for randomly-chosen spreading sequences, the $SINR$ becomes a random variable. This is because the $SINR$ is a function of the covariance matrix which is random in this case. However, when K and N tend towards infinity while the system load is a fixed value, the $SINR$ will have a closed-form expression. In such a situation, the CDMA system is considered as a large system. From [45], it can be written as

$$M_i = \mathbf{s}_1^H (\mathbf{S}_1 \mathbf{A}_1 \mathbf{S}_1^H)^i \mathbf{s}_1 \simeq \text{trace}(\mathbf{S}_1 \mathbf{A}_1 \mathbf{S}_1^H)^i. \quad (4.13)$$

According to [54], $\text{trace}(\mathbf{S}_1 \mathbf{A}_1 \mathbf{S}_1^H)^i = E[\lambda^i]$ where $E[\lambda^i]$ is the i th moment of the eigenvalues of the matrix $\mathbf{S}_1 \mathbf{A}_1 \mathbf{S}_1^H$. In order to find moments, definitions and coefficients are the same as in Chapter 2.

4.3 Numerical Results and Discussions

The performance of the PPIC receiver strongly depends on the value of the PCF. This factor which is a function of the system load, the number of interference cancellation stages, and the SNR should be chosen properly. Otherwise, a wrong selection of this factor results in a poor performance. For all figures, it is assumed that $a_1^2 = 1$. Figure 4.1 shows the large-system performance of the PPIC receiver versus PCF when $\beta = 0.5$, $m = 8$, and $SNR = 12dB$. As is seen, the optimum performance is achieved when PCF is picked between 0.16 and 0.17. Therefore, by choosing an appropriate PCF obtained in this figure, the optimum performance of the PPIC receiver for the CDMA system over a fading channel is obtained to be shown in Figure 4.2.

Figure 4.2 compares the large-system performance of a CDMA system over a Rayleigh frequency-flat fading channel with different linear multiuser receivers where the expression for the performance of the PPIC receiver is according to (4.10) and the expressions for the performance of the MMSE and SUMF receivers are taken from [47]. By applying the tool introduced in this chapter, the SINR is found more

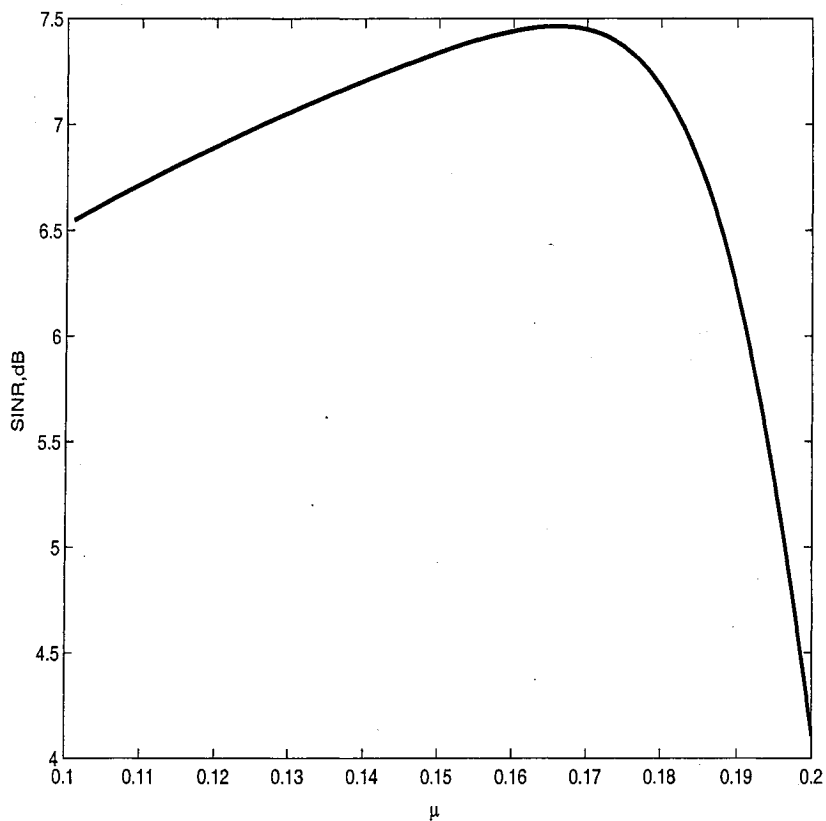


Figure 4.1: Large-system performance of the PPIC receiver for CDMA system over a Rayleigh-fading channel versus PCF ($\beta = 0.5$, $m = 8$, and $SNR = 12dB$).

accurately compared to numerical simulation. Furthermore, this result is obtained with major saving in the processing time compared to numerical simulations. This is due to the fact that simulation results need to be averaged for a large number of samples as will be seen in Figure 4.6. Therefore, by knowing the system load, the PCF, the number of interference cancellation stages, the SNR and the type of fading channel, the performance can be calculated easily for different situations.

Figure 4.3 shows the performance of a synchronous CDMA system over an AWGN channel with different linear multiuser receivers. It is worth noting that the reason that the performance of the PPIC receiver for equal-power case is better than

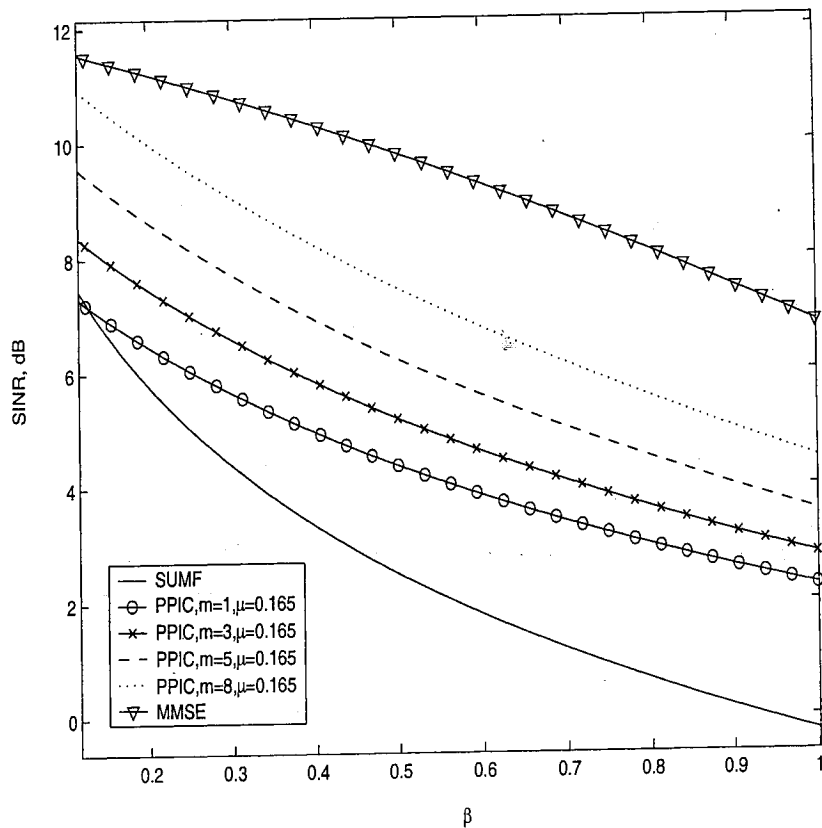


Figure 4.2: Comparison of the Large-system SINR of synchronous CDMA with SUMF, MMSE, and PPIC ($m = 1, 3, 5, 8$) receivers over a Rayleigh-fading channel for $SNR = 12dB$.

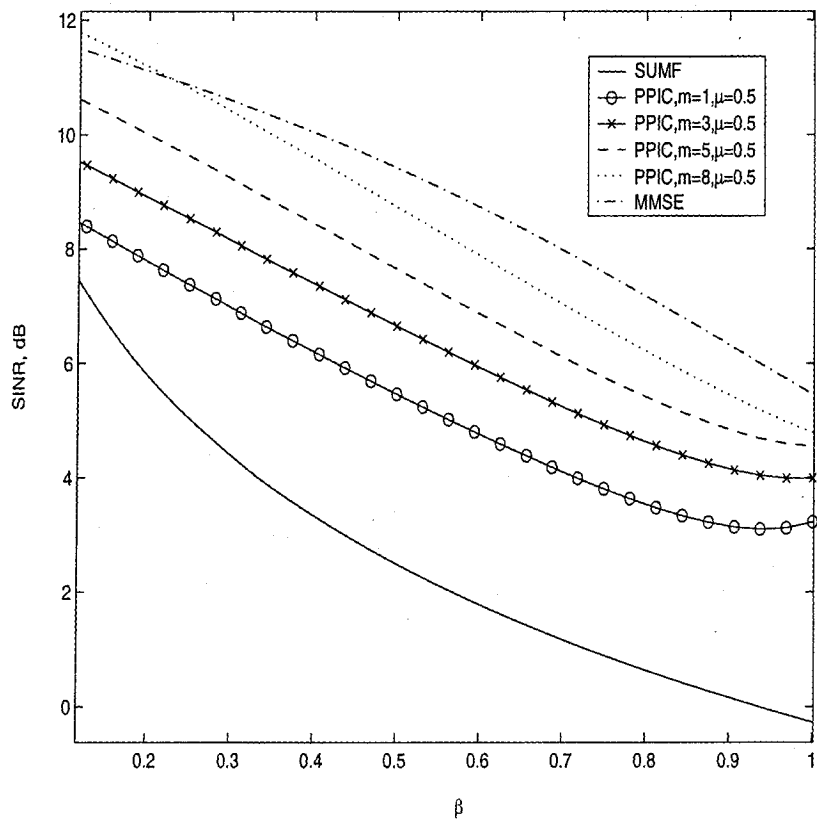


Figure 4.3: Large-system SINR of synchronous CDMA with SUMF, MMSE, and PPIC ($m = 1, 3, 5, 8$) receivers over AWGN channel for $SNR = 12dB$.

fading case is because for synchronous, equal-power case a higher partial cancellation factor (μ) is applied. This is due to the fact that in equal-power case, the multiuser system can estimate the MAI with more reliability. Therefore, more interference cancellation is feasible. However, when the users arrive at the receiver with different power levels and, furthermore, it is assumed that no power control is in place, the multiuser system experiences more MAI with less reliability to be estimated. This results in applying a smaller PCF.

Figure 4.4 depicts the performance improvement of the multistage linear PPIC receiver for a fixed system load when the number of interference cancellation stages increases. This figure shows that in order to achieve the performance of the MMSE receiver, many stages of interference cancellation are needed. This can be considered as a drawback for this receiver.

Figure 4.5 shows the bit error rate (BER) improvement of the PPIC receiver versus the number of interference cancellation stages. The BER at the m th stage is approximately defined as $P_b = Q(\sqrt{SINR_m^{PPIC}})$ where

$$Q(x) = 1/(\sqrt{2\pi}) \int_x^\infty \exp(-t^2/2) dt. \quad (4.14)$$

It should be noted that since the MMSE receiver maximizes the SINR [47], it offers a better performance in fading condition. This results in a larger gap between the performances of these two receivers for a CDMA system over a fading channel.

Figure 4.6 shows the values of N for which a CDMA system can be considered large. Numerical simulations are run for 1000 samples. In this figure, simulation results for different processing gains are compared with the analytical result obtained according to (4.10). It is seen that as the processing gain becomes larger, the simulated performance tends to the analytical result such that for $N \geq 32$ we can assume that we deal with a large system. Therefore, it is possible to use the analytical formula for practical applications while the error remains negligible.

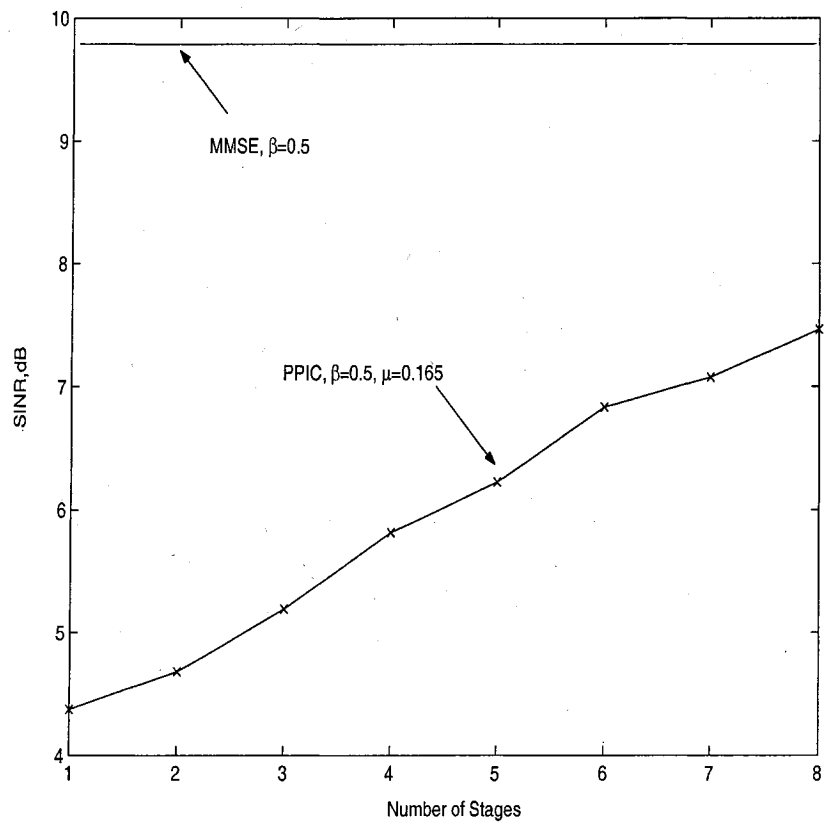


Figure 4.4: SINR improvement of the multistage PPIC receiver for a CDMA system over a Rayleigh-fading channel versus the number of interference cancellation stages, $SNR = 12$.

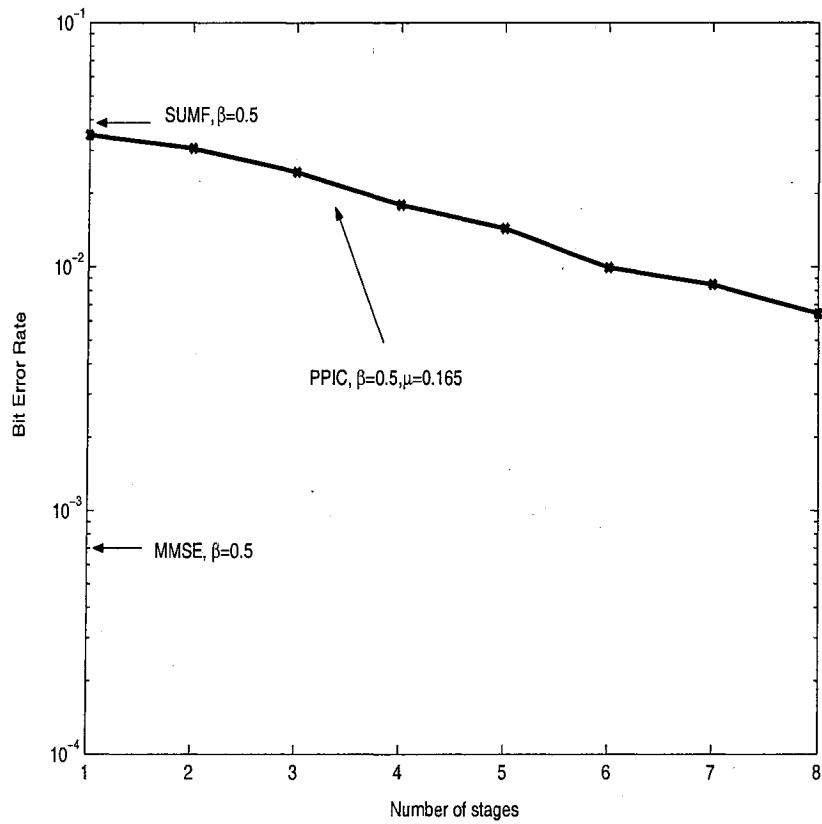


Figure 4.5: BER improvement of the multistage PPIC receiver for a CDMA system over a Rayleigh-fading channel for different stages, $SNR = 12$.

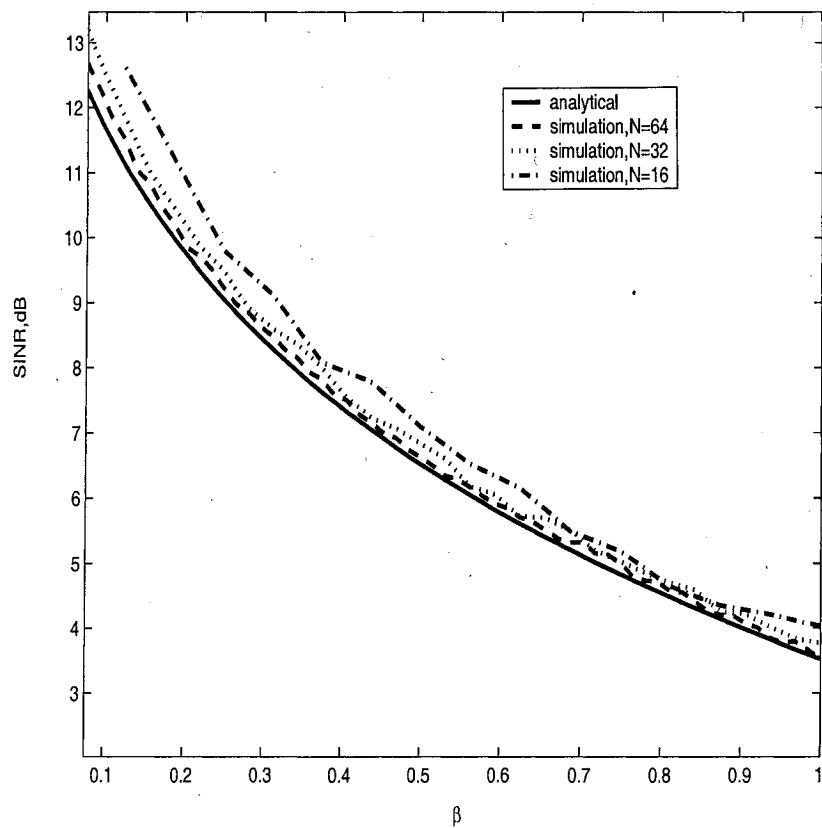


Figure 4.6: Comparison of the large-system analytical and simulation results for a CDMA system over a Rayleigh-fading channel with PPIC receiver, $N = 16, 32,$ and 64 , $SNR = 12$ dB, $m = 1$, and $\mu = 0.165$.

4.4 Summary

A closed-form expression for the large-system performance of the multistage linear partial parallel interference cancellation receiver for the CDMA system over a frequency-flat fading channel was introduced in this thesis. It was shown that the large-system performance has a closed-form expression that is a function of the system load, the partial cancellation factor, the number of interference cancellation stages, the SNR, and the received powers of interfering users. By using the proposed tool, the performance of the PPIC can be calculated more precisely with a considerable saving on the processing time compared to the numerical simulation. It was also shown that practically, for the processing gain of 32 or more, we can assume that the CDMA system is a large system. Delving into the receiver proposed in this chapter, one may point out the following drawbacks. First of all, many stages of interference cancellation are needed in order to provide the same performance as that of the MMSE receiver. In addition, it is not clear that how to find the optimum PCF analytically for different conditions in terms of the system load and the SNR. Chapter 5, addresses these issues.

Chapter 5

Large-System Design and Analysis of Multistage Linear PPIC Receiver with a Variable PCF

This chapter introduces a multistage linear partial parallel interference cancellation (PPIC) receiver whose performance converges to that of the minimum mean-squared error (MMSE) receiver by applying a variable PCF. The figure of merit for evaluating the performance is the signal to interference-plus-noise ratio (SINR) that is calculated under a large system condition. It will be shown that the large-system performance is a function of the number of the interference cancellation stages, the moments of the eigenvalues of the covariance matrix, and the signal to noise ratio (SNR). Compared to the existing multistage linear PPIC receivers, our proposed scheme has the following benefits: a) Its performance converges to that of the MMSE receiver with a lower number of interference cancellation stages, b) it is more robust when dealing with higher system loads and SNR levels, and c) the performance is found directly without using any orthogonalization algorithm [60].

This chapter introduces the multistage linear multiuser receivers in Section 5.1. Some numerical results are presented in Section 5.2; and conclusions are given in Section 5.3.

5.1 MMSE-Based Multistage Multiuser Receiver with a variable PCF

The introducing multiuser receiver is an MMSE-based multistage linear PPIC receiver with a variable PCF for different interference cancellation stages. In this receiver, we take the background noise into consideration when designing the demodulator. Compared to the receiver proposed in [45], the performance of our proposed scheme converges to that of the MMSE receiver with fewer stages of interference cancellation for the same channel condition. Compared to the receiver proposed in [50], the performance of our scheme is superior for high system loads and high Signal to Noise Ratio (**SNR**) levels. This means that our proposed scheme employs a more efficient approach to reduce the MAI. Finally, compared to the method proposed in [4] and [5], the SINR is calculated without using any orthogonalization algorithm. This results in less complexity. By generalizing what was proposed in [45], the linear iterative method becomes

$$\mathbf{x}_{1,m} = \mu_m \mathbf{r} + (\mathbf{I} - \mu_m \mathbf{B}_1) \mathbf{x}_{1,m-1} \quad (5.1)$$

where $\mathbf{x}_{1,i}$ is an $N \times 1$ spread signal at stage i for $i = 0, 1, \dots, m$, μ_i is the PCF at stage i , and

$$\mathbf{B}_1 = \mathbf{S}_1 \mathbf{A}_1 \mathbf{S}_1^H + \frac{\sigma^2}{P}. \quad (5.2)$$

The matrix $\mathbf{S}_1 \mathbf{A}_1 \mathbf{S}_1^H$ is called the covariance matrix and the decision statistic for the first user at the stage m is defined as

$$b_{1,m} = a_1 \mathbf{s}_1^H \cdot \mathbf{x}_{1,m} = a_1 \mathbf{c}_{1,m}^H \cdot \mathbf{r} \quad (5.3)$$

It is assumed that $\mathbf{x}_{1,0} = \mu_0 \mathbf{r}$. Now, using a technique similar to what was proposed in [44], we get

$$\begin{aligned} \mathbf{x}_{1,m} - \mathbf{B}_1^{-1} \mathbf{r} &= \mu_m \mathbf{r} + (\mathbf{I} - \mu_m \mathbf{B}_1) \mathbf{x}_{1,m-1} - \mathbf{B}_1^{-1} \mathbf{r} \\ &= (\mathbf{I} - \mu_m \mathbf{B}_1) \mathbf{x}_{1,m-1} - (\mathbf{I} - \mu_m \mathbf{B}_1) \mathbf{B}_1^{-1} \mathbf{r} \end{aligned}$$

$$= (\mathbf{I} - \mu_m \mathbf{B}_1)(\mathbf{x}_{1,m-1} - \mathbf{B}_1^{-1} \mathbf{r}) \quad (5.4)$$

It should be noted that there are some differences between (5.4) and what was proposed in [44]. First of all, the decision statistic at stage $m = 0$ is a nonzero value defined as $b_{1,0} = a_1 \mu_0 \mathbf{s}_1^H \cdot \mathbf{r}$ while $b_{1,0}$ is assumed to be zero in [44]. Secondly, in our definitions, the matrix \mathbf{B}_1 is an $N \times N$, while it is a $K \times K$ matrix in [44]. Continuing the recursion, we get

$$\begin{aligned} \mathbf{x}_{1,m} - \mathbf{B}_1^{-1} \mathbf{r} &= \prod_{i=1}^m (\mathbf{I} - \mu_i \mathbf{B}_1)(\mathbf{x}_{1,0} - \mathbf{B}_1^{-1} \mathbf{r}) \\ &= \prod_{i=1}^m (\mathbf{I} - \mu_i \mathbf{B}_1)(\mu_0 - \mathbf{B}_1^{-1}) \mathbf{r} \end{aligned} \quad (5.5)$$

Eventually, (5.5) can be written as

$$\mathbf{x}_{1,m} = \left[\mathbf{I} - \prod_{i=0}^m (\mathbf{I} - \mu_i \mathbf{B}_1) \right] \mathbf{B}_1^{-1} \mathbf{r} \quad (5.6)$$

Using (5.3), the m -stage demodulator is found as

$$\mathbf{c}_{1,m} = \left[\mathbf{I} - \prod_{i=0}^m (\mathbf{I} - \mu_i \mathbf{B}_1) \right] \mathbf{B}_1^{-1} \mathbf{s}_1 \quad (5.7)$$

The decision statistics of user 1 at the stage m becomes

$$\tilde{b}_1 = a_1 \mathbf{s}_1^H \left[\mathbf{I} - \prod_{i=0}^m (\mathbf{I} - \mu_i \mathbf{B}_1) \right] \mathbf{B}_1^{-1} \mathbf{r} = -a_1 \mathbf{s}_1^H \left[\sum_{i=0}^m \theta_i \mathbf{B}_1^i \right] \mathbf{r}. \quad (5.8)$$

Define

$$\tilde{\mathbf{b}}_1 = -a_1 \boldsymbol{\theta} \cdot \mathbf{z} \quad (5.9)$$

where $\boldsymbol{\theta}$ is defined according to (2.30) and

$$\mathbf{z} = \begin{bmatrix} a_1 \mathbf{s}_1^H \\ a_1 \mathbf{s}_1^H \mathbf{B}_1 \\ \vdots \\ a_1 \mathbf{s}_1^H \mathbf{B}_1^m \end{bmatrix} \mathbf{r} \quad (5.10)$$

We further define

$$\Lambda_r = \mathbf{s}_1^H \mathbf{B}_1^r \mathbf{s}_1 \quad (5.11)$$

Therefore, the $(m+1) \times 1$ vector \mathbf{z} can be written as

$$\mathbf{z} = a_1^2 b_1 \mathbf{M} + a_1 \mathbf{N} \quad (5.12)$$

with

$$\mathbf{M} = \begin{bmatrix} \Lambda_0 \\ \Lambda_1 \\ \vdots \\ \Lambda_m \end{bmatrix} \quad (5.13)$$

and

$$\Lambda_i = \sum_{i=0}^m \binom{m}{i} \left(\frac{\sigma^2}{P} \right)^{(m-i)} M_i, \quad (5.14)$$

It is assumed that $\Lambda_0 = M_0$. Finally, the $(m+1) \times 1$ matrix \mathbf{N} is defined as

$$\mathbf{N} = \begin{bmatrix} \mathbf{s}_1 \cdot (\mathbf{S}_1 \mathbf{A}_1 \mathbf{b}_1 + \mathbf{n}) \\ \mathbf{s}_1 \cdot \mathbf{B}_1 (\mathbf{S}_1 \mathbf{A}_1 \mathbf{b}_1 + \mathbf{n}) \\ \vdots \\ \mathbf{s}_1 \cdot \mathbf{B}_1^m (\mathbf{S}_1 \mathbf{A}_1 \mathbf{b}_1 + \mathbf{n}) \end{bmatrix} \quad (5.15)$$

The expressions for optimum PCF and SINR remain the same as (2.28) and (2.29) except that the definition of \mathbf{M} is according to (5.13) and the matrix \mathbf{R} is an $(m+1) \times (m+1)$ Hankel matrix with the first column as

$$[\Lambda_1, \Lambda_2, \dots, \Lambda_{m+1}]^H \quad (5.16)$$

and the last row as

$$[\Lambda_{m+1}, \Lambda_{m+2}, \dots, \Lambda_{2m+1}] \quad (5.17)$$

As will be seen in Section 5.2, compared with the other receivers introduced earlier, our proposed receiver has the following benefits. First of all, compared to the MMSE-based multistage linear PPIC receiver with a constant PCF (which

hereafter, is called the first scheme), the performance of our scheme converges to that of the MMSE receiver with fewer stages of interference cancellation by introducing a small complexity in order to recalculate the PCF (μ_i) from the vector $\boldsymbol{\theta}$. Moreover, in comparison with the decorrelator-based multistage linear PPIC receiver with variable PCF (which hereafter, is called the second method), the performance of our proposed method is superior, while the complexity is almost the same. The second advantage becomes more significant for higher system loads and higher SNR levels.

5.2 Numerical Results and Discussion

For all numerical calculations, purely random spreading sequences are assumed.

5.2.1 Equal-Power Case

Figure 5.1 shows the SINR of the scheme presented in Section 2.2.2 (hereafter, it is called the first scheme) for a large CDMA system over an AWGN channel versus system load for a fixed SNR level. The expressions for SINR of the MMSE and SUMF receivers are taken from [47] and the expression for calculating the optimum PCF of the PPIC receiver is taken from [6]. It is seen from this figure that for about 15 stages of interference cancellation, the performance of the PPIC receiver becomes almost the same as that of the MMSE receiver for a low to moderate system load. However, there is a larger gap for moderate to high system load.

Figure 5.2 shows the SINR of the first scheme for a large CDMA system over an AWGN channel versus SNR for a fixed system load. It is seen from this figure that the performance of the PPIC receiver becomes the same as that of the MMSE receiver for low to moderate SNR levels. However, for a moderate to high SNR level, there is a larger gap between the performances of PPIC and MMSE receivers. As a result, in order to obtain the performance of the MMSE receiver for higher SNR

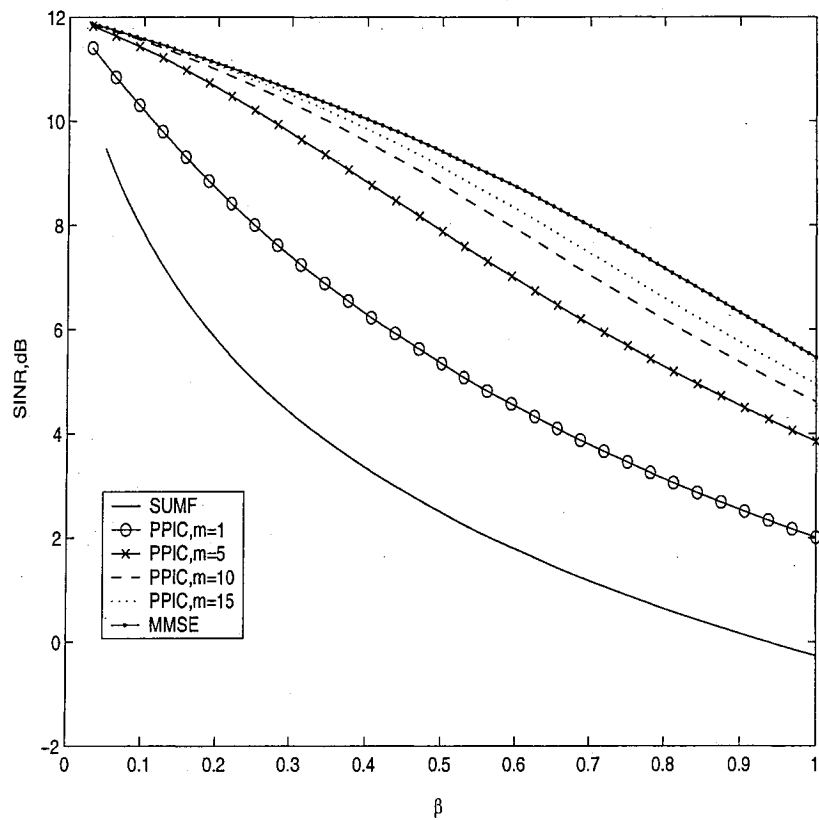


Figure 5.1: SINR of the MMSE-based multistage linear PPIC receiver with constant PCF for a large CDMA system over an AWGN channel versus system load, SNR= 12.0 dB.

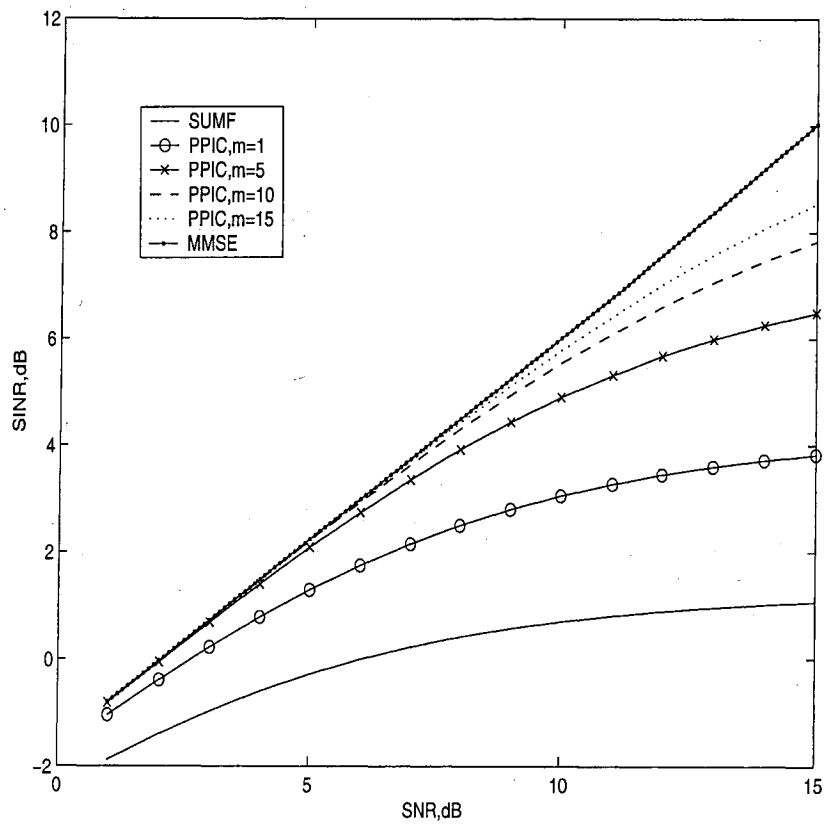


Figure 5.2: SINR of the MMSE-based multistage linear PPIC receiver with constant PCF for a large CDMA system over an AWGN channel versus SNR, $\beta = 0.75$.

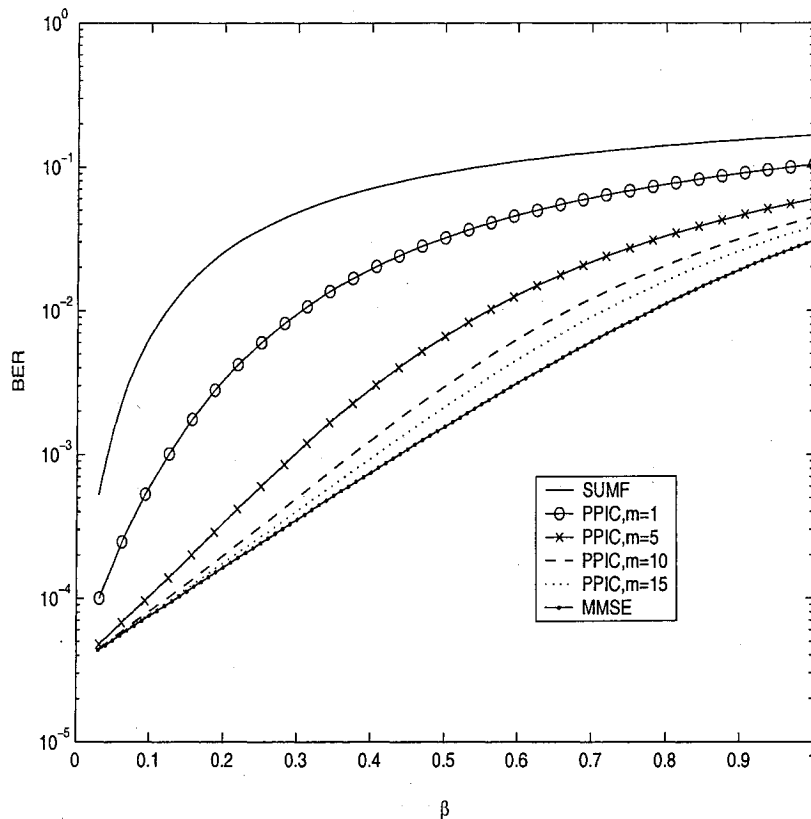


Figure 5.3: BER of the MMSE-based multistage linear PPIC receiver with constant PCF for a large CDMA system over an AWGN channel versus system load, SNR= 12.0 dB.

levels, more stages of interference cancellation are needed.

Figures 5.3 and 5.4 show the BER of the first method for a large CDMA system over an AWGN channel for different system loads and SNR levels, respectively. It is noted that the bit error rate (BER) at the m th stage is approximately defined as $P_b = Q(\sqrt{SINR_m^{PPIC}})$ where $Q(x) = 1/(\sqrt{2\pi}) \int_x^\infty \exp(-t^2/2) dt$. As is seen, these two figures once more show the gaps between the performances of PPIC and MMSE receivers for higher system loads and SNR levels.

By investigating Figures 5.1 to 5.4 one may conclude the following facts. Firstly, in order to force the performance of the first scheme to converge to that

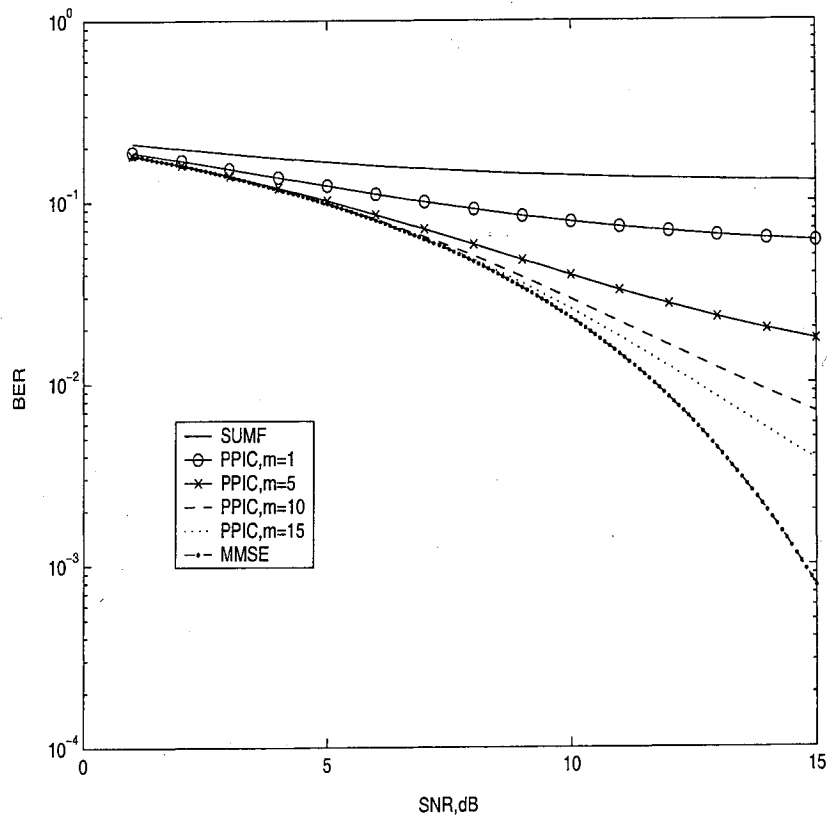


Figure 5.4: BER of the MMSE-based multistage linear PPIC receiver with constant PCF for a large CDMA system over an AWGN channel versus SNR, $\beta = 0.75$.

of the MMSE receiver, a large number of interference cancellation stages is required. Secondly, despite having a large number of interference cancellation stages, the performance begins to deviate from that of the MMSE receiver for high system loads and high SNR levels. In order to overcome these drawbacks, the second scheme was proposed in [50] and also introduced in Section 2.2.3 whose performance converges to that of the decorrelator receiver that is evaluated by Figures 5.5 to 5.8.

Figure 5.5 shows the SINR of the second scheme for a large CDMA system over an AWGN channel versus system load for a fixed SNR. When comparing this figure with Figure 5.1, the following benefits are attributed to this receiver. First of all, the performance of this receiver becomes exactly the same as that of the decorrelator receiver with fewer stages of interference cancellation. Secondly, for a moderate SNR level, this performance is achieved regardless of the system load.

Figure 5.6 shows the SINR of the second scheme for a large CDMA system over an AWGN channel versus SNR for a fixed system load. This figure shows that the second scheme is suitable for moderate to high SNR levels. This is due to the fact that at low SNR levels, the decorrelator receiver is dominated by the background noise rather than the MAI. However, for higher SNR levels, the MAI is more dominating.

Figures 5.7 and 5.8 show the BER of the second method for a large CDMA system over an AWGN channel for different system loads and SNR levels, respectively. These two figures prove the same fact that the performance of the second scheme becomes the same as that of the decorrelator receiver for fewer stages of interference cancellation.

Investigating Figures 5.5 to 5.8 demonstrates the advantages of this scheme over the previous one. However, comparing Figures 5.1 to 5.4 with Figures 5.5 to 5.8, respectively, shows a large degradation in performance of the second scheme when the system is highly loaded. In order to resolve this problem, we propose an MMSE-based multistage linear PPIC receiver whose performance becomes the same

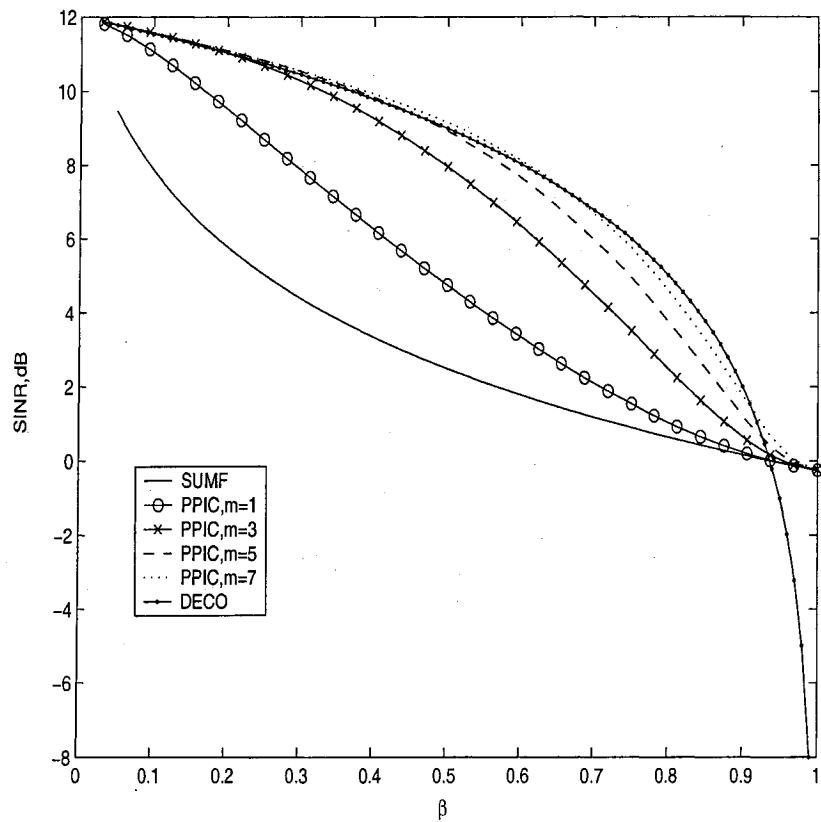


Figure 5.5: SINR of the decorrelator-based multistage linear PPIC receiver with different PCF for a large CDMA system over an AWGN channel versus system load, SNR= 12.0 dB.

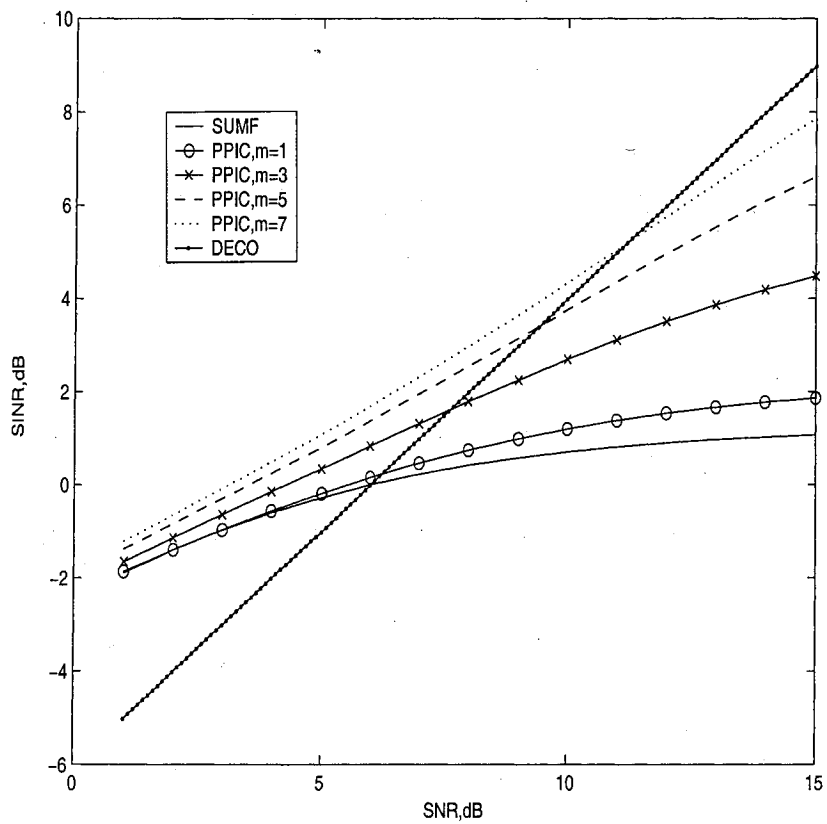


Figure 5.6: SINR of the decorrelator-based multistage linear PPIC receiver with variable PCF for a large CDMA system over an AWGN channel versus SNR, $\beta = 0.75$.

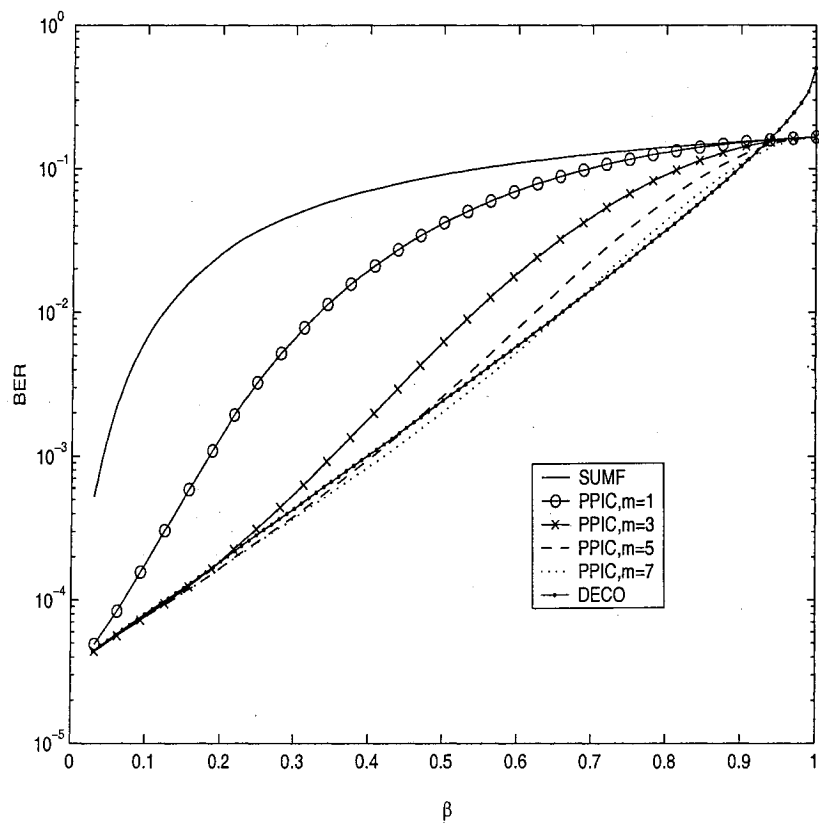


Figure 5.7: BER of the Decorrelator-based multistage linear PPIC receiver with variable PCF for a large CDMA system over an AWGN channel versus system load, SNR= 12.0 dB.

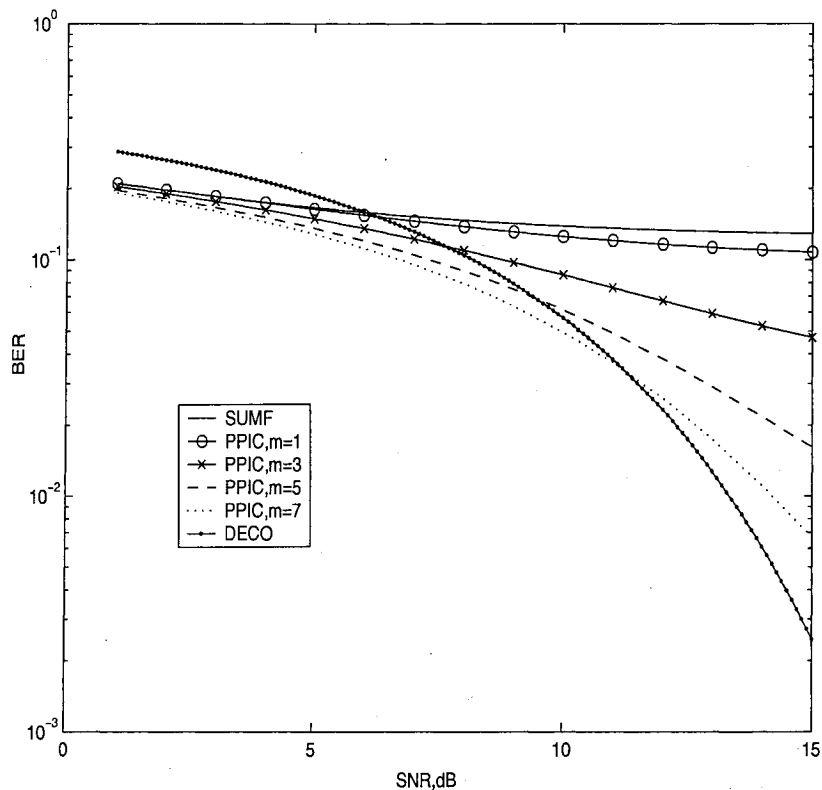


Figure 5.8: BER of the decorrelator-based multistage linear PPIC receiver with variable PCF for a large CDMA system over an AWGN channel versus SNR, $\beta = 0.75$.

as that of the MMSE receiver for all system loads. The efficiency of our proposed scheme is gauged through Figures 5.9 to 5.12.

Figure 5.9 shows the SINR of our proposed scheme for a large CDMA system over an AWGN channel versus system load for a fixed SNR level. Compared to the first scheme, these benefits are noticeable. Firstly, the performance of our proposed method tends to become the same as that of the MMSE receiver with a lower number of interference cancellation stages. Secondly, this performance is achieved for all system loads. Compared to the second method, the performance of our proposed method is always superior since in our proposed method, the background noise is

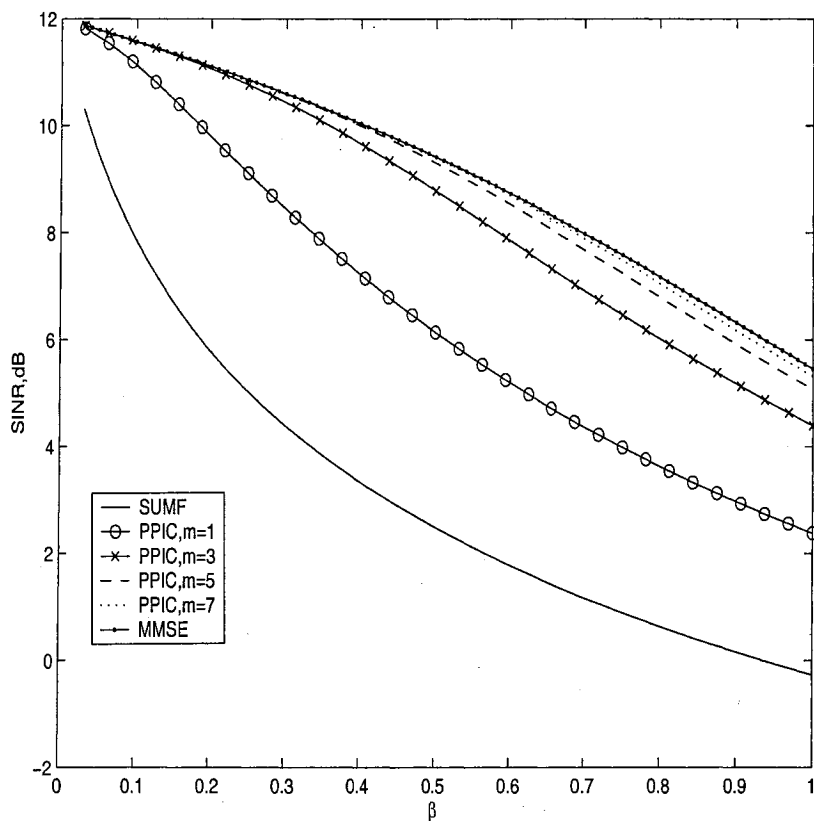


Figure 5.9: SINR of the MMSE-based multistage linear PPIC receiver with variable PCF for a large CDMA system over an AWGN channel versus system load, SNR=12.0 dB.

taken into consideration when cancelling the MAI.

Figure 5.10 shows the SINR of our proposed scheme for a large CDMA system over an AWGN channel versus SNR for a fixed system load. As is seen, another advantage of our proposed scheme is that its performance tends to become the same as that of the MMSE receiver for almost all SNR levels.

Figures 5.11 and 5.12 show the BER of our proposed scheme for a large CDMA system over an AWGN channel for different system loads and SNR levels, respectively.

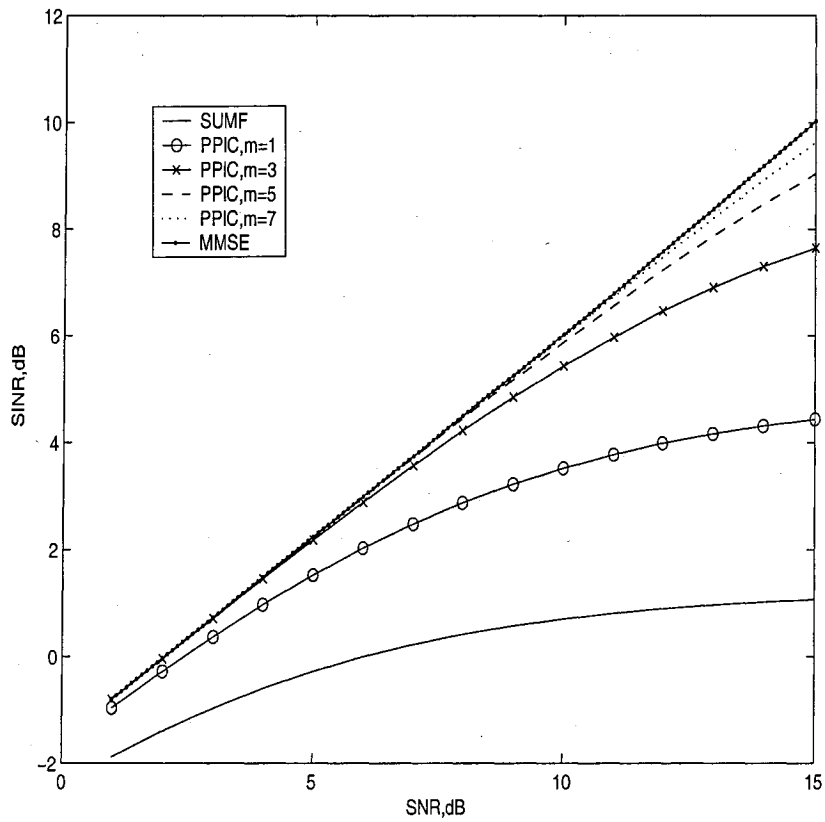


Figure 5.10: SINR of the multistage linear PPIC receiver with variable PCF for a large CDMA system over an AWGN channel versus SNR, $\beta = 0.75$.

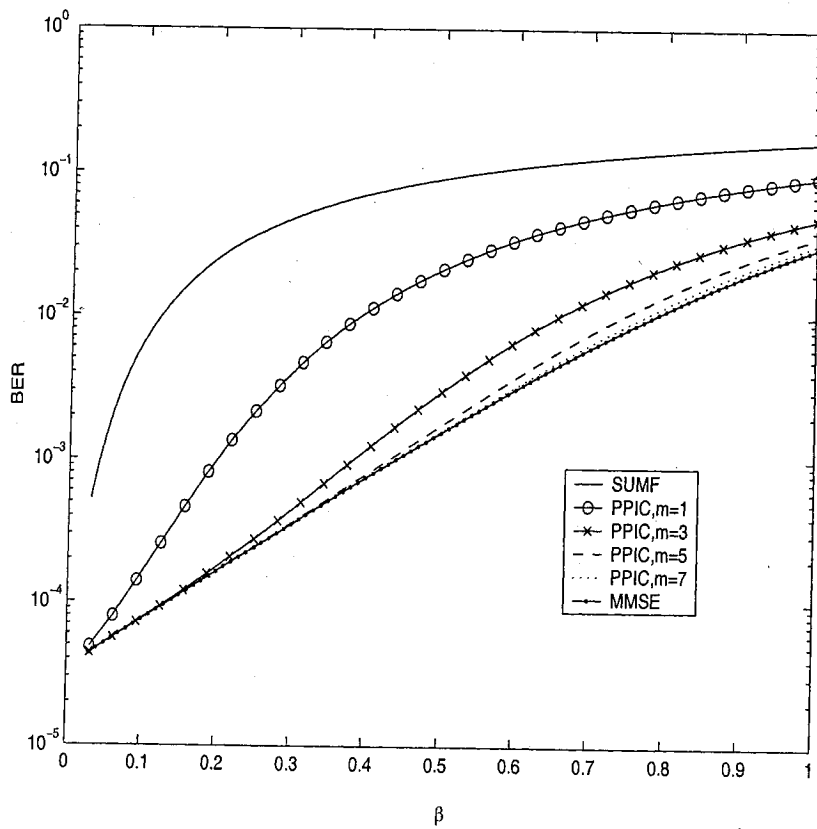


Figure 5.11: BER of the MMSE-based multistage linear PPIC receiver with variable PCF for a large CDMA system over an AWGN channel versus system load, SNR=12.0 dB.

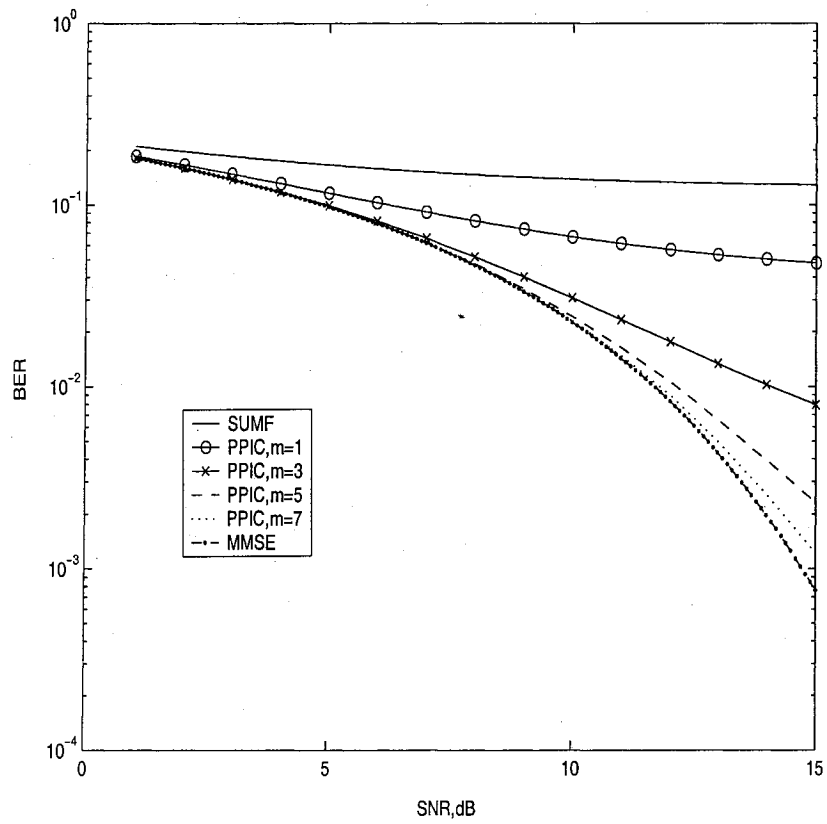


Figure 5.12: BER of the MMSE-based multistage linear PPIC receiver with variable PCF for a large CDMA system over an AWGN channel versus SNR, $\beta = 0.75$.

5.2.2 Unequal-Power Case

When the channel is not AWGN, employing the first scheme becomes more difficult since it is not clear how to calculate the optimum PCF. In Chapter 4, the optimum PCF for a special case of SNR= 12.0 dB and $\beta = 0.75$ was found by numerical calculation. By applying the same method, the optimum PCF is found to be about 0.165 for different system loads when SNR= 12.0 dB.

Figure 5.13 shows the SINR of the first scheme for a large CDMA system over a Rayleigh frequency-flat fading channel versus system load for a fixed SNR level. In all calculations, it is assumed that the channel gain for the first user is $a_1^2 = 1$.

Figure 5.14 shows the SINR of our proposed method for a large CDMA system over a Rayleigh frequency-flat fading channel versus system load for a fixed SNR level. The expressions for the SINR of the MMSE and SUMF receivers for a Rayleigh frequency-flat fading channel are according to [47], [7], and [8]. Comparing Figure 5.14 with Figure 5.13 again shows that our proposed method is superior for the following reasons. Compared to the first method, the calculation of the optimum PCF is possible according to (2.28). Compared to the second method, a better performance is achieved for higher system loads since the background noise is considered to cancel the MAI. For the sake of brevity, we do not include that comparison.

Figure 5.15 shows the SINR of our proposed scheme for a large CDMA system over a Rayleigh frequency-flat fading channel versus SNR for a fixed system load.

Figures 5.16 and 5.17 show the BER of our proposed scheme for a large CDMA system over a Rayleigh frequency-flat fading channel for different system loads and SNR levels, respectively.

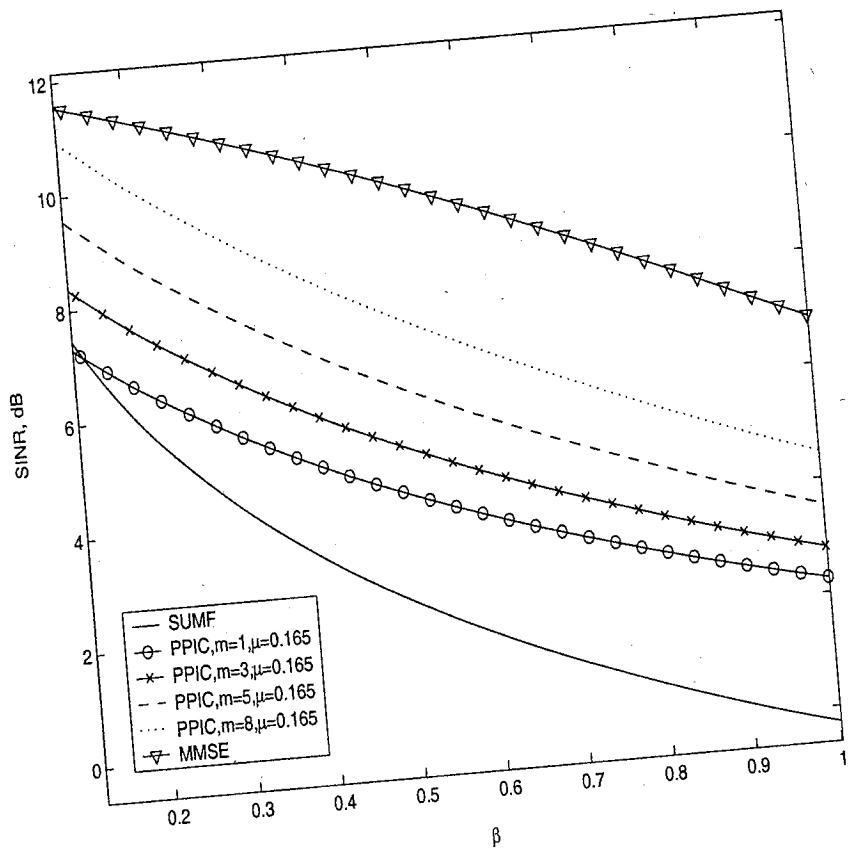


Figure 5.13: SINR of the MMSE-based multistage linear PPIC receiver with constant PCF for a large CDMA system over a Rayleigh frequency-flat fading channel versus system load, SNR= 12.0 dB.

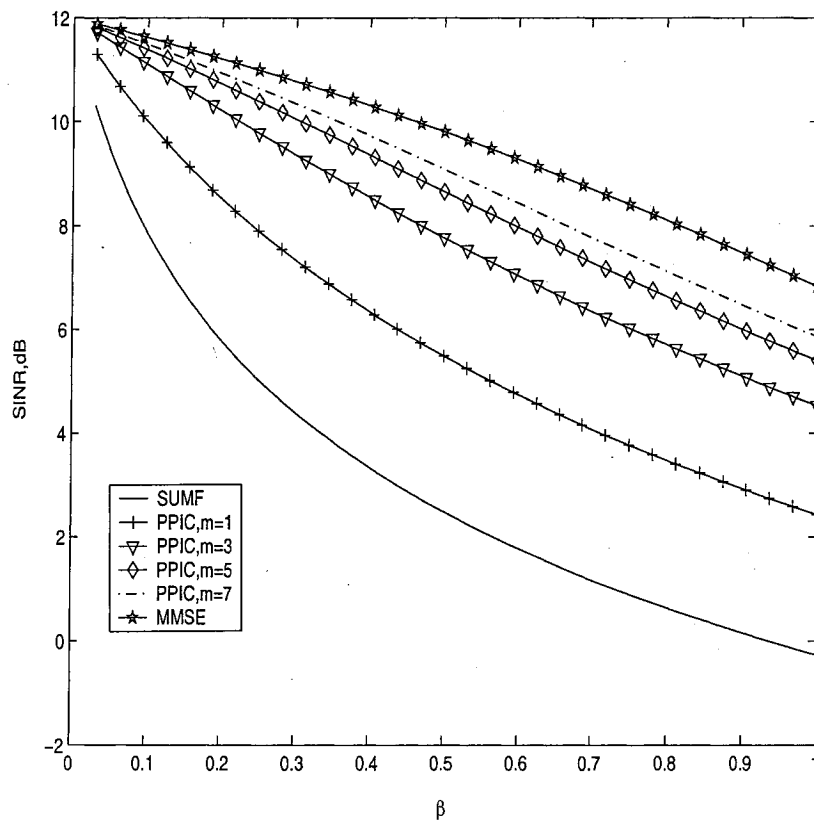


Figure 5.14: SINR of the MMSE-based multistage linear PPIC receiver with variable PCF for a large CDMA system over a Rayleigh frequency-flat fading channel versus system load, SNR= 12.0 dB.

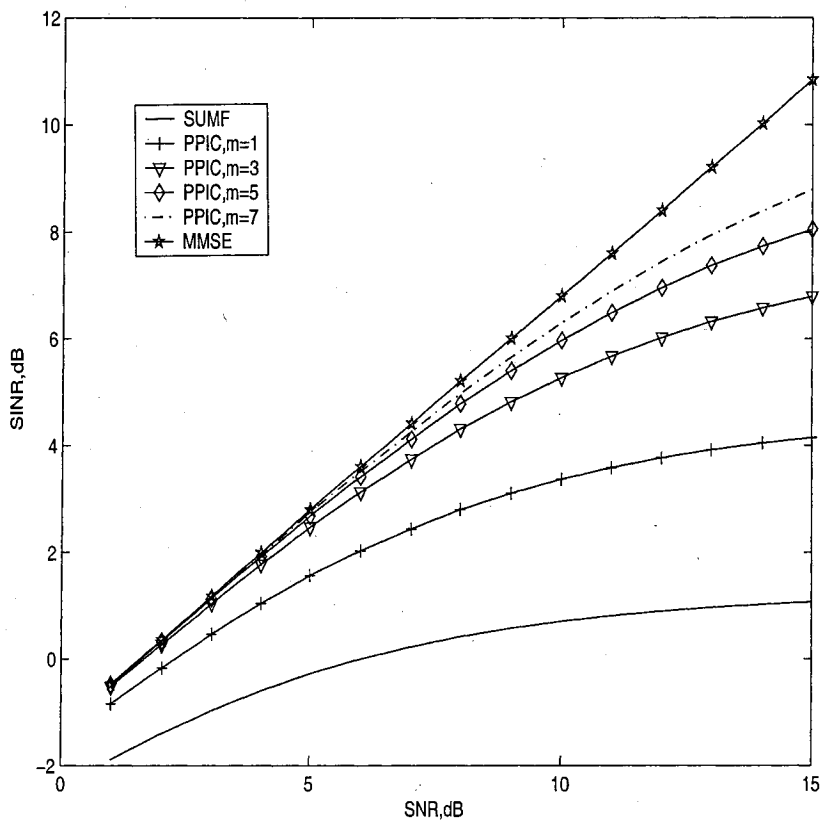


Figure 5.15: SINR of the MMSE-based multistage linear PPIC receiver with variable PCF for a large CDMA system over a Rayleigh frequency-flat fading channel versus SNR, $\beta = 0.75$.

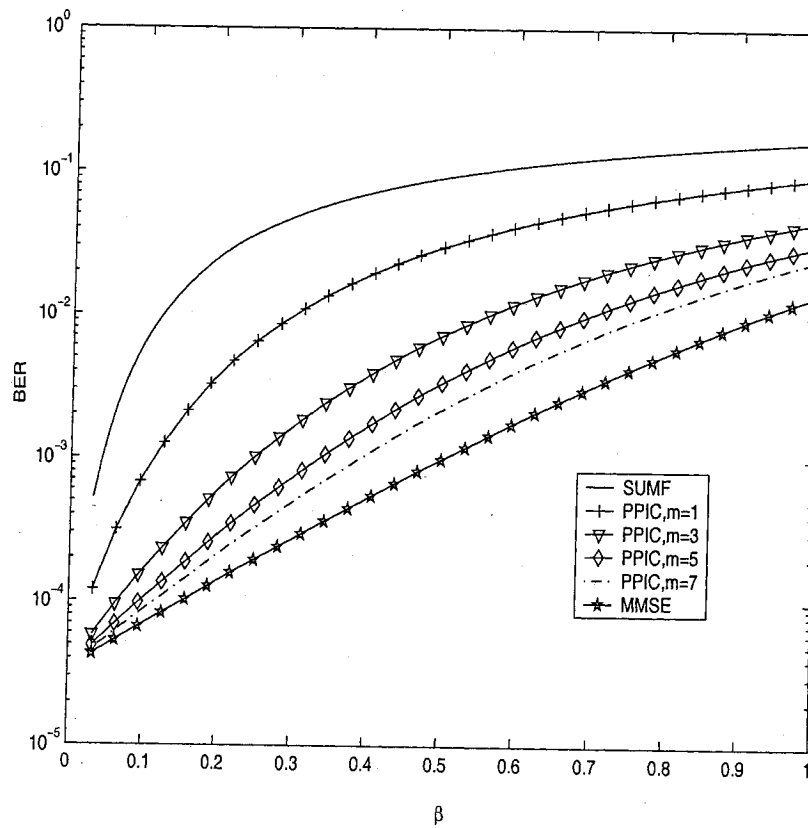


Figure 5.16: BER of the MMSE-based multistage linear PPIC receiver with variable PCF for a large CDMA system over a Rayleigh frequency-flat fading channel versus system load, SNR= 12.0 dB.

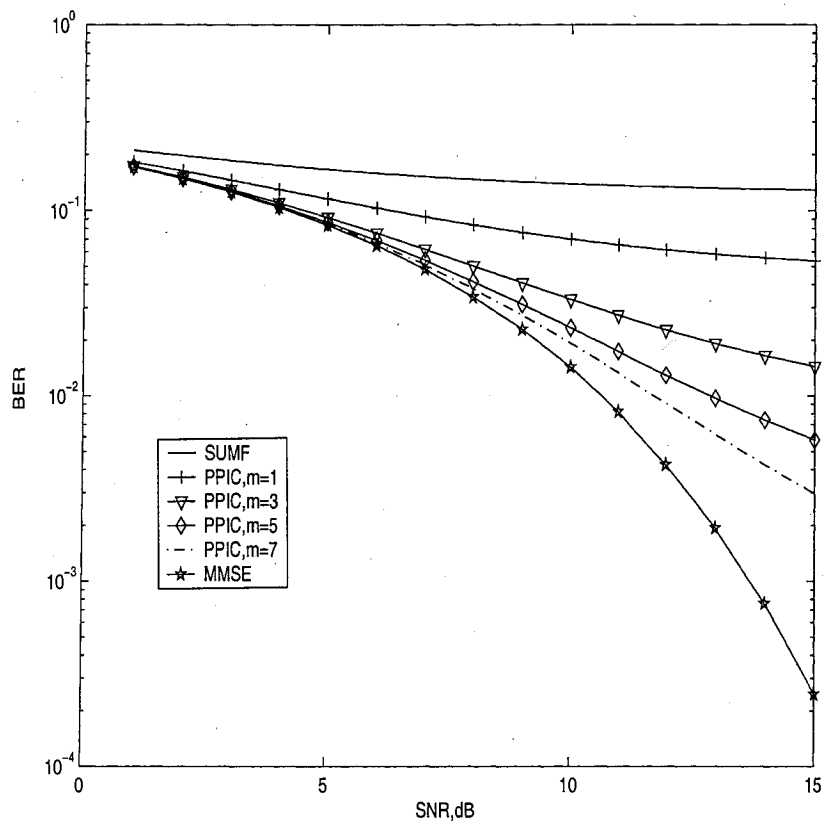


Figure 5.17: BER of the MMSE-based multistage linear PPIC receiver with variable PCF for a large CDMA system over a Rayleigh frequency-flat fading channel versus SNR, $\beta = 0.75$.

5.3 Summary

We introduced a multistage linear partial parallel interference cancellation (PPIC) receiver whose performance converges to that of the minimum mean-squared error (MMSE) receiver by applying a variable PCF. It was shown that the signal to interference-plus-noise ratio (SINR) is a function of the number of interference cancellation stages, the moments of the eigenvalues of the covariance matrix, and the signal to noise ratio (SNR). For a large CDMA system, the SINR has a closed-form expression since the moments of the eigenvalues of the large covariance matrix have closed-form expressions. Compared to the existing schemes for the multistage linear PPIC receiver, our proposed scheme provides the following benefits. First of all, with fewer stages of interference cancellation, its performance converges to that of the MMSE receiver that provides the best performance among the linear multiuser receivers. Secondly, our proposed receiver is more robust for high system loads and high SNR levels; and finally, the expression for the performance is found directly without using any orthogonalization algorithm. In the next chapter, we extend our proposed multistage linear multiuser receiver to a multipath fading case.

Chapter 6

Multistage Multiuser Detection and Channel Estimation over Multipath Fading Channels

This chapter introduces a simple method to design and analyze a multistage linear multiuser (MLMU) receiver for a synchronous direct-sequence (DS-) code division multiple access (CDMA) system over a multipath fading channel. The figure of merit to evaluate the performance is the signal to noise-plus-interference ratio (SINR). Finding a closed-form expression for the SINR in an asynchronous case is not possible. Therefore, we assume the system to be synchronous. Compared to other recently-proposed methods, our proposed method offers a more efficient approach to analyzing the large-system performance by introducing a new expression for the covariance matrix of the interference. In addition, a simple multistage scheme to estimate the multipath channel gains is introduced. Through numerical examples, it will be shown that the performance of the MLMU receiver will converge to that of the minimum mean-squared error (MMSE) receiver. The proposed data and channel estimation schemes with some numerical examples are presented in Sections 6.1

and 6.2, respectively. Finally, conclusions are drawn in section 6.3.

6.1 Data Estimation

In [50], when designing multiuser receiver, the same multipath fading channel gains were assigned to different users. Moreover, the performance of the MLMU receiver converges to that of the decorrelator receiver since the inverse matrix of the interference (the MAI plus the background noise) term was approximated by only a polynomial in the MAI. Compared to [50], we consider different and independent multipath channel gains for different users. In addition, unlike [50], by applying our proposed scheme, the performance of the MLMU receiver will tend to become the same as that of the MMSE receiver. This is due to the fact that in our method, the inverse matrix of the interference term is approximated through the way that the background noise is considered in the polynomial expansion. Finally, since we consider the distribution of the channel gains, unlike [50], which deals with only downlink communication, our proposed method can be applied to both downlink and uplink communications. From Chapter 2, for the m -stage multistage linear multiuser (MLMU) receiver, the decision statistic can be written as

$$\tilde{b}_1 = \mathbf{a}_1^H \mathbf{s}_1^H \left(\sum_{i=0}^m x_i \mathbf{B}_1^i \right) \cdot \mathbf{r} \quad (6.1)$$

where x_i is a scalar coefficient and $\mathbf{B}_1 = \mathbf{S}_1 \mathbf{A}_1 \mathbf{S}_1^H + (\sigma^2/P)\mathbf{I}$. The following theorem gives the expression for the large-system performance of the MLMU receiver for a multipath fading channel. The proof is given in Appendix A. The expressions for channel gains and covariance matrices for the interference (the MAI plus the background noise) term are different compared to [50] and [51]. It is further assumed that the average of the channel gain for the first user is $E[\mathbf{a}_1^H \mathbf{a}_1] = 1$. Otherwise, the performance will be multiplied by the given average.

Theorem 6.1.1 *The signal to noise-plus-interference ratio (SINR) of the MLMU receiver in a multipath fading channel with L distinct paths for the first user at the stage m becomes :*

$$SINR_{1,m} = \mathbf{\Lambda}^H \mathbf{R}^{-1} \mathbf{\Lambda} \quad (6.2)$$

where $\mathbf{\Lambda}$ is an $(m+1) \times 1$ vector defined as $\mathbf{\Lambda} = [\Lambda_0, \Lambda_1, \dots, \Lambda_m]^H$ with $\Lambda_i = \sum_{j=0}^i \binom{i}{j} (\sigma^2/P)^{(i-j)} M_j$ and M_i is the i -th moment of the eigenvalues of the matrix $\mathbf{S}_1 \mathbf{A}_1 \mathbf{S}_1^H$. Furthermore, the $(m+1) \times (m+1)$ matrix \mathbf{R} is called the covariance matrix of the interference term defined as

$$\mathbf{R} = E[\mathbf{N}\mathbf{N}^H] = \begin{bmatrix} \Lambda_1 & \Lambda_2 & \dots & \Lambda_{m+1} \\ \Lambda_2 & \Lambda_3 & \dots & \Lambda_{m+2} \\ \vdots & & & \\ \Lambda_{m+1} & \Lambda_{m+2} & \dots & \Lambda_{2m+1} \end{bmatrix} \quad (6.3)$$

Proof: See Appendix A. □

Having chosen the spreading sequences randomly, for small K and N , the performance of any multiuser receiver will become a random value. However, by letting K and N tend towards infinity while the system load $\beta = K/N$ is held constant, the performance will converge to a deterministic value. In such a condition, the CDMA system is considered a large system. For a large-system scenario, it can be shown that [45]

$$M_i = \mathbf{s}_1^H (\mathbf{S}_1 \mathbf{A}_1 \mathbf{S}_1^H)^i \mathbf{s}_1 \simeq \text{trace}(\mathbf{S}_1 \mathbf{A}_1 \mathbf{S}_1^H)^i = E[\lambda^i] \quad (6.4)$$

The following theorem gives the expression for the moments of the eigenvalues of the covariance matrix for the MAI term.

Theorem 6.1.2 For a multipath fading channel with L distinct paths, the i th moment of the eigenvalues of the matrix $\mathbf{S}_1 \mathbf{A}_1 \mathbf{S}_1^H$ becomes

$$M_i = E[\lambda^i] = \sum_{j=1}^i \beta^j L^j \sum_{m_1+\dots+m_j=m} c(m_1, \dots, m_j) E[\Delta^{m_1}] \dots E[\Delta^{m_j}] \quad (6.5)$$

where $\beta = K/N$ is the system load and Δ is a nonnegative random variable whose distribution is the limit distribution of matrix \mathbf{A}_1 . All other coefficients are found according to Chapter 2.

Proof: The proof is the extension of the results found in Chapter 2 to a multipath fading case as follows. The matrix $\mathbf{A}_1 = \text{diag}[a_2^2, \dots, a_2^K]$ is a $(K-1)L \times (K-1)$ matrix that can be decomposed to L independent $(K-1) \times (K-1)$ matrices. Since the same distribution is assumed for the elements of all matrices, the moments of the eigenvalues of the matrix $\mathbf{S}_1 \mathbf{A}_1 \mathbf{S}_1^H$ will become L times any $(K-1) \times (K-1)$ matrix resulting from decomposition. \square

In order to evaluate the performance of our proposed multiuser receiver, some numerical examples are provided. The channel is assumed to be a multipath Rayleigh fading channel with L independent paths for each user. Figure 6.1 shows the large-system SINR improvement of the MLMU receiver in a multipath fading channel versus system load for fixed SNR and number of resolvable paths. As is seen from this figure, the performance of the MLMU receiver converges to that of the MMSE receiver as the number of interference cancellation stages increases. Moreover, this performance is achieved with much less complexity compared to the MMSE receiver.

Figure 6.2 shows the large-system SINR of the MLMU receiver versus the SNR when the system load and the number of resolvable paths are fixed. This figure shows that the performance of the multistage linear multiuser receiver becomes almost the same as that of the MMSE receiver after a few stages of interference cancellation when the SNR level is from low to moderate. However, for moderate to high SNR levels, there is a larger gap between the performances of MLMU and MMSE receivers.

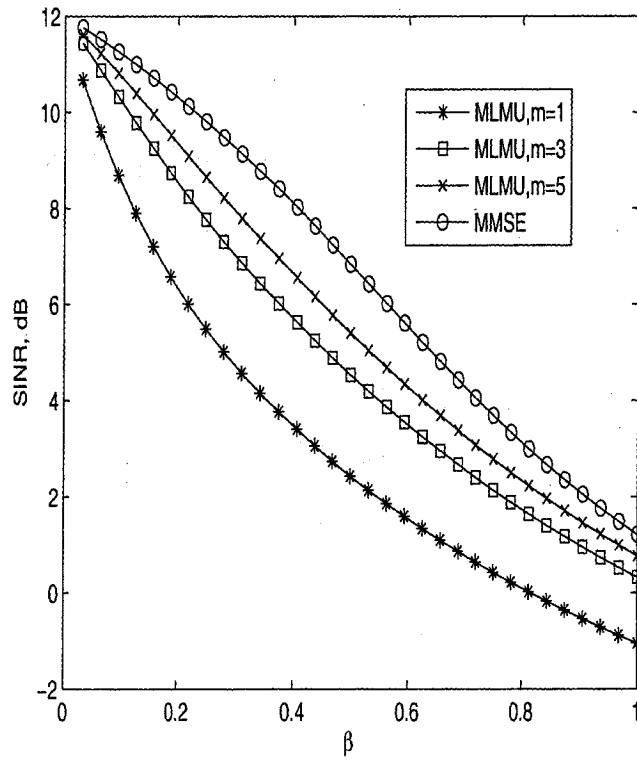


Figure 6.1: Large-system SINR of the MMSE-based MLMU receiver in a multipath fading channel versus system load for $L = 2$ and $SNR = 12.0$ dB.

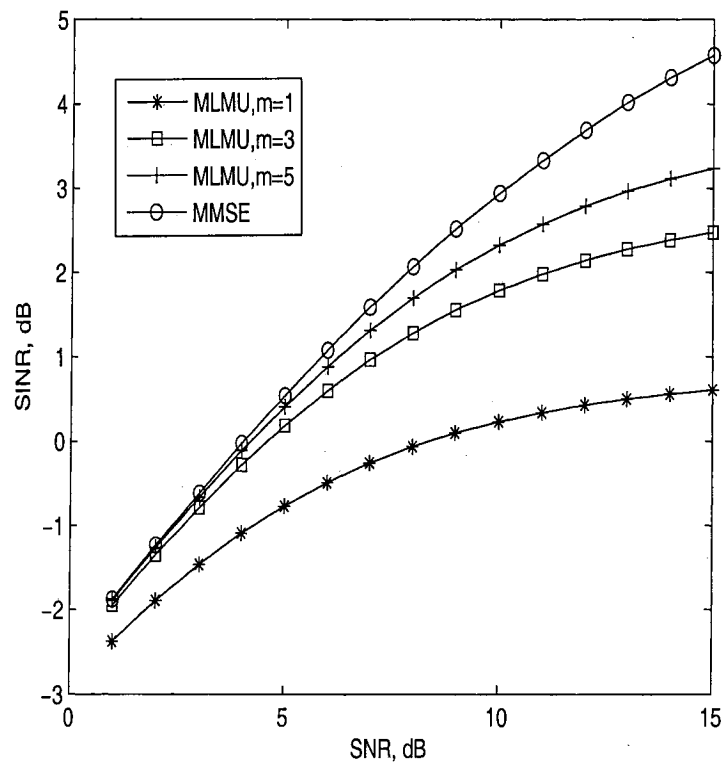


Figure 6.2: Large-system SINR of the MMSE-based MLMU receiver in a multipath fading channel versus SNR for $L = 3$ and $\beta = 0.5$.

Figure 6.3 shows the large-system performance of the MLMU receiver in a multipath fading channel versus the number of resolvable paths when the SNR and the system load are known. As is seen, the performance degrades very fast as the number of paths increases.

Figure 6.4 shows the bit error rate (BER) improvement of the MLMU receiver in a multipath fading environment versus the system load. In this figure, it is assumed that $P_b = Q(\sqrt{SINR_m^{PPIC}})$ where $Q(x) = 1/(\sqrt{2\pi}) \int_x^\infty \exp(-t^2/2) dt$. This figure once more shows that the performance of the MLMU receiver converges to that of the MMSE receiver.

Figures 6.5 and 6.6 show the BER of the MLMU receiver versus the SNR and the number of resolvable paths, respectively.

6.2 Channel Estimation

Concerning the channel estimation problem, an iterative method for channel estimation was proposed in [56]. However, it does not consider the large-system case. In [57] and [58], a channel estimation method for the large-system case was introduced only for a single path fading channel. Finally, in [51], a multistage channel estimation for the large system case in a multipath fading channel was proposed. We introduce a simple multistage channel estimation scheme. This is done by introducing a new expression for the covariance matrix of the interference term, compared to [50] and [51], which results in a simpler and more efficient approach to large-system analysis. The moments of the covariance matrix of the signature sequences and channel gains will be found as well. In this thesis, the SINR, the estimated channel gains and the corresponding MSEs are expressed in terms of the SNR, which makes the expressions functions of more familiar terms. In [50] and [51], the expressions were functions of the noise level. From Chapter 2, we approximate the estimate of the

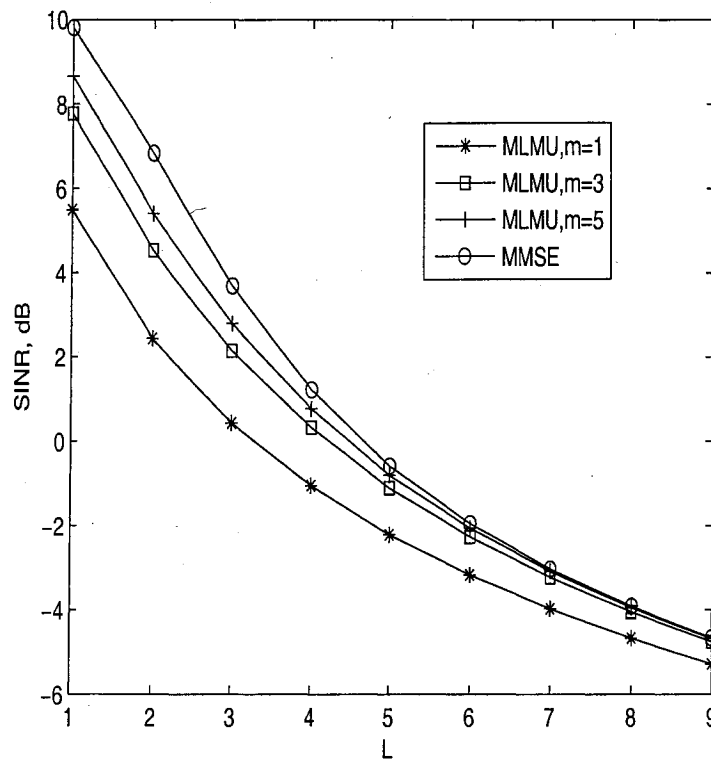


Figure 6.3: Large-system SINR of the MMSE-based MLMU receiver in a multipath fading channel versus the number of resolvable paths for $SNR = 12.0$ dB and $\beta = 0.5$.

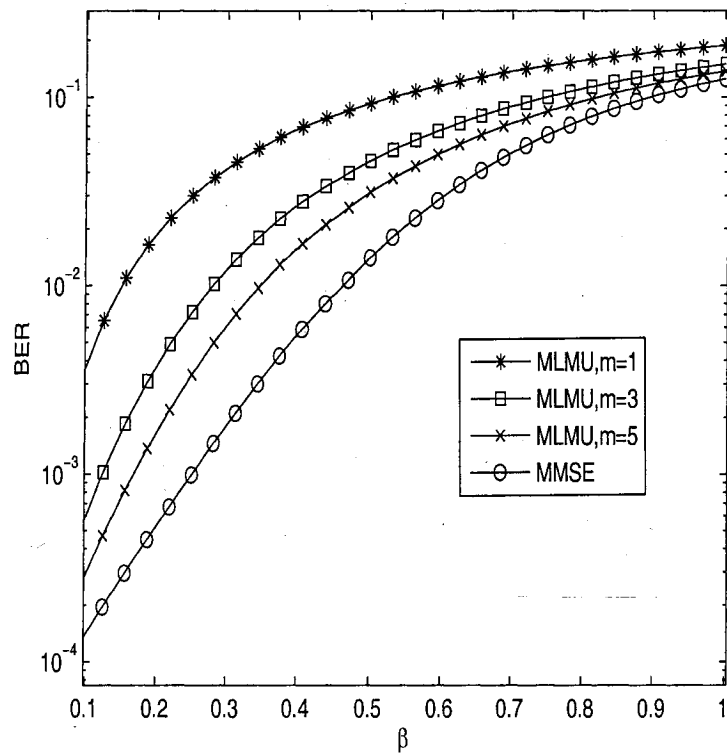


Figure 6.4: Large-system BER of the MMSE-based MLMU receiver in a multipath fading channel versus system load for $L = 2$ and $SNR = 12.0$ dB.

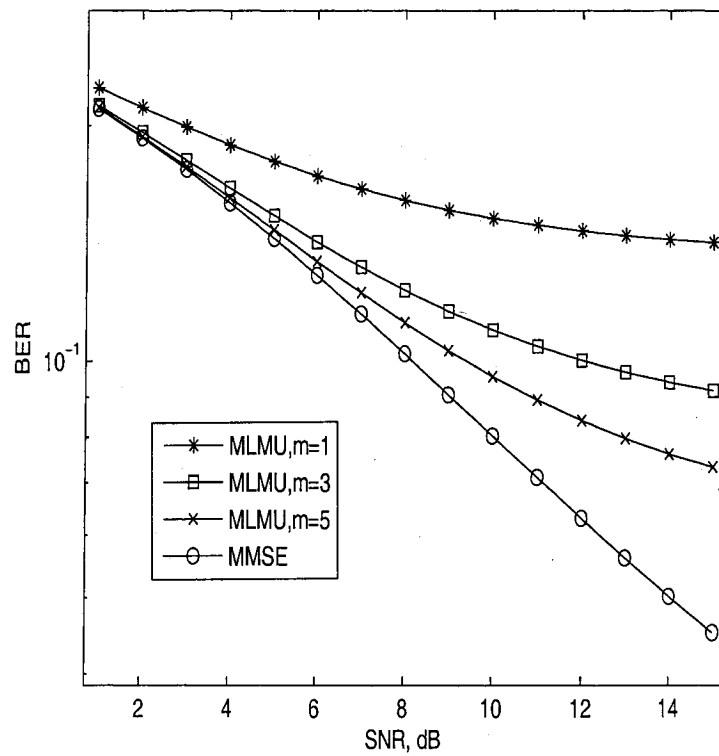


Figure 6.5: Large-system BER of the MMSE-based MLMU receiver in a multipath fading channel versus SNR for $L = 3$ and $\beta = 0.5$.

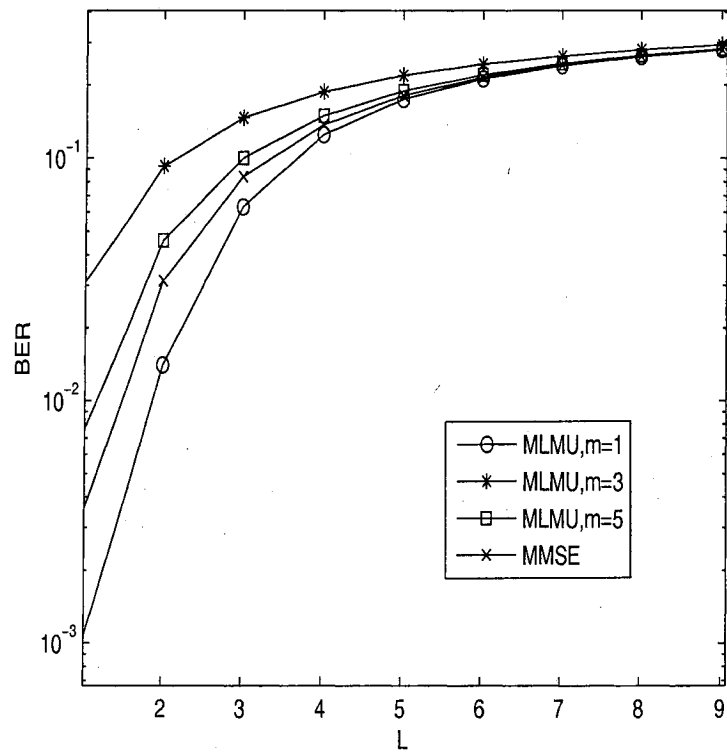


Figure 6.6: Large-system BER of the MMSE-based MLMU receiver in a multipath fading channel versus L for $SNR = 12.0$ dB and $\beta = 0.5$.

channel gain for the first user and the first path as

$$\tilde{a}_{11} = \tau^{-1/2} \bar{\mathbf{s}}_{11}^H \left(\sum_{i=0}^m X_i \mathbf{B}_1^i \right) \bar{\mathbf{r}} \quad (6.6)$$

where X_i is a scalar and

$$\mathbf{B}_1 = \bar{\mathbf{S}}_{11} \mathbf{A}_{11} \bar{\mathbf{S}}_{11}^H + \frac{1}{\tau} \frac{\sigma^2}{P} \mathbf{I} \quad (6.7)$$

Theorem 6.2.1 *The large-system multistage MSE_{11} at the stage m is*

$$MSE_{11}^m = (\mathbf{X}\Lambda)(\mathbf{X}\Lambda)^H + \mathbf{X}\mathbf{R}\mathbf{X}^H + 1 - 2\mathbf{X}\Lambda \quad (6.8)$$

where it is minimum when
$$\mathbf{X} = \frac{\mathbf{R}^{-1}\Lambda}{\Lambda^H \mathbf{R}^{-1}\Lambda + 1} \quad (6.9)$$

and the definitions of Λ and \mathbf{R} are according to Theorem 6.1.1.

Proof: See Appendix B. □

The following theorem, gives the moments that are required to calculate Λ and \mathbf{R} .

Theorem 6.2.2 *For a multipath fading channel with L distinct paths and τ training symbols, the large-system i th moment of the eigenvalues of the matrix $\bar{\mathbf{S}}_{11} \mathbf{A}_{11} \bar{\mathbf{S}}_{11}^H$ becomes*

$$M_i = E[\lambda^i] = \sum_{j=1}^i \left(\frac{\beta L}{\tau} \right)^j \sum_{m_1 + \dots + m_j = m} c(m_1, \dots, m_j) E[\Delta^{m_1}] \dots E[\Delta^{m_j}] \quad (6.10)$$

Proof: The proof is the same as Theorem 6.1.2 except that in order to cancel the effect of training symbols, the moments are divided by the number of training symbols. All coefficients are defined according to Theorem 6.1.2. □

The multistage channel estimation scheme introduced in this section has the following advantages compared to the scheme proposed in [51]. First of all, the estimated channel gains and their corresponding MSEs are calculated in a simpler fashion. This is due to the fact that we introduce a new expression for the covariance matrix of the interference term. Moreover, the found estimates and their related

MSEs are functions of the SNR instead of the background noise level only, which makes the expressions as functions of more familiar terms.

In order to gauge the efficiency of our proposed estimation method, some numerical examples follow. Figure 6.7 shows the large-system MSE of the proposed multistage channel estimation versus system load for fixed SNR, number of training symbols, and number of resolvable paths. As is seen from this figure, the multistage MSE converges to that of the MMSE case. The reason that the multistage estimation scheme does not provide the same performance as that of the MMSE case is because the number of training sequences should be larger as Figure 6.8 proves this matter.

Figure 6.8 shows the large-system MSE of the proposed multistage channel estimation versus the number of training symbols for known system load, SNR, and number of resolvable paths.

Figure 6.9 shows the large-system MSE of the multistage channel estimation versus the number of resolvable paths when the system load, the SNR, and the number of training symbols are available. Finally, Figure 6.10 shows the large-system MSE of the multistage channel estimation versus the SNR for known system load, number of training symbols, and number of resolvable paths.

6.3 Summary

In this chapter, we introduced a simple method to analyze the large-system performance of the multistage linear multiuser (MLMU) receiver for a CDMA system over a multipath fading channel. Unlike the previously proposed methods, we considered different multipath fading coefficients for different users. Moreover, we gave a new expression for the covariance matrix of the interference term which resulted in a simpler and more efficient approach to find the performance. We also introduced a simple multistage method to estimate the fading channel gains. Numerical examples showed that the performance of the MLMU receiver converges to that of the MMSE receiver with much more affordable complexity, compared to the MMSE case.

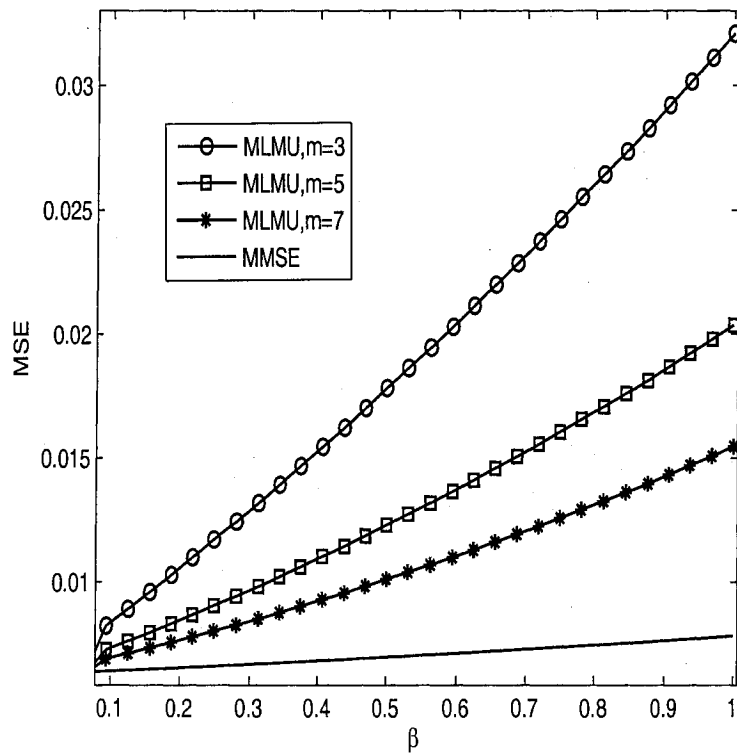


Figure 6.7: Large-system multistage MSE versus system load. $\tau = 10$, $L = 2$, and $SNR = 12.0$ dB.

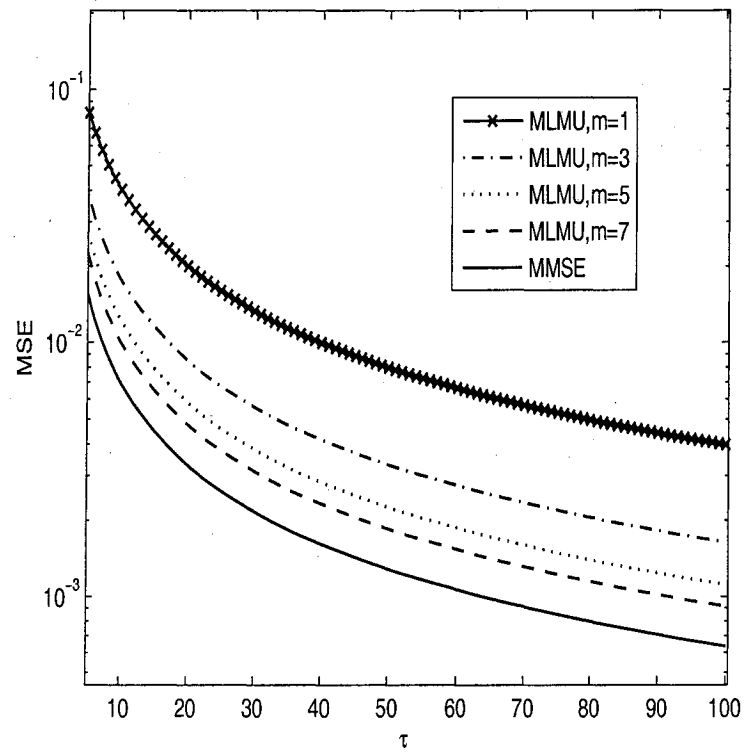


Figure 6.8: Large-system multistage MSE versus number of training symbols. $\beta = 0.5$, $L = 2$, and $SNR = 12.0$ dB.

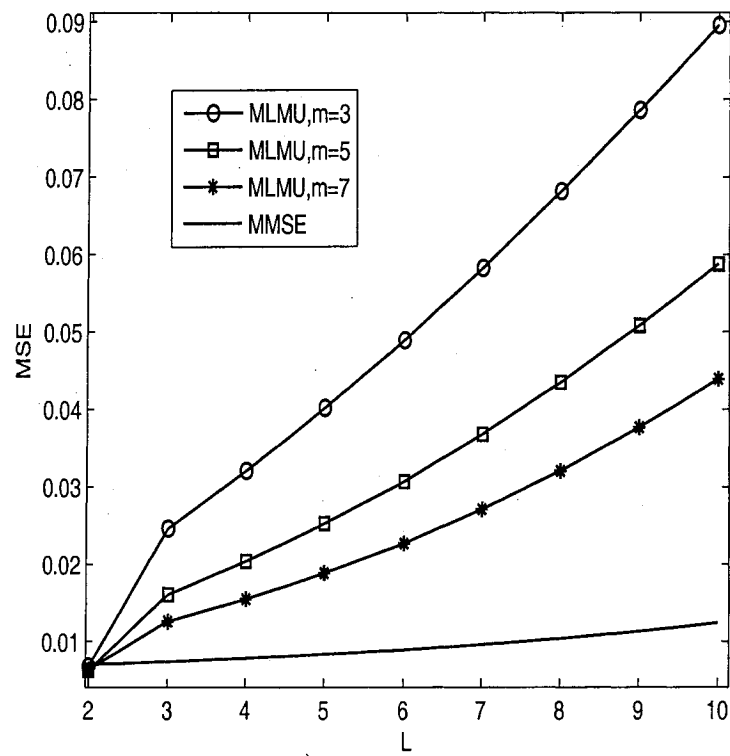


Figure 6.9: Large-system multistage MSE versus number of resolvable paths. $\tau = 10$, $\beta = 0.5$, and $SNR = 12.0$ dB.

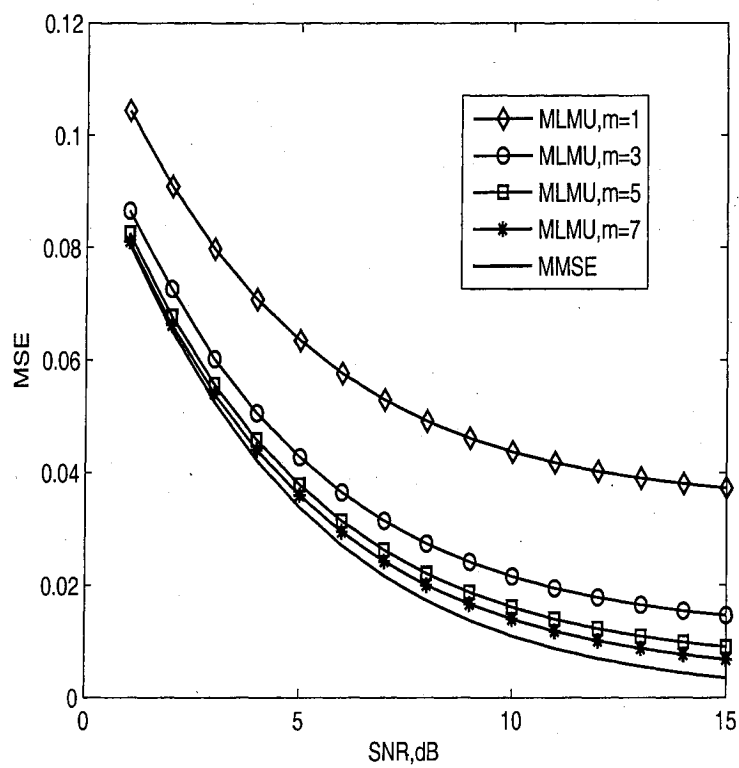


Figure 6.10: Large-system multistage MSE versus SNR. $\tau = 10$, $\beta = 0.5$, and $L = 2$.

Chapter 7

Multistage PPIC Receiver for Asynchronous CDMA Systems

This chapter introduces a low-complexity multistage linear partial parallel interference cancellation (PPIC) receiver for an asynchronous DS-CDMA system. This receiver is suitable for satellite systems using either CDMA or a combination of time division multiple access (TDMA) and CDMA [59]. The figure of merit to evaluate the performance is the signal-to-interference-plus-noise ratio (SINR) that will be calculated by using the moments of the eigenvalues of the covariance matrix. The optimum performance of the investigating receiver will be established by adjusting different system parameters such as the partial cancellation factor (PCF), the number of interference cancellation stages, the system load, and the signal to noise ratio (SNR). It will be seen that the SINR of the PPIC receiver converges to that of the minimum mean-squared error (MMSE) receiver with much less complexity compared to the MMSE receiver.

The proposed multistage linear PPIC receiver is presented in Section 7.1. The behavior of the proposed scheme is investigated in Section 7.2 by tuning different system parameters in order to find the region where the system achieves its optimum performance. Finally, conclusions are included in Section 7.3.

7.1 Multistage Linear PPIC Receiver

For an m -stage partial parallel interference cancellation (PPIC) receiver with the PCF of μ , the demodulator \mathbf{c}_1 is defined as

$$\mathbf{c}_{1,m}^{PPIC} = \mu \left(\sum_{i=0}^m \left[\mathbf{I} - \mu (\mathbf{S}_1 \mathbf{S}_1^H + \frac{\sigma^2}{P} \mathbf{I}) \right]^i \right) \mathbf{s}_1 \quad (7.1)$$

where \mathbf{S}_1 is defined according to (2.63). The definition in (7.1) is the extension of the demodulator \mathbf{c}_1 introduced in [45] to an asynchronous case. The SINR for asynchronous PPIC receiver for the first user is defined as

$$SINR_{1,m}^{PPIC} = \frac{(\eta_m)^2}{\nu_m} \quad (7.2)$$

where by doing the same manipulation introduced in [45], we get

$$\eta_m = \sum_{i=0}^m (-\mu)^i \sum_{j=0}^i \left(\frac{\sigma^2}{P} - \frac{1}{\mu} \right)^{i-j} \binom{i}{j} M_j \quad (7.3)$$

and

$$\nu_m = \sum_{i=0}^m \sum_{j=0}^m (-\mu)^{i+j} \sum_{l=0}^{i+j} \left(\frac{\sigma^2}{P} - \frac{1}{\mu} \right)^{i+j-l} \binom{i+j}{l} \times \left(M_{l+1} + \frac{\sigma^2}{P} M_l \right) \quad (7.4)$$

with

$$M_i = \mathbf{s}_1^H (\mathbf{S}_1 \mathbf{S}_1^H)^i \mathbf{s}_1 \quad (7.5)$$

Note that the extreme cases of our proposed receiver are single-user matched-filter (SUMF) and minimum mean-squared error (MMSE) receivers (i.e., $m = 0$ and $m \rightarrow \infty$, respectively).

7.2 Performance Evaluation

The performance evaluation of the investigating receiver is done by tuning different parameters of the multistage linear PPIC receiver in an asynchronous environment

where it is assumed that all users arrive at the receiver with the same power level. Extension of the system to an unequal-power case is possible through the lines of [46]. For all simulations, purely random signature sequences are considered, although it is assumed that these signature sequences are known to the receiver. All simulations are averaged over 1000 samples.

7.2.1 Performance Versus Number of Stages

In order to find out the optimum number of interference cancellation stages (m), the performance improvement of the multistage linear PPIC receiver versus the number of the interference cancellation stages is investigated in Figure 7.1 by adjusting the PCF (μ) for fixed SNR and system load ($\beta = K/N$). As this figure indicates, the value of the PCF has a crucial impact on the performance of the multistage linear PPIC receiver such that a wrong selection of this factor will result in a poor performance. Therefore, the anomalies in the figure show the unstable regions due to an improper selection of the PCF. This means that for a given SNR, system load and number of interference cancellation stages, the PCF has to be selected from stable regions in order to obtain the best performance. As is seen, by letting the PCF be any value between 0.3 and 0.5, the optimum performance is achieved.

Figure 7.2 depicts the performance improvement of the multistage linear PPIC receiver versus the number of interference cancellation stages when the SNR, the system load, and the PCF are known. As is seen from this figure, the performance of the multistage linear PPIC receiver converges to that of the MMSE receiver as the number of interference cancellation stages increases. However, unlike the MMSE case, this performance is achieved without any need to calculate the inverse of the covariance matrix of signature sequences which results in a much less complexity. In summary, by choosing a proper PCF, the performance of the MMSE receiver is almost achieved when the number of interference cancellation stages is greater than 15.

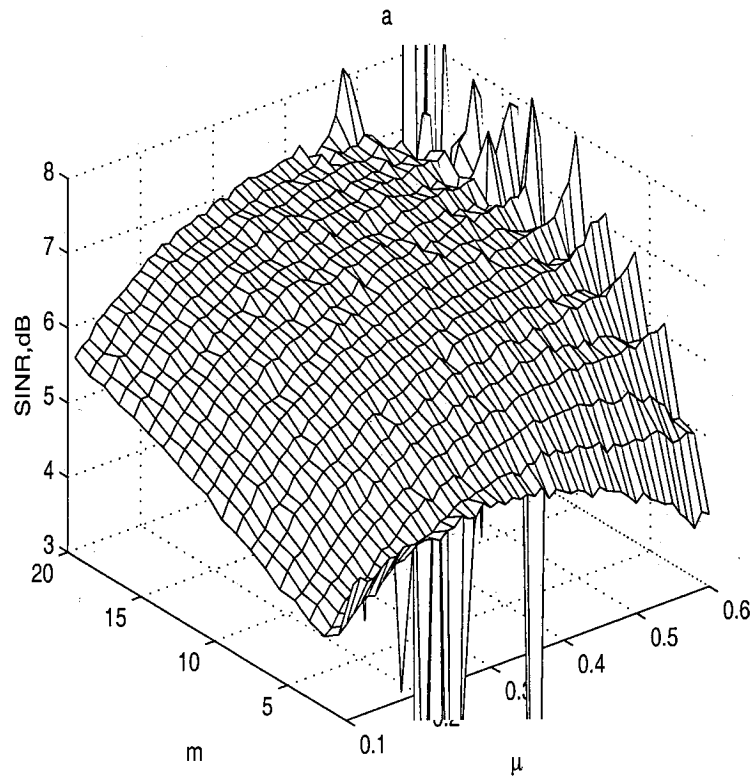


Figure 7.1: SINR improvement of the multistage linear PPIC receiver for an asynchronous CDMA system over an AWGN channel versus PCF (μ) and the number of the interference cancellation stages (m), $SNR = 12.0dB$, $K = 16$, $N = 32$ (system load $\beta = K/N = 0.5$).

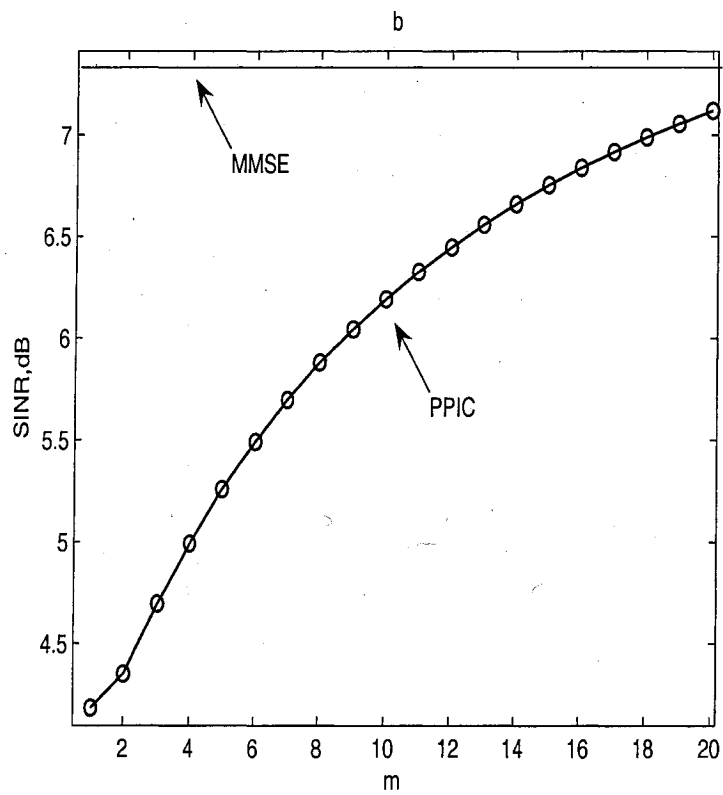


Figure 7.2: SINR improvement of the multistage linear PPIC receiver for an asynchronous CDMA system over an AWGN channel versus m , $SNR = 12.0dB$, $K = 16$, $N = 32$ ($\beta = 0.5$), and $\mu = 0.4$.

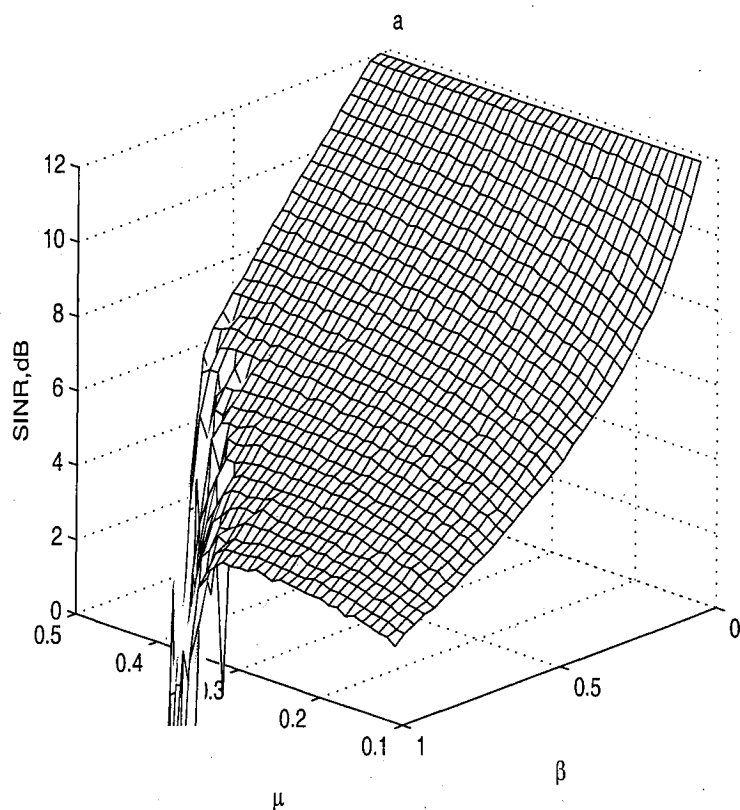


Figure 7.3: SINR of the multistage linear PPIC receiver for an asynchronous CDMA system over an AWGN channel versus μ and β , $SNR = 12.0dB$, $N = 32$, $m = 15$.

7.2.2 Performance Versus System Load

Figure 7.3 shows the performance of the multistage linear PPIC receiver versus PCF and system load when the SNR and the number of interference cancellation stages are known. According to this figure, in order to obtain the best performance, the PCF should be picked up between 0.2 and 0.4, especially, when the system is highly loaded (*i.e.*, $\beta \rightarrow 1$).

Figure 7.4 shows the performance of the multistage linear PPIC receiver versus system load for fixed SNR, number of interference cancellation, and PCF. As is perceived from this figure, the performance of the multistage linear PPIC receiver

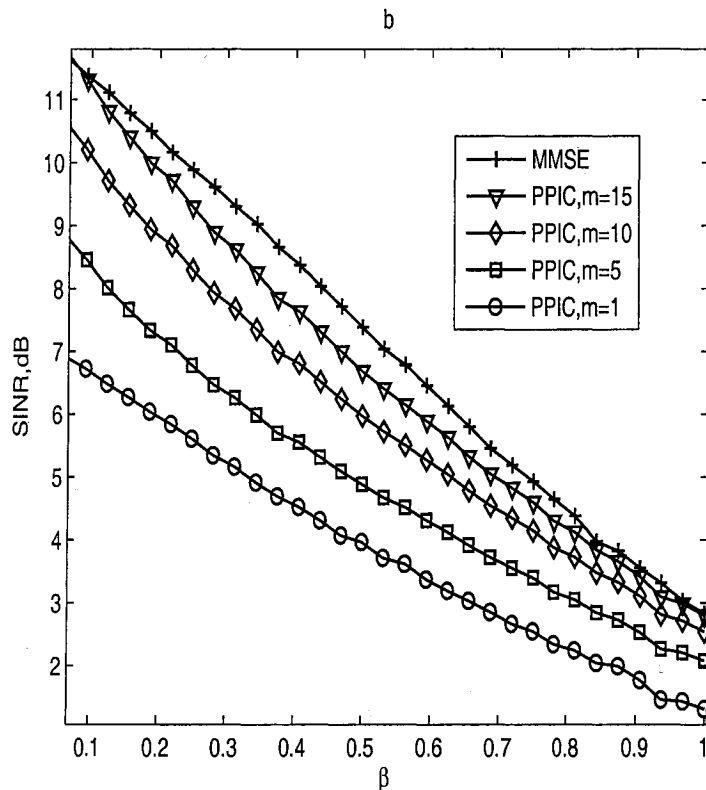


Figure 7.4: SINR of the multistage linear PPIC receiver for an asynchronous CDMA system over an AWGN channel versus β , $SNR = 12.0dB$, $N = 32$, $m = 15$, and $\mu = 0.3$.

converges to that of the MMSE receiver as the number of interference cancellation stages increases.

7.2.3 Performance Versus SNR

Figure 7.5 shows the performance of the multistage linear PPIC receiver versus PCF and SNR when the system load and the number of interference cancellation stages are known. From this figure, the best performance is achieved when the PCF is chosen between 0.3 and 0.5 for moderate to high SNR levels.

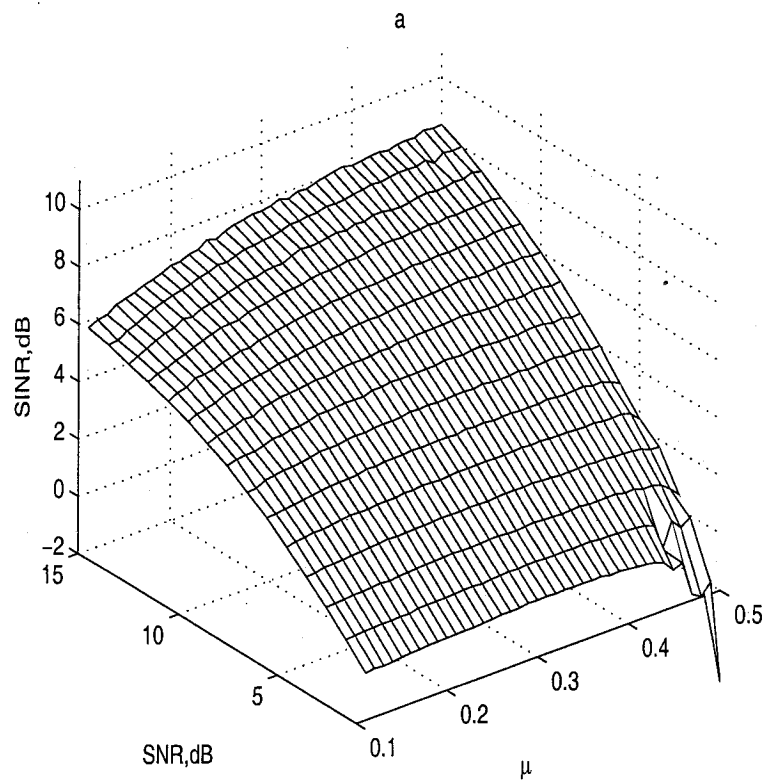


Figure 7.5: SINR of the multistage linear PPIC receiver for an asynchronous CDMA system over an AWGN channel versus μ and SNR, $N = 32$, $K = 16$, $m = 15$.

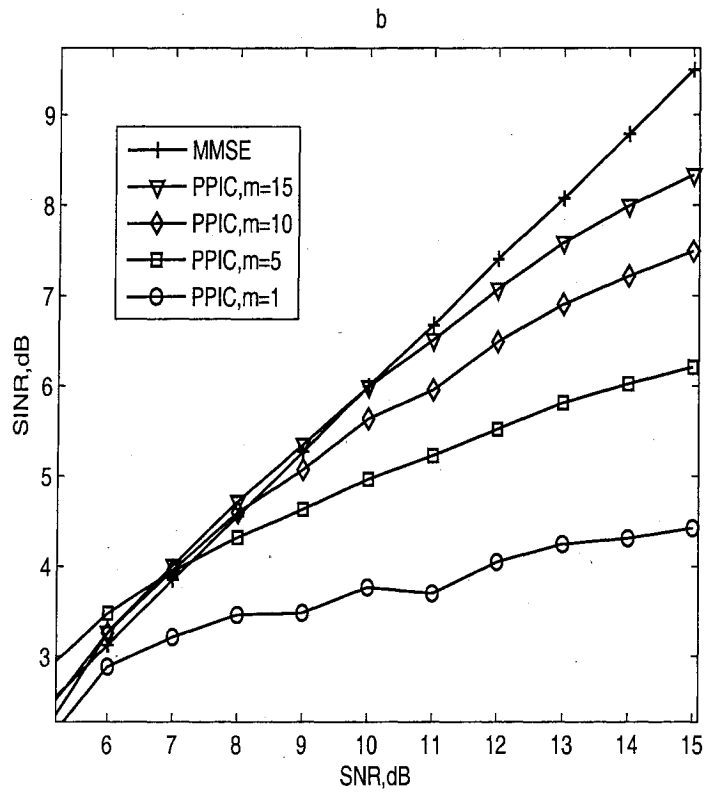


Figure 7.6: SINR of the multistage linear PPIC receiver for an asynchronous CDMA system over an AWGN channel versus μ and SNR, $N = 32$, $K = 16$, $m = 15$, $\mu = 0.5$.

Figure 7.6 shows the performance of the multistage linear PPIC receiver versus SNR for fixed system load, number of interference cancellation, and PCF. Once again, it is seen that the performance of the multistage linear PPIC receiver converges to that of the MMSE receiver for moderate to high SNR levels as the number of interference cancellation stages increases.

It is noted that compared to the results obtained in [45] and [47], the performances of PPIC and MMSE receivers are significantly degraded due to asynchrony.

Regarding all simulation results, the best performance is achieved when the PCF is between 0.3 and 0.5; and the number of stages is greater than 15 for a moderate to high SNR level.

7.3 Summary

In this chapter, we introduced a multistage linear partial parallel interference cancellation (PPIC) receiver for an asynchronous CDMA system. Since the proposed receiver provides a good compromise among the performance, the complexity, and the processing delay, it is suitable for satellite communication systems using either CDMA or evolutionary CDMA (combination of CDMA and TDMA). The performance of our proposed receiver was evaluated by using the moments of the eigenvalues of the covariance matrix. By investigating the behavior of the introduced scheme, the appropriate regions to choose the partial cancellation factor and the number of interference cancellation stages were determined. In this case, the performance of the multistage PPIC receiver converges to that of the MMSE receiver with less complexity compared to the MMSE receiver.

Chapter 8

Conclusions and Suggestions for Future Work

8.1 Conclusions

In this thesis, we introduced a simple approach for calculating the optimum partial cancellation factors (PCF) for the partial parallel interference cancellation (PPIC) receiver in a synchronous CDMA system over AWGN and frequency-flat fading channels. These factors were found for a case where the number of active users and the processing gain tend towards infinity while their ratio is finite. The found PCF is a function of the number of interference cancellation stages, the moments of the eigenvalues of the covariance matrix, the system load, and the signal-to-noise ratio (SNR). Simulation results showed that by using our proposed method, the performance of the PPIC receiver converges to that of the minimum mean-squared error (MMSE) receiver. When comparing our method with the previously proposed methods, one can point out some advantages. Firstly, it is less complex due to the fact that the calculated PCFs are explicit functions of the moments of the eigenvalues of the covariance matrix. Secondly, there is no need to know the number of interference cancellation stages *a priori*. Finally, there is no need for the

PCFs to be ordered. This last advantage results in even more simplicity in circuitry.

We found a closed-form expression for the large-system performance of the multistage linear partial parallel interference cancellation receiver for the CDMA system over a frequency-flat fading channel. It was shown that the large-system performance has a closed-form expression that is a function of the system load, the partial cancellation factor, the number of interference cancellation stages, the SNR, and the received powers of interfering users. Using the proposed tool, the performance of the PPIC can be calculated more precisely with a considerable saving on the processing time compared to the numerical simulations.

We also introduced a multistage linear PPIC receiver whose performance converges to that of the MMSE receiver by applying a variable PCF. It was shown that the signal to interference-plus-noise ratio (SINR) is a function of the number of interference cancellation stages, the moments of the eigenvalues of the covariance matrix and the SNR. Compared to the existing schemes for the multistage linear PPIC receiver, our proposed scheme provides the following benefits. First of all, with fewer stages of interference cancellation, its performance converges to that of the MMSE receiver that provides the best performance among the linear multiuser receivers. Secondly, our proposed receiver is more robust for high system loads and high SNR levels; and finally, the expression for the performance is found directly without using any orthogonalization algorithm.

We extended our proposed scheme to analyze the large-system performance of the multistage linear multiuser (MLMU) receiver for a CDMA system over a multipath fading channel. Unlike the previously proposed methods, we considered different multipath fading coefficients for different users. Moreover, we proposed a new expression for the covariance matrix of the interference term which resulted in a more efficient and simpler approach to find the performance. We also introduced a simple multistage method to estimate the fading channel gains. Numerical examples show that by using our approach for data and channel estimation, the performance

of the MLMU receiver will converge to that of the MMSE receiver with much more affordable complexity, compared to the MMSE case.

Regarding asynchronous case, we introduced a multistage linear PPIC receiver for an asynchronous CDMA system. Since the proposed receiver provides a good compromise among the performance, the complexity and the processing delay, it is suitable for satellite communication systems using either CDMA or evolutionary CDMA (combination of CDMA and TDMA). The performance of our proposed receiver was evaluated by using the moments of the eigenvalues of the covariance matrix. By investigating the behavior of the introduced scheme, the proper regions to choose the partial cancellation factor and the number of interference cancellation stages were determined. In this case, the performance of the multistage PPIC receiver converges to that of the MMSE receiver with less complexity.

8.2 Directions for Further Research

The topics for further research are

- Large-system design and analysis of the MLMU receiver for asynchronous CDMA systems.
- Large-system design and analysis of the MLMU receiver for coded CDMA systems with different coding schemes.
- Multistage channel estimation of asynchronous CDMA system over multipath fading channels.
- Multistage channel estimation of coded CDMA systems with different coding schemes.

Appendix A

Proof of Theorem 6.1.1

The decision statistic can be written as

$$\tilde{b}_1 = \mathbf{x} \cdot \mathbf{Z} \quad (\text{A.1})$$

with

$$\mathbf{x} = [x_0, x_1, \dots, x_m] \quad (\text{A.2})$$

and

$$\mathbf{Z} = \begin{bmatrix} \mathbf{a}_1^H \mathbf{s}_1^H \\ \mathbf{a}_1^H \mathbf{s}_1^H \mathbf{B}_1 \\ \vdots \\ \mathbf{a}_1^H \mathbf{s}_1^H \mathbf{B}_1^m \end{bmatrix} \cdot \mathbf{r}. \quad (\text{A.3})$$

Eventually, the vector \mathbf{z} can be written as

$$\mathbf{Z} = b_1 \mathbf{M} + \mathbf{N} \quad (\text{A.4})$$

where the second term of (A.4) is the interference (the MAI plus the background noise) term and

$$\mathbf{M} = \begin{bmatrix} \mathbf{a}_1^H \mathbf{s}_1^H \mathbf{s}_1 \mathbf{a}_1 \\ \mathbf{a}_1^H \mathbf{s}_1^H \mathbf{B}_1 \mathbf{s}_1 \mathbf{a}_1 \\ \vdots \\ \mathbf{a}_1^H \mathbf{s}_1^H \mathbf{B}_1^m \mathbf{s}_1 \mathbf{a}_1 \end{bmatrix} \quad (\text{A.5})$$

and

$$\mathbf{N} = \begin{bmatrix} \mathbf{a}_1^H \mathbf{s}_1^H (\mathbf{S}_1 \mathbf{A}_1^{1/2} \mathbf{b}_1 + \mathbf{n}) \\ \mathbf{a}_1^H \mathbf{s}_1^H \mathbf{B}_1 (\mathbf{S}_1 \mathbf{A}_1^{1/2} \mathbf{b}_1 + \mathbf{n}) \\ \vdots \\ \mathbf{a}_1^H \mathbf{s}_1^H \mathbf{B}_1^m (\mathbf{S}_1 \mathbf{A}_1^{1/2} \mathbf{b}_1 + \mathbf{n}) \end{bmatrix} \quad (\text{A.6})$$

The MSE is defined as

$$\begin{aligned} \text{MSE}_1 &= E[|\tilde{b}_1 - b_1|^2] = E[|\mathbf{xZ} - b_1|^2] \\ &= E[(\mathbf{xZ})(\mathbf{Zx})^H + 1 - 2b_1 \mathbf{xZ}] \\ &= \mathbf{x} \boldsymbol{\Lambda} \mathbf{x}^H + \mathbf{xR} \mathbf{x}^H + 1 - 2\mathbf{x}\boldsymbol{\Lambda} \end{aligned} \quad (\text{A.7})$$

where

$$\begin{aligned} \boldsymbol{\Lambda} = E[\mathbf{M}] &= E \begin{bmatrix} \mathbf{a}_1^H \mathbf{s}_1^H \mathbf{s}_1 \mathbf{a}_1 \\ \mathbf{a}_1^H \mathbf{s}_1^H \mathbf{B}_1 \mathbf{s}_1 \mathbf{a}_1 \\ \vdots \\ \mathbf{a}_1^H \mathbf{s}_1^H \mathbf{B}_1^m \mathbf{s}_1 \mathbf{a}_1 \end{bmatrix} \\ &= \begin{bmatrix} M_0 \\ M_1 + \frac{\sigma^2}{P} \\ \vdots \\ \sum_{i=0}^m \binom{m}{i} \left(\frac{\sigma^2}{P}\right)^{(m-i)} M_i \end{bmatrix} \\ &= \begin{bmatrix} \Lambda_0 \\ \Lambda_1 \\ \vdots \\ \Lambda_m \end{bmatrix} \end{aligned} \quad (\text{A.8})$$

with $\Lambda_0 = M_0$, $M_i = E[\mathbf{a}_1^H \mathbf{s}_1^H (\mathbf{S}_1 \mathbf{A}_1 \mathbf{S}_1^H)^i \mathbf{s}_1 \mathbf{a}_1]$, and

$$\Lambda_i = \sum_{j=0}^i \binom{i}{j} \left(\frac{\sigma^2}{P}\right)^{(i-j)} M_j. \quad (\text{A.9})$$

The $(m + 1) \times (m + 1)$ covariance matrix R of the MAI plus noise term is calculated as

$$\mathbf{R} = E[\mathbf{N}\mathbf{N}^H] = \begin{bmatrix} \Lambda_1 & \Lambda_2 & \dots & \Lambda_{m+1} \\ \Lambda_2 & \Lambda_3 & \dots & \Lambda_{m+2} \\ \vdots & & & \\ \Lambda_{m+1} & \Lambda_{m+2} & \dots & \Lambda_{2m+1} \end{bmatrix} \quad (\text{A.10})$$

Finding the derivative of (A.7) w.r.t. \mathbf{x} and equating to zero yields

$$\mathbf{x} = \frac{\mathbf{R}^{-1}\boldsymbol{\Lambda}}{1 + \boldsymbol{\Lambda}^H \mathbf{R}^{-1} \boldsymbol{\Lambda}} \quad (\text{A.11})$$

The decision statistic by substituting (A.4) into (A.1) becomes

$$\tilde{b}_1 = \mathbf{x} \cdot \mathbf{Z} = \mathbf{x}(b_1 \mathbf{M} + \mathbf{N}) = b_1 \mathbf{x} \mathbf{M} + \mathbf{x} \mathbf{N} \quad (\text{A.12})$$

where the first term in (A.12) is the useful signal and the second term is the MAI plus the background noise. The SINR by substituting for \mathbf{x} from (A.11) is calculated as

$$SINR_1 = \frac{E[(b_1 \mathbf{x} \mathbf{M})^2]}{E[(\mathbf{x} \mathbf{N})^2]} = \boldsymbol{\Lambda}^H \mathbf{R}^{-1} \boldsymbol{\Lambda}. \quad (\text{A.13})$$

Appendix B

Proof of Theorem 6.2.1

The estimated channel gain for the first user and the first path can be written as

$$\tilde{a}_{11} = \mathbf{X} \cdot \mathbf{Z} \quad (\text{B.1})$$

with

$$\mathbf{X} = [X_0, X_1, \dots, X_m] \quad (\text{B.2})$$

and

$$\mathbf{Z} = \tau^{-1/2} \begin{bmatrix} \bar{\mathbf{s}}_{11}^H \\ \bar{\mathbf{s}}_{11}^H \mathbf{B}_1 \\ \vdots \\ \bar{\mathbf{s}}_{11}^H \mathbf{B}_1^m \end{bmatrix} \cdot \mathbf{r}. \quad (\text{B.3})$$

Eventually,

$$\mathbf{Z} = a_{11} \mathbf{M} + \tau^{-1/2} \mathbf{N} \quad (\text{B.4})$$

where

$$\mathbf{M} = \begin{bmatrix} \bar{\mathbf{s}}_{11}^H \bar{\mathbf{s}}_{11} \\ \bar{\mathbf{s}}_{11}^H \mathbf{B}_1 \bar{\mathbf{s}}_{11} \\ \vdots \\ \bar{\mathbf{s}}_{11}^H \mathbf{B}_1^m \bar{\mathbf{s}}_{11} \end{bmatrix} \quad (\text{B.5})$$

and

$$\mathbf{N} = \begin{bmatrix} \bar{\mathbf{s}}_{11}^H (\tau^{1/2} \bar{\mathbf{S}}_{11} \mathbf{a}_{11} + \bar{\mathbf{n}}) \\ \bar{\mathbf{s}}_{11}^H \mathbf{B}_1 (\tau^{1/2} \bar{\mathbf{S}}_{11} \mathbf{a}_{11} + \bar{\mathbf{n}}) \\ \vdots \\ \bar{\mathbf{s}}_{11}^H \mathbf{B}_1^m (\tau^{1/2} \bar{\mathbf{S}}_{11} \mathbf{a}_{11} + \bar{\mathbf{n}}) \end{bmatrix} \quad (\text{B.6})$$

The MSE is defined as

$$\begin{aligned} \text{MSE}_{11} &= E[|\tilde{a}_{11} - a_{11}|^2] = E[|\mathbf{XZ} - a_{11}|^2] \\ &= E[(\mathbf{XZ})(\mathbf{XZ})^H + 1 - 2a_{11}\mathbf{XZ}] \\ &= (\mathbf{X}\Lambda)(\mathbf{X}\Lambda)^H + \mathbf{X}\mathbf{R}\mathbf{X}^H + 1 - 2\mathbf{X}\Lambda \end{aligned} \quad (\text{B.7})$$

where

$$\begin{aligned} \Lambda = E[\mathbf{M}] &= E \begin{bmatrix} \bar{\mathbf{s}}_{11}^H \bar{\mathbf{s}}_{11} \\ \bar{\mathbf{s}}_{11}^H \mathbf{B}_1 \bar{\mathbf{s}}_{11} \\ \vdots \\ \bar{\mathbf{s}}_{11}^H \mathbf{B}_1^m \bar{\mathbf{s}}_{11} \end{bmatrix} \\ &= \begin{bmatrix} M_0 \\ M_1 + \frac{1}{\tau} \cdot \frac{\sigma^2}{P} \\ \vdots \\ \sum_{i=0}^m \binom{m}{i} \left(\frac{1}{\tau} \cdot \frac{\sigma^2}{P}\right)^{(m-i)} M_i \end{bmatrix} \\ &= \begin{bmatrix} \Lambda_0 \\ \Lambda_1 \\ \vdots \\ \Lambda_m \end{bmatrix} \end{aligned} \quad (\text{B.8})$$

with $M_i = E[\bar{\mathbf{s}}_{11}^H (\bar{\mathbf{S}}_{11} \mathbf{A}_{11} \bar{\mathbf{S}}_{11}^H)^i \bar{\mathbf{s}}_{11}]$ and

$$\Lambda_i = \sum_{j=0}^i \binom{i}{j} \left(\frac{1}{\tau} \cdot \frac{\sigma^2}{P}\right)^{(i-j)} M_j. \quad (\text{B.9})$$

The $(m+1) \times (m+1)$ covariance matrix R of the MAI plus noise term is calculated as

$$\mathbf{R} = E[\mathbf{N}\mathbf{N}^H] = \begin{bmatrix} \Lambda_1 & \Lambda_2 & \dots & \Lambda_{m+1} \\ \Lambda_2 & \Lambda_3 & \dots & \Lambda_{m+2} \\ \vdots & & & \\ \Lambda_{m+1} & \Lambda_{m+2} & \dots & \Lambda_{2m+1} \end{bmatrix} \quad (\text{B.10})$$

Finding the derivative of (B.7) w.r.t. \mathbf{X} and equating to zero yields

$$\mathbf{X} = \frac{\mathbf{R}^{-1}\boldsymbol{\Lambda}}{1 + \boldsymbol{\Lambda}^H \mathbf{R}^{-1} \boldsymbol{\Lambda}}. \quad (\text{B.11})$$

Bibliography

- [1] R. Prasad, T. Ojanpera, "A survey on CDMA: evolution towards wideband CDMA," in *Proc. IEEE Int. Symp. Spread Spect. Techol. Appl.*, vol. 1, pp. 323-331, Sep.2-4, 1998.
- [2] S. Verdu, *Multiuser Detection*, Cambridge, U.K.: Cambridge Univ. Press, 1998.
- [3] D. Guo, S. Verdu, and L.K. Rasmussen, "Asymptotic normality of linear multiuser receiver outputs," *IEEE Trans. Inform. Theory*, vol. 48, pp. 1-16, Dec. 2002.
- [4] L.G.F. Trichard, J.S. Evans, and I.B. Collings, "Optimal linear multistage receivers and the recursive large system SIR," in *Proc. IEEE Int. Symp. Information Theory*, pp. 21-21, Jun.30-Jul.5, 2002.
- [5] L.G.F. Trichard, J.S. Evans, and I.B. Collings, "Optimal linear multistage receivers with unequal power users," in *Proc. IEEE Int. Symp. Information Theory*, pp. 390-390, Jun.29-Jul.4, 2003.
- [6] N. Albeanu and T.J. Lim, "Optimization of linear iterative interference-cancellation receivers for CDMA communications," *IEEE Trans. Commun.*, vol. 52, pp. 376-379, Mar. 2004.
- [7] K. Yu, J.S. Evans, and I.B. Collings, "Performance analysis of LMMSE receivers for M-ary QAM in Rayleigh faded CDMA channels," *IEEE Trans. Veh. Technol.*, vol. 52, pp. 1242-1253, Sep. 2003.

- [8] S. Shamai and S. Verdu, "The impact of frequency-flat fading on the spectral efficiency of CDMA," *IEEE Trans. Inform. Theory*, vol. 47, pp. 1302-1327, May 2001.
- [9] R.R. Muller and S. Verdu, "Design and analysis of low-complexity interference mitigation on vector channels," *IEEE J. Select. Areas Commun.*, vol. 19, pp. 1429-1441, Aug. 2001.
- [10] M. Debbah, W. Hachem, P. Loubaton, and M. de Courville, "MMSE analysis of certain large isometric random precoded systems," *IEEE Trans. Inform. Theory*, vol. 49, pp. 1293-1311, May 2003.
- [11] S. Verdu and S. Shamai, "Spectral efficiency of CDMA with random spreading," *IEEE Trans. Inform. Theory*, vol. 45, pp. 622-640, Mar. 1999.
- [12] A. Abdi, H. Hashemi, and S. Nader-Esfahani, "On the PDF of the sum of random vectors" *IEEE Trans. Commun.*, vol. 48, pp. 7-12, Jan. 2000.
- [13] S. Verdu, "Multiple-access channels with memory with and without frame synchronism" *IEEE Trans. Inform. Theory*, vol. 35, pp. 605-619, May 1989.
- [14] R.S. Cheng and S. Verdu, "The effect of asynchronism on the total capacity of Gaussian multiple-access channels" *IEEE Trans. Inform. Theory*, vol. 38, pp. 2-13, Jan. 1992.
- [15] S. Verdu, "The capacity region of the symbol-asynchronous Gaussian multiple-access channel" *IEEE Trans. Inform. Theory*, vol. 35, pp. 733-751, Jul. 1989.
- [16] R.K. Mallik, "On multivariate Rayleigh and exponential distributions," *IEEE Trans. Inform. Theory*, vol. 49, pp. 1499-1515, Jun. 2003.
- [17] A.D. Wyner, "Recent results in the Shannon theory," *IEEE Trans. Inform. Theory*, vol. 20, pp. 2-10, Jan. 1974.

- [18] D. Guo and S. Verdu, *Multiuser detection and statistical mechanics*, in Communications, Information and Network Security (V. Bhargava, H. V. Poor, V. Tarokh, and S. Yoon, eds.), ch. 13, pp. 229-277, Kluwer Academic Publishers, 2002.
- [19] R.M. Gray, "On the asymptotic eigenvalue distribution of Toeplitz matrices," *IEEE Trans. Inform. Theory*, vol. 18, pp. 725-730, Nov. 1972.
- [20] D. Jonsson, "Some limit theorems for the eigenvalues of a sample covariance matrix," *J. Multivariate Analysis*, pp. 1-38, Dec. 1982.
- [21] M. Ghotbi and M.R. Soleymani, "Computing partial cancellation factors for PPIC receiver in large CDMA over a fading channel," in *Proc. IEEE VTC Fall*, Los Angeles, USA, Sep. 26-29, 2004.
- [22] M. Ghotbi and M.R. Soleymani, "The impact of fading on the performance of large CDMA with parallel interference cancellation," in *Proc. 22nd Biennial Symp. on Commun.*, Kingston, Canada, May 31-Jun. 3, 2004.
- [23] T. Tanaka, "A statistical-mechanics approach to large-system analysis of CDMA multiuser detectors" *IEEE Trans. Inform. Theory*, vol. 48, pp. 2888-2910, Nov. 2002.
- [24] T. Tanaka and M. Okada, "Approximate Belief Propagation, Density Evolution, and Statistical Neurodynamics for CDMA Multiuser Detection" *IEEE Trans. Inform. Theory*, vol. 51, pp. 700-706, Feb. 2005.
- [25] M. Debbah, P. Loubaton, and M. de Courville, "The spectral efficiency of linear precoders" In *Proc. IEEE Information Theory Workshop*, pp. 90-93, Mar.31-Apr.4, 2003.

- [26] J.W. Silverstein and S.I. Choi, "Analysis of the Limiting Spectral Distribution of Large Dimensional Random Matrices" *J. Multivariate Analysis*, vol. 54, pp. 295-309, Aug. 1995.
- [27] J.W. Silverstein and Z.D. Bai, "On the Empirical Distribution of Eigenvalues of a Class of Large Dimensional Random Matrices" *J. Multivariate Analysis*, vol. 54, pp. 175-192, Aug. 1995.
- [28] C.G.F. Valadon, G.A. Verelst, P. Taaghoh, R. Tafazolli, and B.G. Evans, "Code-division multiple access for provision of mobile multimedia services with a geostationary regenerative payload," *IEEE J. Select. Areas Commun.*, vol. 17, pp. 223-237, Feb. 1999.
- [29] S. Moshavi, "Multi-user detection for DS-CDMA communications," *IEEE Commun. Mag.*, vol. 34, pp. 124-136, Oct. 1996.
- [30] D.R. Brown, M. Motani, V.V. Veeravalli, H.V. Poor, and C.R., Johnson, "On the performance of linear parallel interference cancellation," *IEEE Trans. Inform. Theory*, vol. 47, pp. 1957-1970, Jul. 2001.
- [31] D. Divsalar, M.K. Simon, and D. Raphaeli, "Improved parallel interference cancellation for CDMA," *IEEE Trans. Commun.*, vol. 46, pp. 258-268, Feb. 1998.
- [32] D. Koulakiotis and A. H. Aghvami, "Data detection techniques for DS/CDMA mobile systems: a review," *IEEE Personal Commun.*, vol. 7, pp. 24-34, Jun. 2000.
- [33] M.J. Borran and M. Nasiri-Kenari, "An efficient detection technique for synchronous CDMA communication systems based on the expectation maximization algorithm," *IEEE Trans. Veh. Technol.*, vol. 49, pp. 1663-1668, Sep. 2000.

- [34] R.M. Buehrer, "On the convergence of multistage interference cancellation," in *Proc. IEEE Asilomar Sig. Sys. Comp.*, vol. 1, pp. 634-638, Oct. 1999.
- [35] R.M. Buehrer and S.P. Nicoloso, "Comments on partial parallel interference cancellation for CDMA," *IEEE Trans. Commun.*, vol. 47, pp. 658-661, May 1999.
- [36] P. Shan and T.S. Rappaport, "Parallel interference cancellation (PIC) improvements for CDMA multiuser receivers using partial cancellation of MAI estimates," in *Proc. IEEE Globecom 98*, vol. 6, pp. 3282-3287.
- [37] M. Ghotbi and M.R. Soleymani, "Multiuser detection of DS-CDMA signals using partial parallel interference cancellation in satellite communications," *IEEE J. Select. Areas Commun.*, vol. 22, pp. 584-593, Apr. 2004.
- [38] M. Ghotbi and M.R. Soleymani, "Partial parallel interference cancellation of DS-CDMA satellite signals with amplitude and phase estimation," in *Proc. IEEE Globecom*, Taipei, Taiwan, Nov. 17-21, 2002.
- [39] M. Ghotbi and M.R. Soleymani, "Multistage parallel interference cancellation with power and phase estimation," in *Proc. IEEE VTC Fall*, Vancouver, Canada, Sep. 24-29, 2002.
- [40] D. Guo, L.K. Rasmussen, and T.J. Lim, "Linear parallel interference cancellation in long-code CDMA multiuser detection," *IEEE J. Select. Areas Commun.*, vol. 17, pp. 2074-2081, Dec. 1999.
- [41] P.G. Renucci, "*Optimization of soft interference cancellation in DS-CDMA receivers*," Master's thesis, Virginia Polytechnic Institute and State University, Blacksburg, Virginia, May 1998.

- [42] A.N. Fawzy, A.W. Fayed, and M.M. Riad, "Optimization of partial parallel interference cancellation (PPIC) factor in CDMA systems," in *Proc. IEEE Sys., Man, Cyber.*, 2000, pp. 2375-2380.
- [43] Y.T. Hsieh and W.R. Wu, "An optimum two-stage partial parallel interference canceller for CDMA systems," in *Proc. IEEE Globecom*, vol. 1, pp. 499-503, Nov. 2002.
- [44] D. Guo, "*Linear parallel interference cancellation in CDMA*," M.Eng. thesis, Nat. Univ. Singapore, 1998. [online]:<http://www.princeton.edu/~guo>.
- [45] L.G.F. Trichard, J.S. Evans, and I.B. Collings, "Large system analysis of linear multistage parallel interference cancellation," *IEEE Trans. Commun.*, vol. 50, pp. 1778-1786, Nov. 2002.
- [46] M. Ghotbi and M.R. Soleymani, "Performance of Parallel Interference Cancellation in Large CDMA over a Fading Channel," in *Proc. IEEE Globecom*, Nov. 29-Dec.3, 2004.
- [47] D.N.C. Tse and S.V. Hanly, "Linear multiuser receivers: effective interference, effective bandwidth and user capacity," *IEEE Trans. Inform. Theory*, vol. 45, pp. 641-657, Mar. 1999.
- [48] J. Evans and D.N.C. Tse, "Large system performance of linear multiuser receivers in multipath fading channels," *IEEE Trans. Inform. Theory*, vol. 46, pp. 2059-2078, Sep. 2000.
- [49] Kiran and D.N.C. Tse, "Effective interference and effective bandwidth of linear multiuser receivers in asynchronous CDMA systems," *IEEE Trans. Inform. Theory*, vol. 46, pp. 1426-1447, Jul. 2000.

- [50] W. Hachem, "Simple polynomial detectors for CDMA downlink transmissions on frequency-selective channels," *IEEE Trans. Inform. Theory*, vol. 50, pp. 164-171, Jan. 2004.
- [51] L. Cottatellucci and R.R. Muller, "Asymptotic design and analysis of multi-stage detectors and multistage channel estimators for multipath fading channels," in *Proc. IEEE Int. Symp. Information Theory*, pp. 243-243, 27 Jun.29-Jul.4, 2003.
- [52] L. Cottatellucci, M. Debbah, and R.R. Muller, "Asymptotic design and analysis of multistage detectors for asynchronous CDMA systems," in *Proc. IEEE Int. Symp. Information Theory*, Jun.27-Jul.2, 2004, pp. 509-509.
- [53] L. Cottatellucci and R.R. Muller, "Multistage detectors in asynchronous CDMA systems" In *Proc. IEEE Zurich Seminar on Commun.*, pp. 102-105, Feb.18-Feb.20, 2004.
- [54] L. Li, A.M. Tulino, and S. Verdu, "Asymptotic eigenvalue moments for linear multiuser detection," in *Proc. IEEE Signals, Systems and Computers, Asilomar Conf.*, pp. 1177-1181, Nov. 4-7, 2001.
- [55] M. Ghotbi and M.R. Soleymani, "A simple method for computing partial cancellation factors in CDMA using PPIC receiver," in *Proc. IEEE ICASSP*, Montreal, Canada, May 17-21, 2004.
- [56] A.A. D'Amico, U. Mengali, and M. Morelli, "Channel estimation for the uplink of a DS-CDMA system" *IEEE Trans. Wireless Commun.*, vol. 2, pp. 1132-1137, Nov. 2003.
- [57] J.S. Evans, "Optimal resource allocation for pilot symbol aided multiuser receivers in Rayleigh faded CDMA channels," *IEEE Trans. Commun.*, vol. 50, pp. 1316-1325, Aug. 2002.

- [58] W.G. Phoel and M.L. Honig, "Performance of coded DS-CDMA with pilot-assisted channel estimation and linear interference suppression" *IEEE Trans. Commun.*, vol. 50, pp. 822-832, May 2002.
- [59] M. Ghotbi and M.R. Soleymani, "Performance of an Asynchronous CDMA System with Parallel Interference Cancellation," in *Proc. IEEE VTC Spring*, Milan, Italy, May 17-19, 2004.
- [60] M. Ghotbi and M.R. Soleymani, "Large-System Analysis of Multistage PPIC Receivers," in *Proc IEEE CWIT*, Montreal, Canada, June 2005.